

NAVAL POSTGRADUATE SCHOOL MONTEREY, CALIFORNIA



THESIS

**CONVECTIVE HEAT TRANSFER FROM A
VERTICAL CYLINDER IN A HIGH
AMPLITUDE RESONANT SOUND FIELD**

by

Mark Bridenstine

September, 1996

Thesis Advisor:

Ashok Gopinath

Approved for public release; distribution is unlimited.

19970121 199

DTIC QUALITY INSPECTED 1

REPORT DOCUMENTATION PAGE

Form Approved OMB No. 0704-0188

Public reporting burden for this collection of information is estimated to average 1 hour per response, including the time for reviewing instruction, searching existing data sources, gathering and maintaining the data needed, and completing and reviewing the collection of information. Send comments regarding this burden estimate or any other aspect of this collection of information, including suggestions for reducing this burden, to Washington Headquarters Services, Directorate for Information Operations and Reports, 1215 Jefferson Davis Highway, Suite 1204, Arlington, VA 22202-4302, and to the Office of Management and Budget, Paperwork Reduction Project (0704-0188) Washington DC 20503.

1. AGENCY USE ONLY (Leave blank)	2. REPORT DATE September 1996	3. REPORT TYPE AND DATES COVERED Master's Thesis	
4. TITLE AND SUBTITLE CONVECTIVE HEAT TRANSFER FROM A VERTICAL CYLINDER IN A HIGH AMPLITUDE RESONANT SOUND FIELD		5. FUNDING NUMBERS	
6. AUTHOR(S) Mark Bridenstine		8. PERFORMING ORGANIZATION REPORT NUMBER	
7. PERFORMING ORGANIZATION NAME(S) AND ADDRESS(ES) Naval Postgraduate School Monterey CA 93943-5000		10. SPONSORING/MONITORING AGENCY REPORT NUMBER	
9. SPONSORING/MONITORING AGENCY NAME(S) AND ADDRESS(ES)		11. SUPPLEMENTARY NOTES The views expressed in this thesis are those of the author and do not reflect the official policy or position of the Department of Defense or the U.S. Government.	
12a. DISTRIBUTION/AVAILABILITY STATEMENT Approved for public release; distribution is unlimited.		12b. DISTRIBUTION CODE	
13. ABSTRACT (maximum 200 words) This thesis is part of a continuing study in developing convective heat transfer correlations for a cylinder in a high amplitude zero-mean oscillating flow. The experiment described here utilizes the RTD technique and a steady state heat transfer measurement method with a platinum wire, serving as the test section, positioned across the inner diameter of a cylindrical plexiglass chamber supporting a strong resonant axial acoustic field. Utilizing two different wire diameters of 0.050 mm and 0.127 mm, various pressure ratios, frequencies, and temperature differences, separated flow heat transfer correlations have been developed. This work would find application in the design of heat exchangers for a thermoacoustic engine.			
14. SUBJECT TERMS Thermoacoustic Engines, Heat Exchangers, Oscillatory Flows, Heat Transfer		15. NUMBER OF PAGES 112	
		16. PRICE CODE	
17. SECURITY CLASSIFICATION OF REPORT Unclassified	18. SECURITY CLASSIFICATION OF THIS PAGE Unclassified	19. SECURITY CLASSIFICATION OF ABSTRACT Unclassified	20. LIMITATION OF ABSTRACT UL

NSN 7540-01-280-5500

Standard Form 298 (Rev. 2-89)
Prescribed by ANSI Std. Z39-18 298-102

Approved for public release; distribution is unlimited.

**CONVECTIVE HEAT TRANSFER FROM A VERTICAL CYLINDER IN A
HIGH AMPLITUDE RESONANT SOUND FIELD**

Mark Bridenstine
Lieutenant, United States Navy
B.S.M.E., University of Notre Dame, 1986

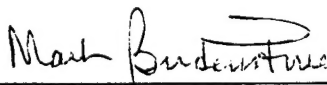
Submitted in partial fulfillment
of the requirements for the degree of

MASTER OF SCIENCE IN MECHANICAL ENGINEERING

from the

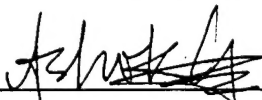
**NAVAL POSTGRADUATE SCHOOL
September 1996**

Author:

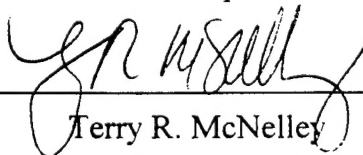


Mark Bridenstine

Approved by:



Ashok Gopinath



Terry R. McNelley

Department of Mechanical Engineering

ABSTRACT

This thesis is part of a continuing study in developing convective heat transfer correlations for a cylinder in a high amplitude zero-mean oscillating flow. The experiment described here utilizes the RTD technique and a steady state heat transfer measurement method with a platinum wire, serving as the test section, positioned across the inner diameter of a cylindrical plexiglass chamber supporting a strong resonant axial acoustic field. Utilizing two different wire diameters of 0.050 mm and 0.127 mm, various pressure ratios, frequencies, and temperature differences, separated flow heat transfer correlations have been developed. This work would find application in the design of heat exchangers for a thermoacoustic engine.

TABLE OF CONTENTS

I. INTRODUCTION	1
II. HISTORICAL.....	3
A. REFRIGERATION	3
1. Vapor Refrigeration Cycle	3
2. Thermoacoustic Cycle.....	4
B. HEAT TRANSFER.....	6
1. Natural/Forced Convection	6
2. Thermoacoustic Streaming	8
III. FLUID MECHANICS.....	11
A. RADIAN WAVELENGTH	11
B. DISPLACEMENT AMPLITUDE.....	12
C. FREQUENCY PARAMETER.....	14
D. REYNOLDS NUMBER	15
E. FLOW SEPARATION	16
IV. EXPERIMENT	19
A. PURPOSE	19
B. EQUIPMENT	20
1. Test Cylinder.....	20
2. Acoustic Chamber.....	21
3. Electronics.....	22
C. PROCEDURE	25
V. RESULTS AND DISCUSSION	31
VI. CONCLUSIONS AND RECOMMENDATIONS	39
APPENDIX A: CALIBRATION	43
APPENDIX B: SAMPLE CALCULATION	49
A. NUSSELT NUMBER	49

B. REYNOLDS NUMBER.....	51
APPENDIX C: UNCERTAINTY ANALYSIS	53
A. PLATINUM WIRE RESISTANCE.....	53
B. NUSSELT NUMBER	55
C. REYNOLDS NUMBER.....	57
APPENDIX D: EXPERIMENTAL DATA	61
LIST OF REFERENCES	95
INITIAL DISTRIBUTION LIST	97

LIST OF FIGURES

Figure 1. Basic Vapor Refrigeration Cycle	3
Figure 2. Basic Thermoacoustic Refrigeration Components	5
Figure 3. Vertical Cylinder Natural Convection	7
Figure 4. Acoustic Streaming Pattern	9
Figure 5. Isothermal "Streaked" Flow	17
Figure 6. Acoustic Chamber and Accessories.....	22
Figure 7. Acoustic Electronics Package.....	23
Figure 8. Heat Transfer Electronics Package.....	24
Figure 9. Standing Wave Velocity Profile in a Circular Cylinder	26
Figure 10. Nusselt Number versus Reynolds Number ($d = 50.8 \mu\text{m}$).....	35
Figure 11. Nusselt Number versus Reynolds Number ($d = 127 \mu\text{m}$).....	36
Figure 12. Nusselt Number versus Reynolds Number (both wires)	37
Figure 13. Curve Fit for Nusselt Number versus Reynolds Number ($d = 50 \mu\text{m}$).....	41
Figure 14. Calibration Chamber.....	44
Figure 15. Platinum Wire Calibration Curve ($d = 50.8 \mu\text{m}$).....	46
Figure 16. Platinum Wire Calibration Curve ($d = 127 \mu\text{m}$).....	47

LIST OF TABLES

Table 1. Platinum Wire Calibration Data ($d = 50.8 \mu\text{m}$)	45
Table 2. Platinum Wire Calibration Data ($d = 127 \mu\text{m}$)	45

LIST OF SYMBOLS, ACRONYMS, AND/OR ABBREVIATIONS

a	test cylinder radius [m]
A	particle displacement [m]
\bar{A}	particle displacement amplitude [m]
A_s	surface area [m ²]
c	speed of sound [m/s]
d	diameter of test cylinder [m]
f	frequency [Hz]
h	convective heat transfer coefficient [W/m ² -K]
HX	heat exchanger
I	current [Amps]
k	thermal conductivity [W/m-K]
KC	Keulegan-Carpenter number
l	length of test cylinder [m]
L	distance from test cylinder to chamber end plate [m]
M	Mach number
Nu	Nusselt number
P_m	mean ambient pressure [Pa]
P_{ref}	reference pressure [Pa]
PR	pressure ratio
R	gas constant [J/kg-K]
Re	Reynolds number
R_{PR}	precision resistor resistance [ohms]
R_s	streaming Reynolds number
R_w	wire resistance [ohms]
RMS	root mean square
RTD	resistance temperature detector
SPL	sound pressure level
t	time [s]
T_c	cold sink temperature [K]
T_h	hot sink temperature [K]
T_s	surface temperature [K]
T_∞	ambient temperature [K]
U	velocity [m/s]
U_0	velocity amplitude [m/s]
V_m	pressure transducer voltage [volts]
V_0	voltage [volts]
V_{PR}	precision resistor voltage [volts]
V_w	platinum wire voltage [volts]
β	amplitude ratio

χ	cylinder length scale
δ	boundary layer thickness [m]
ε	amplitude parameter
γ	ratio of specific heats
λ	wavelength [m]
$\bar{\lambda}$	radian wavelength [m/rad]
Λ	frequency parameter
ν	kinematic viscosity [m ² /s]
ω	radian frequency [rad/s]

I. INTRODUCTION

Pollution free refrigeration is a concept worthy of close inspection in this day and age of an environmentally conscious public. A more far-reaching concern to the masses than the purported global environmental awareness may be the economic impact from a recent international agreement to ban all consumption of chloroflourocarbons (CFCs) by the turn of the century. This will affect everyone in the industrialized world. Technologies are being investigated to supplant or improve present day refrigerants and/or their associated cycles. Researchers, whose interests come from a broad spectrum including academia, space and the automotive industry, seek to provide an alternative to today's refrigeration technology whereby a CFC-free environment remains.

One method, thermoacoustic refrigeration, blends, in part, the disciplines of convective heat transfer and acoustics. Four real world applications of this technology include the Space ThermoAcoustic Refrigerator (STAR) [Ref. 1], a food refrigerator built in the Republic of South Africa, a cryogenic refrigerator for electronics cooling and a device built by the Ford Motor Company for potential automobile uses. Through continued innovation and experimentation these highly specialized designs may soon become distant relatives of a new age of environmentally safe, mass produced, commercial thermoacoustic refrigeration units.

If theory has been put into practice, why not close the book on laboratory experimentation in this field? At present, thermoacoustic refrigerator technology depends on efficient solid to gas heat transfer from its heat exchangers. Lee and Richardson [Ref. 2] reiterate what has been known for a long time, that is, heat transfer coefficients between gases and solid surfaces are small. If the turbulence intensity of the gas free stream is raised, heat transfer rates will increase. Researchers have found that experiments and analysis involving stationary sound fields rather than real turbulent flow are much simpler. Their experiments have shown that under favorable circumstances the presence of oscillations can cause significant increases in gas heat transfer coefficients.

Today's thermoacoustic refrigerators lack the efficiency of modern day vapor compression cycles. Operating at best at about 50% efficiency of conventional refrigerators, there is much room for improvement especially in heat exchanger design. The intent here is to extend the experimental basis for heat exchanger design in thermoacoustic applications. The fundamental flow regimes and the results from varying characteristic parameters within each have not yet been completely analyzed. The motivation for this work is to develop a better understanding of the relationship between high amplitude resonant sound fields and convective heat transfer rates in a gaseous medium and to develop useful correlations for a portion of the wide parameter regime of interest.

II. HISTORICAL

A. REFRIGERATION

1. Vapor Refrigeration Cycle

Vapor compression systems are the most common refrigeration cycles used for both industrial and commercial refrigeration (Figure 1). The working fluid, or refrigerant, in these systems is typically a halogenated hydrocarbon. A measure of efficiency for these cycles, designated the coefficient of performance (COP), comes from the ratio of actual refrigerating effect to the net work required. In theory, the Carnot cycle represents the most efficient cycle. However, several impracticalities arise, therefore, actual systems sacrifice efficiency for a reduction in costs and maintenance.

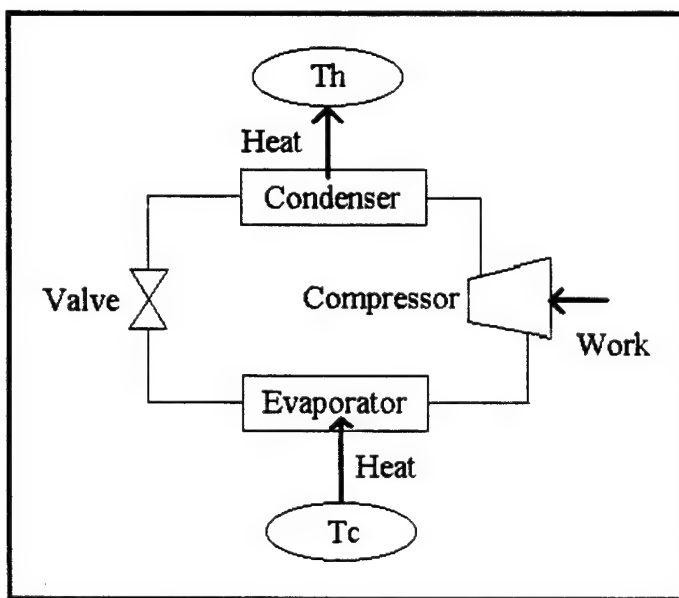


Figure 1. Basic Vapor Refrigeration Cycle

Today's refrigerators grew out of years of theoretical and experimental studies to become efficient, reliable and versatile machines serving numerous applications.

Operating efficiencies on the order of over 90% of Carnot efficiency are not uncommon. Recent international laws requiring an end to the production of environmentally hazardous, ozone-depleting, hydrocarbon refrigerants (i.e., R-11, R-12, R-114) used in many of these systems led to new temporarily acceptable substitutes (i.e., R-134a) and an interest, at least academically, in radically new methods for a future standardized means of refrigeration.

2. Thermoacoustic Cycle

Thermoacoustic refrigeration systems can be described in the following very simplistic way. There are six basic system components illustrated in Figure 2. They include the driver or loudspeaker, two heat exchangers, a "stack," and a sound medium (typically a gas) all enclosed within an acoustic chamber. A resonating sound wave, contained within the acoustic chamber, establishes a sinusoidal varying pressure field with antinodes at the chamber ends. Acoustic theory explains the simultaneous formation of sinusoidal displacement and velocity fields 90 degrees out of phase with the pressure field. They are anchored by nodes at the chamber ends. The sound wave remains stationary, however, the gas molecules within the chamber rapidly move back and forth. By precisely positioning the heat exchange elements (i.e., hot heat exchanger, and cold heat exchanger with a "stack" of low thermal conductivity plates in between) away from the pressure and displacement nodes a "bucket brigade" means of heat transfer between gas particles is created along the length of each plate within the stack. If we assume that a half-wavelength sound wave exists within the chamber of Figure 2, the stack cools at the end facing the driver and heats up at the other end. The magnitude of the temperature gradient is directly related to the pressure ratio created in the chamber. As the pressure amplitude increases so does the temperature difference.

Figure 2 also illustrates a simplified version for one cycle of particle oscillation, [Swift Ref. 3]. A gas particle undergoes adiabatic compression when displaced to position A. Following the laws of thermodynamics, an accompanying temperature rise leaves the particle hotter than the plate. Heat is rejected to the plate, from the particle,

which returns to position B while undergoing adiabatic expansion. A temperature decrease accompanying particle expansion lowers its temperature below that of the plate. Heat flows to the particle and “up” the temperature gradient with subsequent compression and displacement of the particle back to position A. A shallow positive temperature gradient forms across the stack from the cold heat exchanger to the hot heat exchanger through adjacent particle heat transfer across the plates as described above.

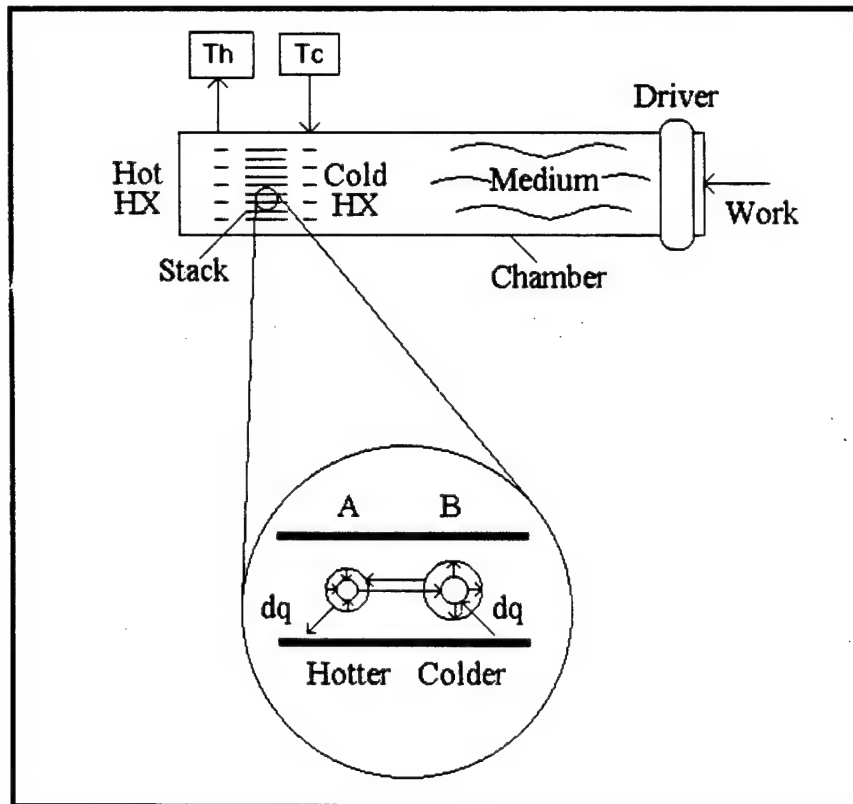


Figure 2. Basic Thermoacoustic Refrigeration Components

In 1993 A. D. Little, Inc., performed a research needs assessment for the Department of Energy [Ref. 4]. They analyzed more than fifteen refrigeration alternatives including substitute refrigerants, improved components and/or alternate cycles. For domestic refrigeration, Little's report concluded that thermoacoustic refrigeration was an

unlikely replacement to vapor compression. Under the categories of priority for research and development, probability of success, and industry involvement, thermoacoustics ranked lowest compared to all other technologies considered. Since that report, however, several corporate sponsored projects, mentioned above in part, affirm the viability of thermoacoustic refrigeration. Steven L. Garrett et al. [Ref. 5] succinctly outline the benefits and predominant technical issues surrounding this technology.

A simple description of the basic flow of heat from one end of the stack to the other, in the presence of an acoustic standing wave, is given above. What has not been considered in great detail is the effect that the same sound wave will have on the heat transfer from the heat exchanger to or from the stack ends. If a gap in physical contact exists between a heat exchanger and the end of the stack, how can we best operate and design the refrigerator to maximize efficient heat transfer across that gap? It is here that significant advances in this technology need to be made both in understanding the theory and incorporating experimental results into design. This study attempts to close the gap between the theory behind thermoacoustic refrigerator heat exchange in a sound field and an efficient heat exchanger design by providing heat transfer correlations in the separated flow regime. It is here that great advances in system efficiency and performance can and need to be made in order to persuade hesitant academics and conservative, potential corporate sponsors of the need for future research, development and investment in this relatively new technology.

B. HEAT TRANSFER

1. Natural/Forced Convection

Generally speaking, there are two distinct modes of convective heat transfer, natural (free) and forced. Each represents a different means by which fluid motion is sustained. The importance of one mode relative to the other is governed by the strength of its respective fluid motion. Forced convection fluid motion, or fluid velocity, is generated by some external forcing condition and, hence, the flow and thermal fields are largely uncoupled. As an example, consider a horizontal cylinder immersed in air.

Assuming that a temperature difference exists between the cylinder and air, a fan used to force air over the cylinder creates the necessary fluid motion for forced convection heat transfer. On the other hand, natural convection fluid motion arises when a body force acts upon a density difference. This density gradient typically results from a temperature difference between the body and the medium. The result is coupled flow and thermal fields, a more difficult problem to solve. Using a vertical cylinder in a quiescent air medium, a temperature difference between the cylinder and air gives way to buoyant forces that create natural convection currents adjacent to the cylinder surface. When the cylinder temperature exceeds that of the air, air adjacent to the cylinder surface is heated. This less dense air rises allowing cooler ambient air to replace it (Figure 3).

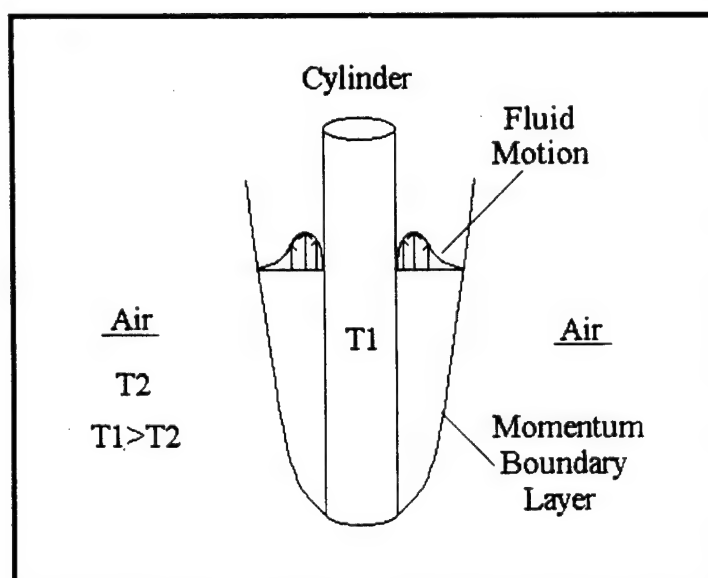


Figure 3. Vertical Cylinder Natural Convection

In all examples of heat transfer, temperature differences give rise to density differences. Therefore, we can say that in the presence of a body force, the effects of natural convection heat transfer are likely to co-exist with forced convection heat transfer. The opposite is not true. The relative importance of these two competing effects is

governed by the ratio of suitably defined Grashof number to Reynolds number (raised to some suitable power). In the limit, as this ratio tends to zero, the buoyancy forces become insignificant. As the ratio tends to infinity, buoyancy forces dominate the forced convection effects. If the two competing effects are comparable in magnitude, mixed or combined convection results.

Analysis of mixed convection flow fields requires knowledge of the two limiting fluid flow cases (i.e., induced buoyant forces and forced convection effects). From Gebhart et al. [Ref. 6], the direction and magnitude of the respective flow fields at any local position along the surface of interest will dictate whether the flow remains attached, separates or reverses. Gebhart et al. present results for differing geometries, surface heating and competing flow field strengths and directions.

2. Thermoacoustic Streaming

Early works regarding the effect of sound and vibration on heat transfer, including Lee and Richardson [Ref. 2], Fand and Cheng [Ref. 7], and Fand and Kaye [Ref. 8, 9], were instrumental in introducing a new fluid flow phenomenon called thermoacoustic streaming. All of the above mentioned authors' research utilized a horizontal heated cylinder in air subjected to a horizontal and transverse stationary sound field. The boundary layer velocity fields established for such an arrangement, when not subjected to a sound field, include azimuthal and radial velocities as expected in natural convection. The former give rise to natural convection currents tangential to the cylinder surface while the latter satisfy continuity requirements and are directed toward the cylinder. The magnitude of these tangential currents far outweigh the seemingly insignificant radial currents. When a sound field is introduced, a new boundary layer flow pattern is superimposed upon the natural convection flow. This acoustic streaming pattern, illustrated by Fand [Ref. 10], is presented in Figure 4. What appear to be two distinct flow patterns, inner and outer streaming layers, are shown. The thickness of the inner layer is exaggerated for clarity. The order of magnitude of the streaming velocities depends upon the intensity of the sound field and, for much of the above work,

corresponds to the radial component of the natural convection currents. The outer streaming flow aids the radial flow at the top and bottom of the cylinder but opposes it on the sides. If the basic boundary layer flow pattern around this cylinder is changed, it is reasonable to assume that the heat transfer may also be affected.

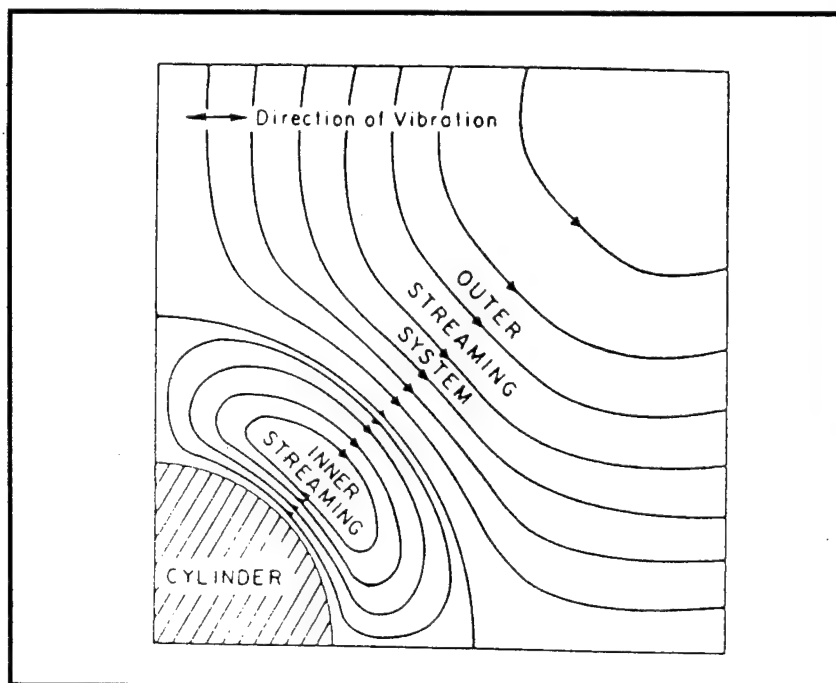


Figure 4. Acoustic Streaming Pattern

In an isothermal experiment this acoustic streaming pattern behavior is well documented. However, when applied to the problem where temperature gradients exist, the streaming pattern deviates from this theory. Several explanations are given in Fand [Ref. 10]. For their specific experiment, Fand and Kaye [Ref. 8] illustrate pictorially the effects of sound on the well known convection flow pattern. Two plumes or vortices form, separate and grow above the cylinder as the sound intensity is increased. The traditional natural convection boundary layer flow is disturbed. Thermoacoustic streaming boundary layer flow, characterized by the two vortices, results. The streaming flows aid heat transfer at the top and bottom but hinder it on the sides. Therefore, a

balance is established whereby the overall heat transfer rate remains unchanged. Lee and Richardson's [Ref. 2] experimental results corroborate this theory noting that sound field intensities below a "critical" sound pressure level (SPL) have no effect on the natural convection heat transfer rate. Once the sound intensity reaches the critical SPL, however, the point of separation for the thermoacoustic vortices has moved down the sides of the cylinder. Streaming velocities separate the boundary layer in the horizontal direction after which the buoyant forces sweep the fluid upwards until the previous area of local reduction in heat transfer is eliminated. The delicate heat transfer balance is compromised yielding an increase in overall heat transfer from the surface. Control of the heat transfer passes from pure natural convection to acoustic streaming.

The above discussion and associated references outline the theory and experimental results regarding attached boundary layer flow for heat transfer from a horizontal cylinder under the influence of a zero-mean oscillating flow. Little data exists concerning the effect such a sound field has on heat transfer from a *vertical* cylinder. More importantly for this research, the theory and experimental data available for *separated flow* heat transfer from a vertical cylinder exposed to a zero-mean oscillating flow is sparse to say the least.

III. FLUID MECHANICS

To extract meaningful results from experiments conducted by numerous researchers using a variety of physical constants and geometric dimensions, it has become common to present them in a general nondimensional form. This methodology reduces the number of variables and links one researcher's data to another, thereby, enabling the engineer the opportunity to efficiently withdraw relevant conclusions regarding the phenomenon for design purposes. Mapping the results in terms of dimensionless parameters also gives the researcher insight into those areas or boundaries not yet completely analyzed. The important parameters necessary to explain the phenomenon of heat transfer from a cylinder in an zero-mean oscillating flow are presented below. Different fluid flow regimes result. This work attempts to extract heat transfer correlations from experimental data collected within the incompressible, separated flow regime.

A. RADIAN WAVELENGTH

Two obvious length scales can be derived from periodic oscillating flow. First, the radian wavelength is defined as

$$\bar{\lambda} = \frac{\lambda}{2\pi} \quad (1)$$

In order to maintain our assumption of incompressibility, the radian wavelength should be larger than the characteristic dimension of the wire, radius, a . Wire radius is an easily measured quantity as is radian wavelength when presented in the form

$$\bar{\lambda} = \frac{\lambda}{2\pi} = \frac{c/f}{2\pi} = \frac{c}{\omega} \quad (2)$$

The dimensionless parameter that results shall be designated, χ . For incompressibility we require

$$\chi = \frac{a}{\lambda} = \frac{a\omega}{c} \ll 1 \quad (3)$$

B. DISPLACEMENT AMPLITUDE

The fluid particles subjected to a time varying sound field will experience a displacement amplitude, \bar{A} . This is the second logical acoustic length scale. One can now begin to appreciate the complexity of this problem. In addition to the common characteristic geometric length scale (e.g. wire radius, a) found in all bluff body fluid flow experiments, two additional acoustic length scales have been introduced.

In order for flow near the wire surface to remain attached, we expect minimal particle displacement relative to the wire diameter near the wire surface. The amplitude parameter, ε , defined as

$$\varepsilon = \frac{\bar{A}}{a} \quad (4)$$

expresses the distance a fluid particle moves relative to the cylinder radius. Its magnitude helps predict the type of flow, separated or attached, along the wire surface. When $\varepsilon \geq 1$ we anticipate separated flow. For ease of measurement we can expand this equation. Consider a sinusoidal time varying signal. A direct relationship exists between particle amplitude and velocity as seen from the following simple scenario. If particle amplitude is defined by

$$A = \bar{A} \cos(\omega t) \quad (5)$$

then particle velocity follows as

$$U = \frac{d(A)}{dt} \quad (6)$$

Consequently,

$$U = \bar{A}\omega \sin(\omega t) \quad (7)$$

The velocity amplitude, U_o , where

$$U_o = \bar{A}\omega \quad (8)$$

produces the direct relationship

$$\bar{A} = \frac{U_o}{\omega} \quad (9)$$

One may now measure velocity amplitude along with frequency, or we can carry the scenario one step further. Morse and Ingard [Ref. 11] present a derivation for the relationship between fluid velocity and pressure change for adiabatic compression of a perfect gas as

$$U_o = \frac{c}{\gamma} \frac{P_o}{P_m} \quad (10)$$

Putting all of this together in a form easily measured by experiment, we have

$$\varepsilon = \frac{c}{a\omega} \left[\frac{P_o}{\gamma P_m} \right] \quad (11)$$

The amplitude parameter by itself is an indication of separated or attached flow. Additionally, when combined with χ , the Mach number results as

$$M = \chi \varepsilon = \left(\frac{a\omega}{c} \right) \left(\frac{U_o}{a\omega} \right) = \frac{U_o}{c} \quad (12)$$

We can reinforce the assumption of incompressible flow when $M \ll 1$. In much of the literature the amplitude parameter is also expressed as the Keulegan-Carpenter number,

$$KC = \pi \varepsilon \quad (13)$$

another dimensionless parameter.

C. FREQUENCY PARAMETER

It is important to include the effects of fluid viscosity when discussing velocity and displacement. Recall Stokes' second problem. This addresses the effect an oscillating plate has on an adjacent viscous fluid. A boundary layer thickness (or Stokes layer) of order

$$\delta = \sqrt{\frac{\nu}{\omega}} \quad (14)$$

dictates how far into the fluid the disturbances created by the oscillating plate can be felt. Solutions to Stokes' second problem show that at a distance greater than approximately 10δ from the plate surface, the amplitude of fluid particle oscillation has decayed to within one percent of the bulk fluid velocity. For boundary layer flows, this Stokes layer thickness is of the same order of magnitude as the inner streaming layer thickness introduced earlier.

A frequency parameter defined by

$$\Lambda^2 = \left(\frac{a}{\delta}\right)^2 = \frac{a^2 \omega}{\nu} \quad (15)$$

relates the characteristic dimension of the body to the Stokes layer thickness.

It has been shown that for $\Lambda^2 \gg 1$, a new, steady, acoustic streaming velocity develops within an outer layer. This steady flow component is of order $O(\epsilon U_0)$ and appears as an apparent slip velocity on the cylinder surface. It decays to zero within the outer layer. Reynolds stresses linked to the oscillating viscous flow in the Stokes layer are the driving force for this new steady flow. Stuart [Ref. 12] provides a mathematical proof of this. In studies of oscillatory flows, sometimes the parameter

$$\beta = \frac{(2a)^2 f}{\nu} = \frac{2}{\pi} \Lambda^2 \quad (16)$$

is used to characterize the flow.

D. REYNOLDS NUMBER

Reynolds number has long been used as a parameter to delineate flow regimes within a given environment. Accurate use of this dimensionless parameter requires the proper definition of velocity and characteristic length. Here, the characteristic length is defined as the cylinder radius, a . And, in an attempt to find appropriate heat transfer correlations, two slightly different definitions for velocity have been employed. The first comes from the steady, acoustic streaming velocity giving us the streaming Reynolds number as

$$R_s = \frac{(\epsilon U_0) a}{\nu} \quad (17)$$

After some manipulation, the streaming Reynolds number can be related to the acoustic parameters introduced above as

$$R_s = \varepsilon^2 \Lambda^2 \quad (18)$$

The second comes from the fluid particle oscillation velocity resulting in

$$\text{Re}_a = \frac{U_0 a}{\nu}, \quad \text{Re}_d = \frac{U_0 (2a)}{\nu} \quad (19)$$

Again, after some rearranging

$$\text{Re}_a = \varepsilon \Lambda^2, \quad \text{Re}_d = 2\varepsilon \Lambda^2 = \beta \cdot KC \quad (20)$$

E. FLOW SEPARATION

Fluid dynamicists (Bearman, Sarpkaya and Williamson to name a few) have long considered the mechanics of flow separation from bluff bodies in an oscillating cross flow. Active areas of research today include: forces induced by the separated flow, a pictorial representation of the wake patterns and numerical solutions that describe the pointwise velocities within these wakes for both two and three dimensional flows. Theoretical hypotheses and experimental results have educated engineers about the effects these flow patterns have on the lift and drag forces imposed upon bodies. The practical application of these studies has dealt mainly with the hydrodynamics of marine structures and vehicles. Extension of these results to heat transfer effects has been minimal.

In 1980 Honji [Ref. 13] presented a paper on his observations of isothermal three-dimensional separated flow from a vertical, oscillating, circular cylinder in water. The resulting photographs of "streaked" flow from various vantage points removed some of

the mystery surrounding the flow instabilities associated with large amplitude oscillations (Figure 5).

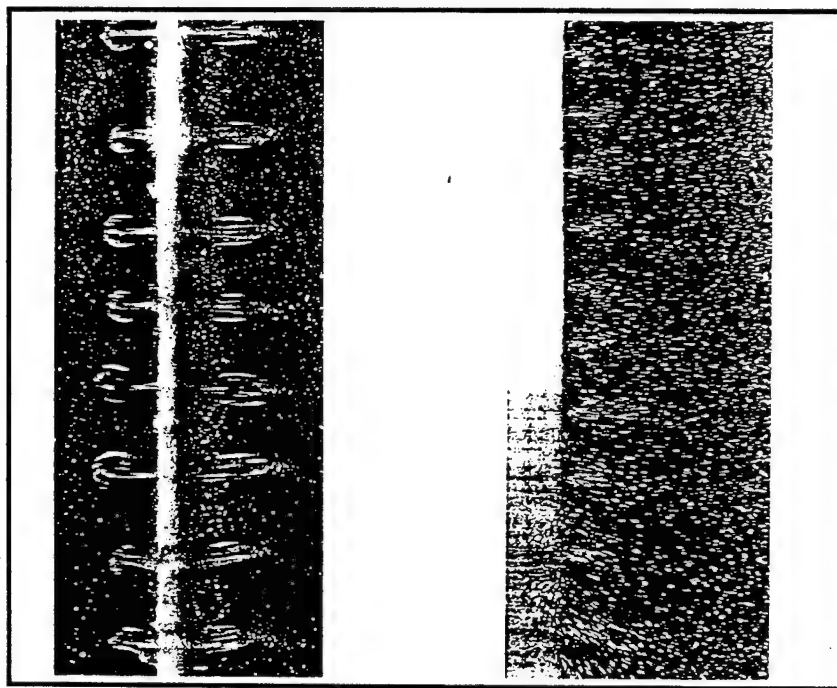


Figure 5. Isothermal "Streaked" Flow

Williamson [Ref. 14] uses several vortex flow regimes, each segregated by Keulegan-Carpenter number, to present pictorially, the formation and movement of vortices, and graphically, the variation in lift and drag forces. He concludes that with an oscillating flow, fluid reversals have a major effect on fluid induced forces. As oscillation amplitude is increased, the frequency per cycle of vortex shedding increases and the angle of vortex departure relative to the incident wave varies, thereby yielding higher induced forces whose oscillations are themselves periodic. Furthermore, the regularity of the vortex pattern appears to break down once a certain amplitude of oscillation is reached, thereby generating a discontinuous and weakened wake pattern. Williamson hypothesizes that three dimensional effects along with destructive vorticity between shed

vortices created in the present half cycle and those created several cycles previous may be the cause.

So, when does flow over a bluff body separate and at what Keulegan-Carpenter number can vortex shedding be observed? Faltinsen [Ref. 15], referencing the works of Bearman, Sarpkaya and Williamson, summarizes the answers to some of these questions. It is commonly agreed upon that once vortices can be seen, separation has occurred. That is not to say, however, that the vortices are necessarily carried away from the vicinity of the body. At very low Keulegan-Carpenter numbers fluid reversal generates mixing of vortices formed in the previous half-cycle with those of the present. The circulation of these are of opposite sense and may cancel each other out. Sarpkaya [Ref. 16] reported separation at a Keulegan-Carpenter number of 1.25. Williamson [Ref. 14] has demonstrated vortex shedding at Keulegan-Carpenter numbers as low as four.

It is clear that significant work has been documented regarding the fluid mechanics associated with flow separation and vortex shedding over a bluff body. It is logically hypothesized here, that similar flow instabilities will arise when temperature gradients, in addition to large amplitude fluid oscillations, are imposed upon a fluid medium near a heated cylinder surface. For this study then, it would seem safe to say that in addition to the previously mentioned requirements for separation, if Keulegan-Carpenter numbers above four are observed, vortex shedding occurs.

IV. EXPERIMENT

A. PURPOSE

Not all problems of science can be solved analytically. Many times it is through experiment that the true nature of a scientific phenomenon is best explained and understood. A small sample of the considerable theory and experimental data concerning the effects of sound on attached boundary layer flow heat transfer from a horizontal cylinder has been presented. The research in this area is hardly exhaustive, however, it far outweighs the available material detailing separated flow heat transfer from a vertical cylinder in the presence of a zero-mean oscillating sound field. What is available concerning separated flows in an isothermal environment has also been presented briefly to introduce the relationship between oscillating fluid amplitude and vortex shedding.

Similar geometric, acoustic and fluid mechanics parameters, presented above, are useful in quantifying experimental results in both cases. Such a standardization allows effective comparisons between different experimental works and provides researchers a "map" on which to track the evolution of analyses until a complete understanding is at hand. It is at this point that a confident assessment of the usefulness of thermoacoustics in commercial heat exchanger design can be made.

Analysis of mean external flows over bluff bodies leads one to solve the boundary layer equations. Friction and convective heat transfer correlations developed from these solutions have proven invaluable to modern engineers in their design of new technologies ranging from spacecraft to golf balls. On the other hand, little has been attempted theoretically or experimentally, to analyze the heat transfer behavior from bodies in zero-mean oscillating flow fields. Simple analogies from mean flow behavior are no longer directly applicable.

Fand and Kaye [Ref. 9] describe related work done by Kubanskii in 1952. His experimental arrangement placed the stationary sound field horizontal and parallel, vice transverse, to the axis of a horizontal heated cylinder. He deduced that fluid near the

cylinder surface moved from the antinodes to the nodes at which point the flows meeting from opposite directions collided to form a single stream that moved away perpendicular to the cylinder in a vortex-type or separated flow fashion. These experiments aim to create similar vortex-type flow but from a vertical cylinder subjected to a transverse sound field. The anticipated driving force for these experiments is forced convection rather than the free convection found by Kubanskii.

B. EQUIPMENT

The approach used here will be similar to that used by Harder [Ref. 17]. Much of the supporting equipment is the same, with the biggest difference coming in the diameter of the test cylinder. A slightly modified acoustic chamber and electric circuit enable the smooth integration of the new test cylinder into the experimental setup.

1. Test Cylinder

Recent heat transfer correlations have been developed using small diameter vertical cylinders in a stationary sound field. George Mozerkewich [Ref. 18] conducted transient heat transfer rate analysis on rhenium and titanium wires of diameter ranging from 0.125 to 2 mm. Don Harder [Ref. 17] utilized a 5 mm diameter copper cylinder with an imbedded cartridge heater to develop steady state heat transfer rate solutions. In the present research, a 0.05 mm (and 0.127 mm) diameter platinum wire acts as both the heater and thermometer for steady state heat transfer analysis. One of the more attractive aspects of platinum is its nearly linear temperature-resistance relation. Upon supplying a known current through the approximately 75 mm length of wire, the voltage drop can be measured and from Ohm's Law resistance is easily calculated.

The wire was attached at each end to a copper stud. A small indentation was made on the flat face of each copper stud to allow pooling of the flux and platinum for increased mechanical integrity. The stud was then washed in a nitric acid solution. This provided a "sticky" surface onto which the flux could better adhere. The platinum wire was then soldered at either end to the threaded copper studs. In order to maintain a relatively constant tension in the wire during both calibration and testing, the lower

copper stud remained free to move vertically, thereby, permitting very short extension and contraction movement during temperature changes.

Imposing a temperature versus resistance linear regression model upon the calibration data (App. A), wire temperature is determined for all experimental runs from the calculated resistance. The importance of accurate resistance measurements across the platinum wire cannot be overemphasized. Very low resistance copper and brass circuit connections were used both in calibration and testing. A Kikusui Model PAR 160A regulated DC power supply provided circuit voltage and current control. Voltage and current resolution are approximately 5 mV and 5 mA, respectively.

2. Acoustic Chamber

Current development of thermoacoustic refrigerators primarily use either U-shaped or straight circular cross-section housings to support the acoustic driver, heat exchangers and stack. Sound is confined quite well, and standing waves can be easily created in such simple structures. Figure 6 depicts a sketch of the acoustic chamber used in these experiments. Harder [Ref. 17] aptly describes the chamber's physical characteristics prior to a few design changes all of which are described below.

Using approximate dimensions, a 1.8 m plexiglass tube of 9 cm outside diameter and 6 mm wall thickness is capped at one end by a JBL Model 2490H acoustic driver and a moveable end plate at the other. The tube is supported by stanchions at various positions along its length. An Endevco piezoresistive pressure transducer embedded in the moveable endplate provides data for pressure ratio and sound pressure level determination within the chamber. An o-ring seal surrounding this endplate permits its easy movement into and out of the chamber while confining the sound wave. Along the length of the chamber are bored two sets of diagonally opposed 12 mm diameter holes. During testing, the platinum wire assembly is placed at one of these locations while the other is blank-capped except for ambient temperature measurements taken inside the chamber.

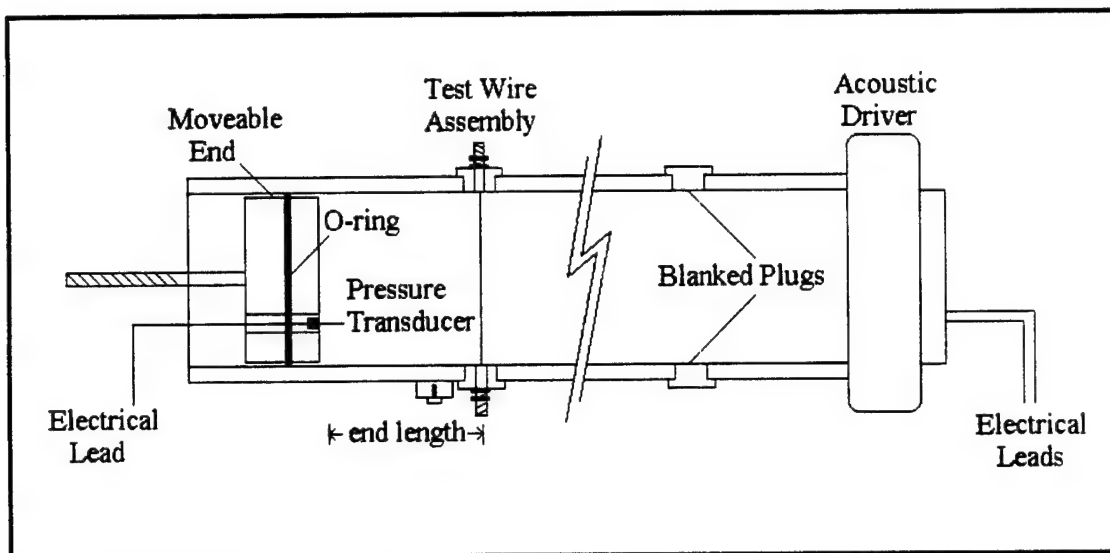


Figure 6. Acoustic Chamber and Accessories

3. Electronics

Several pieces of electronics equipment are used to generate the acoustic signal and then to monitor some of its properties. Figure 7 depicts the interconnecting relationships amongst this equipment. Beginning with a Hewlett Packard Model 33120A waveform generator, the desired waveform (sinusoidal), frequency and amplitude are selected. This signal is fed to a Techron Model 7540 power supply amplifier to boost the signal amplitude until a desired pressure ratio or sound pressure level (SPL) is reached. The amplified waveform enters the acoustic chamber via a JBL Model 2490H acoustic driver located at one end of the chamber. A pressure antinode is established at the moveable endplate located at the opposite end of the acoustic chamber. The standing wave pressure signal is sensed by the pressure transducer and amplified 100 times before it is displayed on a Hewlett Packard Model 34401A multimeter as an AC voltage. It is at this point that the pressure ratio and SPL within the chamber can be determined. Simultaneously, the amplified pressure signal is viewed on an oscilloscope to monitor gross waveform regularity. In series with the oscilloscope, a Hewlett Packard Model 3562A dynamic signal analyzer can record the signal frequency and amplitude for all

harmonics. An indication of harmonic interference from the signal analyzer helps determine exactly which frequency-amplitude combinations establish the optimum acoustic conditions in the chamber prior to the steady state heat transfer rate experimental run.

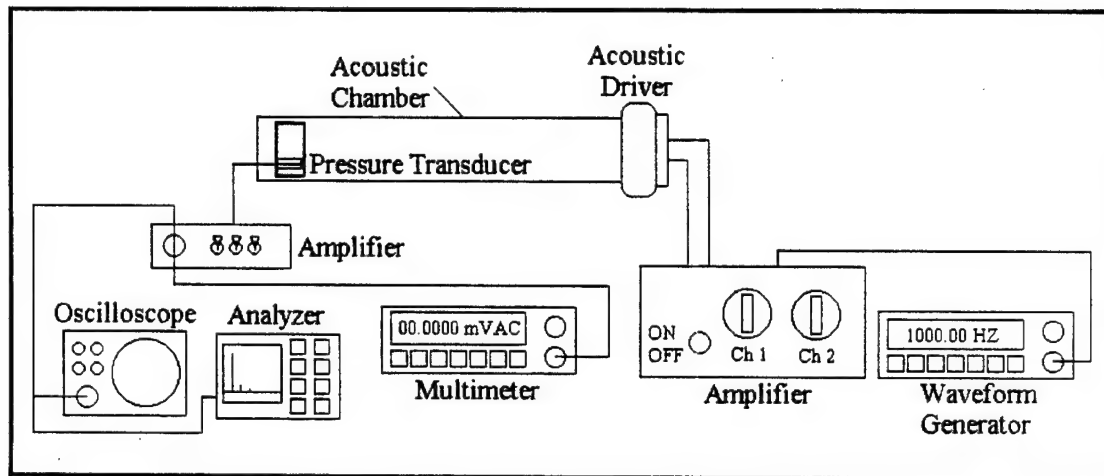


Figure 7. Acoustic Electronics Package

Once the desired acoustic conditions are established, the following additional equipment (Figure 8) is used to establish and monitor the heat transfer characteristics of the experiment. Ambient temperature sensing within the acoustic chamber is performed by manually inserting a T-type thermocouple into the center of the chamber through an upstream, normally capped, hole at the appropriate time. A Keithley Model 740 system scanning thermometer then measures the temperature to an accuracy of $\pm 0.5^{\circ}\text{C}$.

The electrical circuit designed to provide the desired temperature versus resistance characteristics for the platinum wire consists of a known fixed resistance and the platinum wire connected in series with a power supply. The resistor is rated at $98.3\text{ m}\Omega$ with an accuracy of 0.026% and acts both to minimize the power drawn by the platinum wire and to provide a means for accurate circuit current measurement. A Hewlett Packard Model 3478A digital multimeter connected in parallel across both the resistor

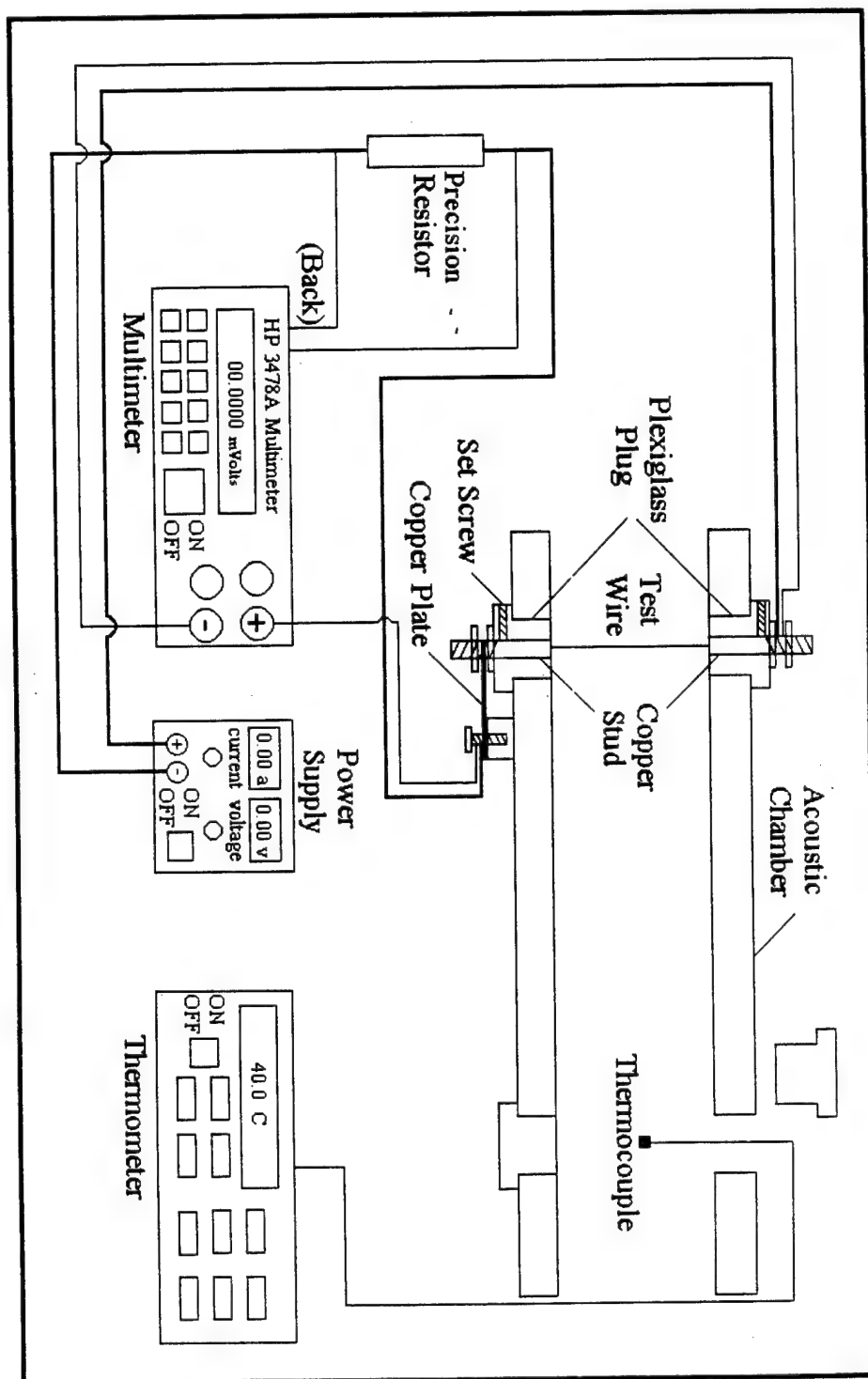


Figure 8. Heat Transfer Electronics Package

and wire accurately measures voltages up to a 5 ½ digit resolution. These measurements are subsequently used to calculate circuit current and wire resistance.

C. PROCEDURE

Prior to inserting the platinum wire into the acoustic chamber, a series of tests were conducted to identify the resonant frequencies for various chamber end lengths, L . With two sets of diagonally opposed holes bored into the chamber wall, the second set being 50 cm offset from the first (Figure 6), end lengths were incremented by 1 cm from a maximum of 73 cm (123 cm) to a minimum of 42 cm (92 cm) by adjusting the position of the moveable endplate. Sine waves starting at 300 Hz, the lower end of the acoustic driver operating range, were introduced into the chamber. Frequency was raised until a resonant condition existed as evidenced by the wave shape seen on the oscilloscope and peak pressure transducer output as read from a multimeter in root mean square (RMS) volts AC. This resonant conditions occurred at roughly 100 Hz increments up to approximately 1900 Hz, the upper end of the acoustic driver operating range. For each resonant state, the frequency, end length, peak RMS voltage for the fundamental and second harmonic frequencies, and maximum pressure transducer output were recorded. The strength of the second harmonic provided a measure of harmonic interference at the velocity antinode. This information established which frequency and end length combinations to use for actual testing.

The geometry of the experimental setup plays an important role in proper test wire positioning. For a given resonant frequency and end length combination, the standing wave velocity created can be depicted as in Figure 9. Test wire placement at maximum sound velocity (antinode) should produce the greatest heat transfer from the wire. Here a simple analogy to forced convection may be helpful. If instead of an acoustic driver, a fan were placed at one end of the chamber (open-ended at the opposite end in this case), the speed of the fan would effect the heat transfer rate. The higher the fan speed, and therefore air velocity in the vicinity of the wire, the higher would be the

heat transfer rate. Similarly for thermoacoustics, the greater the medium velocity near the wire, the greater the anticipated heat transfer rate.

As is evident from Figure 9 any odd multiple of quarter wavelength (i.e., $\lambda/4$, $3\lambda/4$, $5\lambda/4$ etc.) lies at a velocity antinode. From the equation

$$L = \frac{n\lambda}{4}; \quad n = 1, 3, 5 \dots \quad (21)$$

we can determine whether or not a given resonant condition places the test wire at a velocity antinode. Rearranging, we get

$$n = \frac{4L}{\frac{c}{f}}; \quad n = 1, 3, 5 \dots \quad (22)$$

Now, knowing which combinations of resonant frequency and end length were best suited for the fixed geometric conditions, the maximum signal amplitude yielding minimal harmonic interference can be found.

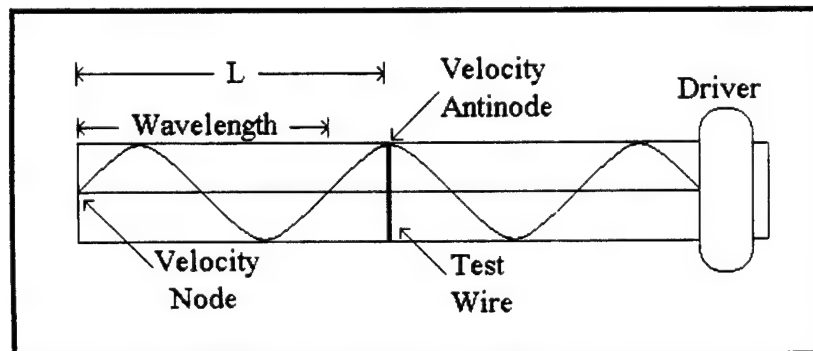


Figure 9. Standing Wave Velocity Profile in a Circular Cylinder

P. D. Richardson [Ref. 19] points out that rather than measuring velocity amplitude with a hot-wire, it is more accurate and convenient to measure pressure

amplitude with a microphone, as done here, since the velocity is directly proportional to the pressure ratio. Recalling that the resonant sound wave pressure is 90 degrees out of phase from the velocity, a pressure antinode exists at the moveable endplate where it is detected by the microphone. The microphone output is amplified 100 times. The signal is then measured by a Hewlett Packard 34401A multimeter as RMS volts AC. The following equation

$$\frac{P_o}{\sqrt{2}} = \frac{\left(\frac{V_o}{\sqrt{2}}\right)}{S} \quad (23)$$

gives the maximum pressure within the chamber. The amplified pressure transducer sensitivity, S , is equal to 0.738 mV/Pa. Solving for pressure, we get

$$P_o = \frac{\left(\frac{V_o}{\sqrt{2}}\right) \text{Volts}}{0.522 \text{Volts/kPa}} \quad (24)$$

Using 101.35 kPa for mean ambient pressure, P_m , we can find the pressure ratio from

$$PR = \frac{P_o}{P_m} * 100\% \quad (25)$$

and sound pressure level (SPL) from

$$SPL = 20 \log_{10} \frac{\frac{P_o}{\sqrt{2}}}{P_{ref}} \quad (26)$$

where P_{ref} is the reference pressure, taken to be 20 μ Pa for gases. In order to cover a wide range of fluid particle amplitudes, the pressure ratios used during the experiment varied from 0.9 to 2.9 percent in 0.1 percent increments or up to the point where harmonic interference became greater than approximately ten percent.

Once the optimum acoustic setpoints were found, the calibrated test wire was positioned within the acoustic chamber. Movement of the wire from its calibration chamber to the experimental acoustic chamber required very delicate maneuvering. Any excessive torsional or axial stress exerted on the copper to platinum wire solder joint separated the joint. After the wire was positioned, the complete electrical circuit was established including all measuring instrumentation. At this point, a comprehensive plan was set forth from which repeated experimental data runs could be made with minimal procedural variance between them. The following description details one such experimental data run.

After an initial equipment warm up period, one frequency and end length combination was set. Acoustic signal amplification was adjusted until the desired pressure ratio was obtained. Fine tuning the frequency ensured a resonant condition within the acoustic chamber. The signal characteristics were monitored on both the oscilloscope and frequency analyzer in order to check the level of harmonic interference. Signal amplifier settings were noted and then the signal was secured. After logging an ambient temperature reading within the chamber, a preset source current and voltage were introduced into the circuit. As the wire heated up, the previously marked signal amplifier settings were re-established. Once steady, after approximately 15 seconds, voltage measurements across the series precision resistor and test wire were taken. As soon as these readings were recorded, the power circuit source and signal amplifier were secured. A second ambient temperature reading within the chamber was logged. Differences between initial and final ambient temperature readings could be as high as 0.3 degrees. All of the above readings were then entered into a spreadsheet where acoustic and heat transfer parameters were calculated. Through trial and error the above procedure was

repeated until the correct source current and voltage were found for the desired temperature difference between the ambient and wire surface. Temperature differences of 8, 16, and 24 degrees (± 0.5 degrees) were targets for each pressure ratio. At some of the highest pressure ratios for the 127 μm diameter wire, temperature differences of 8, 12, and 16 degrees were used because measured wire voltage fluctuations were unacceptably high at 24 degrees. In addition to three different temperature runs per pressure ratio, each voltage reading within a run was taken in triplicate. Averaging the results from three measurements helped minimize the error for a given parameter within a data run.

The above procedure was used at every pressure ratio and for every frequency and end length combination selected. In addition, nearly the same procedure, minus the sound signal, was followed to determine the heat transfer coefficient for natural convection. The results were compared to those presented by Gebhart et al. [Ref. 6] for natural convection from a semi-infinite thin vertical wire in air to validate the procedure. Our enclosed container geometry does not accurately replicate previous experimental setups, therefore, our results do not match those presented by Gebhart. However, our results were of the same order of magnitude. This offered some validity to our experimental setup and procedure.

V. RESULTS AND DISCUSSION

This study investigates the heat transfer characteristics of a thin vertical cylinder in an air medium subjected to a high amplitude zero-mean oscillating flow. Two different wire diameters were individually tested, 50 μm and 127 μm . Both wires were exposed to pressure ratios incremented from 0.9 to 2.9 % while ensuring minimal harmonic interference. Additionally, at each pressure ratio setting, data for three separate temperature differences between the ambient and wire surface were taken. In all, nearly 400 data points were collected. Experimental measurements, applicable heat transfer and acoustic parameter calculations and certain parameter uncertainties are presented in a spreadsheet format found in Appendix D.

Use of such thin wires all but guaranteed separated flows in the high amplitude oscillation environment. The calculated values for the amplitude parameter, (i.e., Keulegan-Carpenter number), which were of $O(10)$, best corroborated this supposition. An early attempt was made to use a relatively thick 254 μm diameter wire with little success. With this wire, resistance measurements were on the order of 100 $\text{m}\Omega$ with a 1°C temperature change. This corresponded to a 0.6 $\text{m}\Omega$ resistance change. Such small values for resistance generated unacceptably high uncertainties for our measurement technique and available equipment, thereby forcing the use of thinner wires.

The first useful experiments were conducted on a 50 μm diameter wire. Initially, a frequency of 1213 Hz with a corresponding end length of 64 cm was used. This combination most closely placed the maximum velocity at the fixed test wire position. During testing, this combination also showed the least harmonic distortion up to a maximum pressure ratio of 2.9 %. No other combination withstood the distortion requirements at such a high pressure ratio.

Next, the effect of acoustic chamber end length was examined. A frequency near 1213 Hz but with an end length different than 64 cm was desired. The one combination available that offered minimal harmonic distortion was a frequency of 1213 Hz at an end

length of 50 cm. The calculated acoustic and heat transfer parameters from these two data sets were compared and noted to be nearly identical for like pressure ratios and temperature differences. It was concluded that different end lengths for a given frequency, while maintaining a zero-mean oscillating flow within the acoustic chamber, do not alter the resulting heat transfer correlations. In order to gather a more diverse set of data, two additional frequencies and associated end lengths were tested. The results at 1053 Hz ($L = 58$ cm) and 564 Hz ($L = 47$ cm) are presented in Appendix D.

Once the 50 μm diameter wire data was organized, a systematic interpretation began. To examine the effects of acoustics on heat transfer, several Nusselt number correlations were investigated using the amplitude and frequency parameters individually and in combination with each other. Nusselt number as a function of Reynolds number, not streaming Reynolds number, provided the best fit to the raw data (Figure 10). From this data, a curve fit yielded the correlation

$$Nu = 0.062 Re^{1.14} \quad (27)$$

Nusselt number errors reached as high as 13 %, while the Reynolds number error was approximately 5 %. Again, the forced convection analogy can be invoked here to help explain these results. Reynolds number is a function of particle velocity for a given cylinder diameter. It has been shown that particle velocity is directly proportional to the pressure ratio, therefore, as the pressure ratio increases so does the Reynolds number. For increasing fluid velocity we expect greater heat transfer and that is precisely what we see in these results.

To extend the range of data and to ensure a suitable Nusselt number correlation had been found, an additional set of data, using the same physical and acoustic parameters as above, was generated for a 127 μm diameter wire. A graph of this data for Nusselt number versus Reynolds number is shown in Figure 11. For this wire, Nusselt number

errors were in the range of 4-15 %, while the Reynolds number error was approximately 2 %.

A graph of the complete set of data from both wires is presented in Figure 12. It was expected that the thicker wire data would fall on top of that for the thinner wire over the common Reynolds numbers, and that the trend of monotonically increasing Nusselt number with Reynolds number would continue into a new higher Reynolds number regime. Neither of these hypotheses were accurately realized. However, within the Reynolds number overlap region for the two wires one can see that even though the data does not strictly overlap, the slopes of the two data sets are comparable.

Obviously, the thicker wire data yielded much more interesting results (Figure 11). A steady increase followed by a peak and subsequent drop in Nusselt number occurs for all three frequencies. As the frequency increases, it appears that the rate at which the Nusselt number drops and the magnitude of the drop also increase. Similarly, for increasing frequency, the drop in Nusselt number occurs at a lower Reynolds number. A discussion of these results follows.

For a given wire diameter (i.e., $127\text{ }\mu\text{m}$), increasing frequency corresponds to an increase in β . Physically speaking, the ratio of wire radius, a , to Stokes layer thickness, δ , increases. Similarly stated, the effects of the Stokes fluid oscillations do not extend as far into the bulk fluid. Consequently, one could conclude that the effects of Stokes flow interaction with the shed vortices is reduced. Any mixing effect associated with this interaction fades resulting in a lower heat transfer rate. In Figure 11, three curves are evident, one for each of three frequencies with β of $O(1)$. The high frequency (β) curve sits below the low frequency (β) curve indicating less heat transfer for a higher frequency as theorized. Furthermore, rather than applying simply a Reynolds number dependence for the heat transfer correlation (Equation 27), we now see a possible β dependence as well. Reviewing Figure 10, the $50.8\text{ }\mu\text{m}$ diameter wire β dependence is not as evident. Here β is of $O(0.1)$. Quite possibly, β becomes influential only when of $O(1)$ or higher.

To explain the sudden Nusselt number drops at high Reynolds number, Williamson's results [Ref. 14] may be helpful. Recalling the work of Williamson, flows yielding high Keulegan-Carpenter numbers evoke separation and varying vortex shedding wake patterns which he groups into KC number regimes. This study includes KC numbers ranging from 14 to 200. If these vortex patterns proceed with some regularity a steady increase in Nusselt number with KC may be expected. However, if between acoustic half-cycles, vortex interference, out of phase vortex shedding along the cylinder length or a loss of regularity in vortex shedding occur, one might expect a disruption in the steady heat transfer from the cylinder. One possible cause, as noted by Williamson, could be an intermittent and random change in the vortex shedding mode (i.e., one side of the cylinder suddenly becoming the preferred side for vortex shedding). Once this change occurs a regularity to the vortex shedding should reappear. Figure 11 gives a limited glimpse at this possibility. The 1213 Hz data shows that a minimum Nusselt number is reached after which an upturn in the curve may be indicative of a return to vortex shedding regularity. The data to support this is far from conclusive, but the hypothesis is in keeping with Williamson's results regarding lift force coefficient fluctuations.

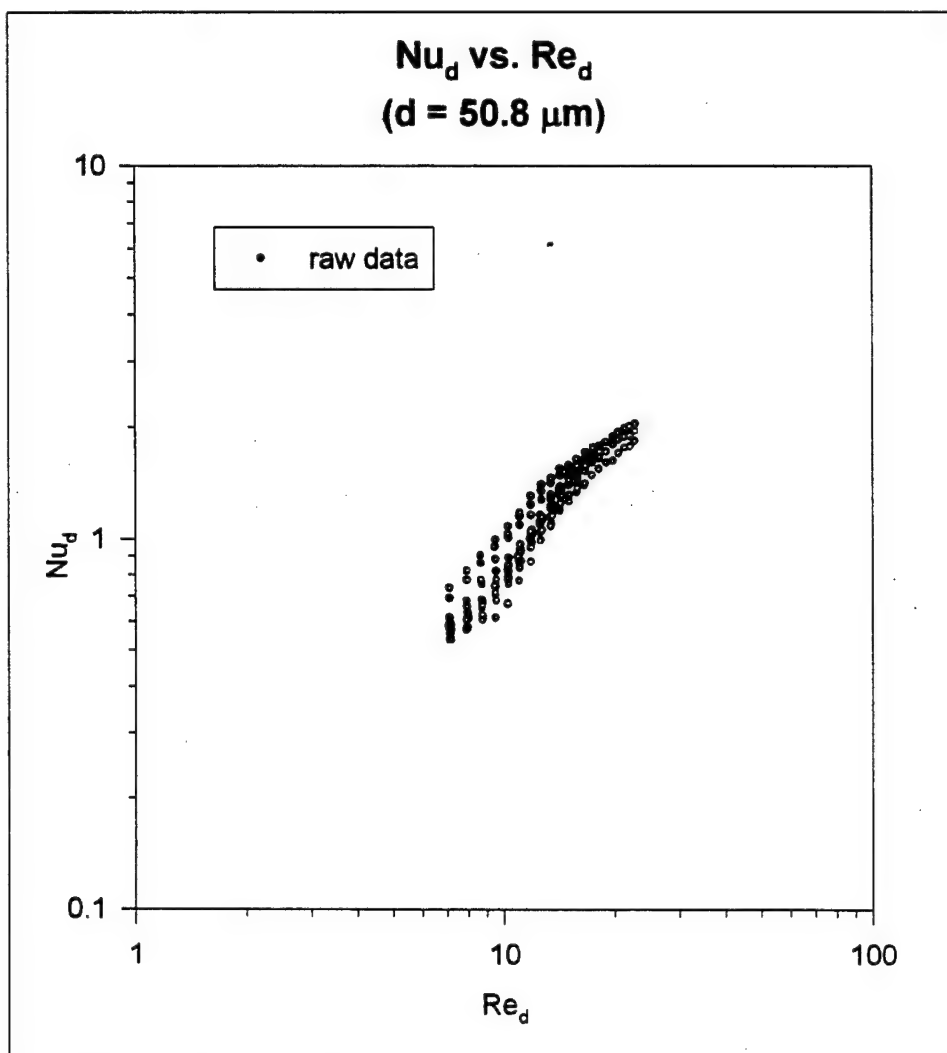


Figure 10. Nusselt Number versus Reynolds Number ($d = 50.8 \mu\text{m}$)

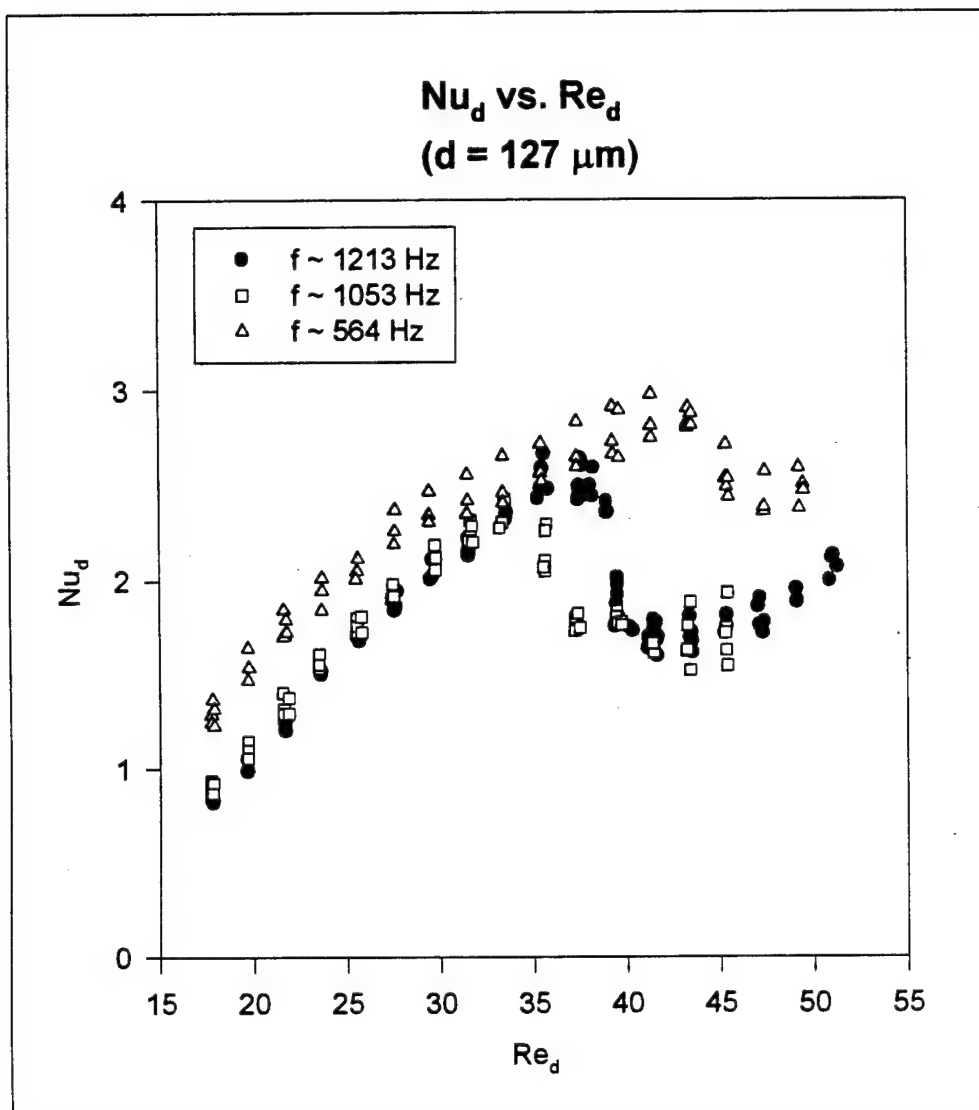


Figure 11. Nusselt Number versus Reynolds Number ($d = 127 \mu m$)

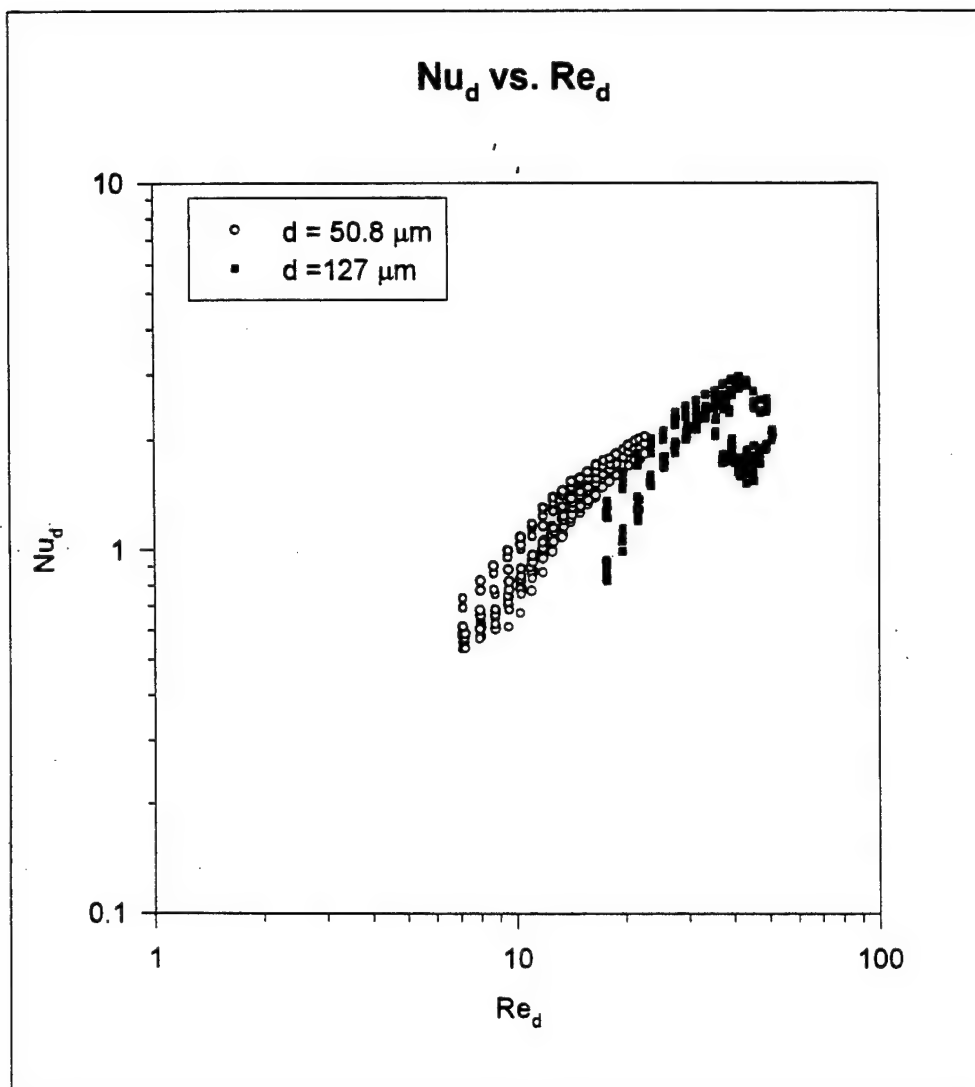


Figure 12. Nusselt Number versus Reynolds Number (both wires)

VI. CONCLUSIONS AND RECOMMENDATIONS

The motivation for this study was two-fold. First was the desire to gain an understanding of the underlying fluid mechanics for oscillating flow over a bluff body. Second was the need to develop useful heat transfer correlations for high amplitude oscillating flow over a vertical cylinder for application in the design of more efficient thermoacoustic engines. The experiments performed utilized a varying set of acoustic parameters for two different cylinder diameters. Two regimes of varying heat transfer mechanisms are discussed.

Conventional studies of oscillating flow over bluff bodies deal with large β values for varying Keulegan-Carpenter numbers. This study has experimented with very low β and, subsequently, two regimes of differing heat transfer mechanisms have been identified.

For β of $O(0.1)$ and over a wide range of moderate to high KC numbers (35 to 200), Equation (27) provides a good curve fit to the data and a correlation for the Nusselt number as a function of Reynolds number (Figure 13). In this case, the oscillating Stokes flow interacts with vortex shedding for a combined mechanism of heat transfer. What has not been considered in these experiments is the effect of Prandtl number. Generally speaking, Nusselt number is a function of both Reynolds number and Prandtl number for forced flow over a cylinder. This is an area for expanded research.

For β of $O(1)$ and over a wide range of moderate to high KC numbers (14 to 86), no definitive correlation has been developed. An introduction to vortex shedding and its effect on heat transfer in this regime has been discussed, but additional data would help solidify these results. In particular, doubling the diameter of the test cylinder, while maintaining KC high enough for vortex shedding, would generate a set of data by which several hypothesis presented above could be validated. Would a thicker wire, and therefore a larger β , generate curves with similar slope but lower heat transfer? If a peak and sudden drop in Nusselt number occurred, would it be at a lower Reynolds number as

the trend from these results indicates? The answers to these questions and validation of the results for β of $O(1)$ will come from future research.

Once a confident explanation of the mechanisms that control heat transfer for low β values has been found, expanded research should include arrays of cylinders. Analysis of two or more cylinders of variable separation distance arranged as either aligned with the sound wave, staggered or side-by-side is a logical next step to developing heat transfer correlations for operational heat exchangers. A removable section of the acoustic chamber would facilitate test platform interchangeability, make calibration easier and minimize handling of these delicate structures. And finally, use of an automated data acquisition system would provide more uniformity in data taking and speed up the entire testing process.

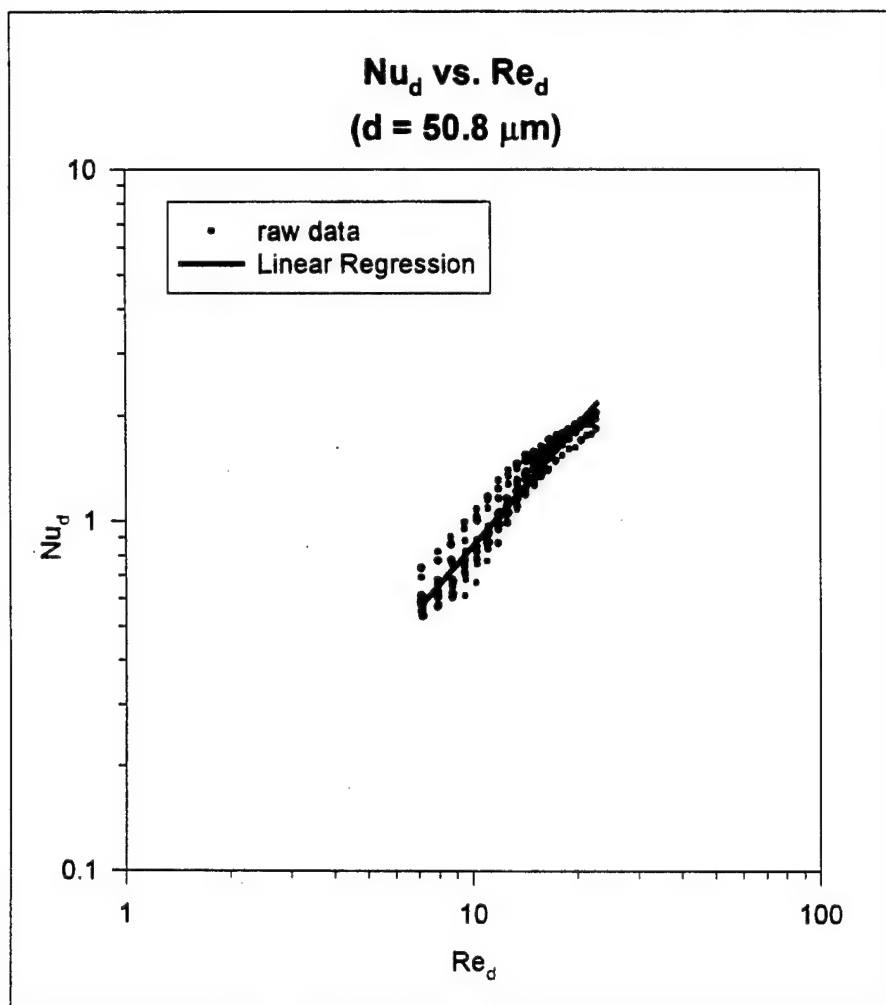


Figure 13. Curve Fit for Nusselt Number versus Reynolds Number ($d = 50 \mu m$)

APPENDIX A: CALIBRATION

One of the most basic measurements required in order to effectively develop heat transfer correlations is temperature. The two temperature measurements of concern here are of the ambient air within the acoustic chamber and the surface of the platinum wire. Thermoresistive elements, like a platinum wire, provide a nearly linear temperature-resistance relation. A preliminary step to the experimentation was to determine this relation through calibration. Ambient air temperature measurements were made with a calibrated T-type thermocouple.

The platinum wire was mounted in a calibration chamber cut from the same plexiglass tube stock used to make the acoustic chamber. All connectors, electric circuitry and equipment were identical to those used throughout experimentation. Once assembled, as in Figure 14, the calibration chamber, along with a T-type thermocouple, was immersed in a Rosemont Engineering Model 913A ethyl glycol bath. An associated Rosemont Engineering Model 920A commutating bridge provided the reference temperature as measured by a precision temperature probe. A four wire bridge electrical circuit was used to keep the lead resistance as low as possible relative to the platinum wire resistance [Ref. 20].

Numerous resistance versus temperature measurements were taken between 20°C and 50°C, the experimental temperature range of interest. Tables 1 and 2 show the measured wire resistance and associated precision temperature values for the two wire diameters. Column T1 gives the calculated temperature resulting from the linear regression equations. The error is simply the percent difference between the measured and calculated temperatures. Figures 15 and 16 show the statistical linear regression curves superimposed upon the raw data. The following two equations were used throughout the data reduction phase of the experiment for the 50.8 μm and 127 μm diameter wires cases, respectively

$$\text{Temperature (}^{\circ}\text{C)} = 59.8156 * \text{Resistance (}\Omega\text{)} - 224.2799 \quad (\text{A.1})$$

$$\text{Temperature (}^{\circ}\text{C)} = 436.112 * \text{Resistance (}\Omega\text{)} - 261.8139 \quad (\text{A.2})$$

Finally, a calibration data run was made for the 127 μm diameter wire using the actual electric circuit employed in the experiment. Assuming a very high forced convection heat transfer coefficient within the ethyl glycol bath, and applying a low power to the platinum wire, temperature differences between the wire surface and the fluid are assumed insignificant. Voltage measurements were made and wire resistances were calculated. Wire resistance was plotted against the precision temperature to generate an independent calibration curve as seen in Figure 16. The results from these two different calibration techniques were compared and showed a small change in slope and intercept of the calibration curve. The four wire bridge calibration results from both platinum wires were used in all experimental calculations in order to maintain some measure of consistency.

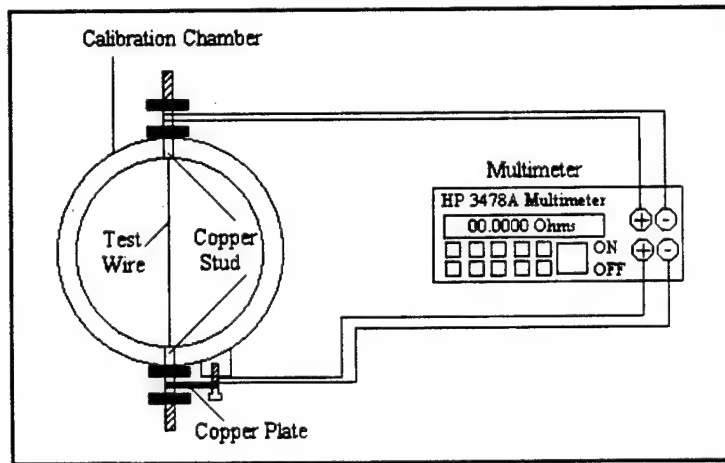


Figure 14. Calibration Chamber

Finally, calibration of the T-type thermocouple, using the same Rosemont Engineering calibration equipment, yielded results within 0.1°C of the reference temperature.

R(w) (W)	T (C)	T1 (C)	error (%)
4.0859	19.87	20.12	1.246
4.1081	21.25	21.45	0.926
4.1395	23.27	23.33	0.243
4.1752	25.56	25.46	0.384
4.2166	28.12	27.94	0.649
4.2465	29.94	29.73	0.716
4.2879	32.29	32.20	0.269
4.3241	34.44	34.37	0.207
4.3810	37.86	37.77	0.232
4.4443	41.37	41.56	0.454
4.5041	44.93	45.14	0.455
4.5631	48.54	48.66	0.256
4.6272	52.2	52.50	0.569
4.5486	47.98	47.80	0.382
4.5100	45.89	45.49	0.883

Table 1. Platinum Wire Calibration Data ($d = 50.8 \mu\text{m}$)

R(w) (Ω)	T (C)	T1 (C)	error (%)
0.6439	19.36	19.00	1.902
0.6493	21.50	21.35	0.685
0.6542	23.52	23.49	0.125
0.6592	25.55	25.67	0.472
0.6639	27.60	27.72	0.436
0.6691	29.93	29.99	0.196
0.6746	32.28	32.39	0.331
0.6796	34.39	34.57	0.514
0.6849	36.79	36.88	0.242
0.6900	38.94	39.10	0.418
0.6953	41.37	41.41	0.108
0.7006	43.61	43.73	0.266
0.7060	46.03	46.08	0.111
0.7116	48.61	48.52	0.178
0.7160	50.78	50.44	0.669
0.7040	45.29	45.21	0.179
0.6931	40.55	40.46	0.234
0.6823	35.72	35.75	0.071
0.6710	30.81	30.82	0.024
0.6614	26.58	26.63	0.190

Table 2. Platinum Wire Calibration Data ($d = 127 \mu\text{m}$)

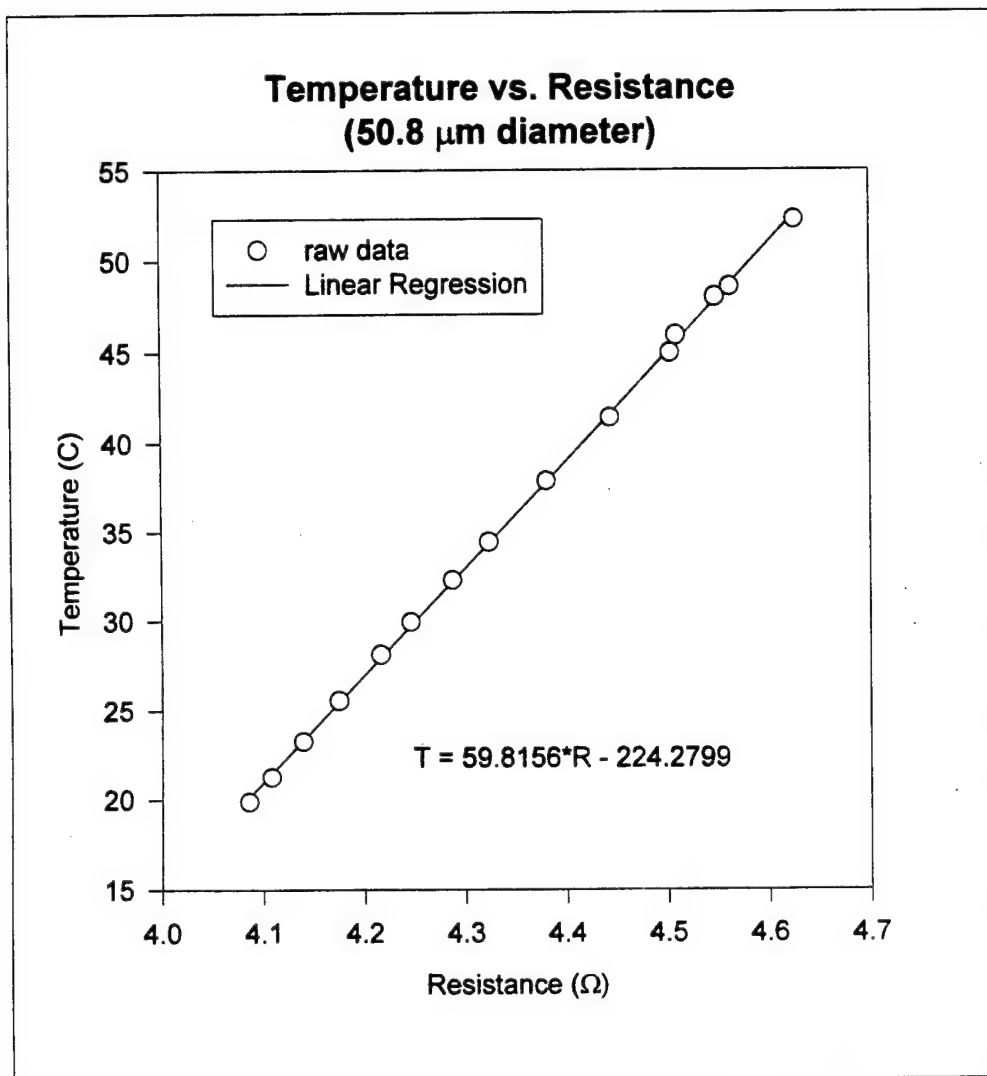


Figure 15. Platinum Wire Calibration Curve ($d = 50.8 \mu\text{m}$)

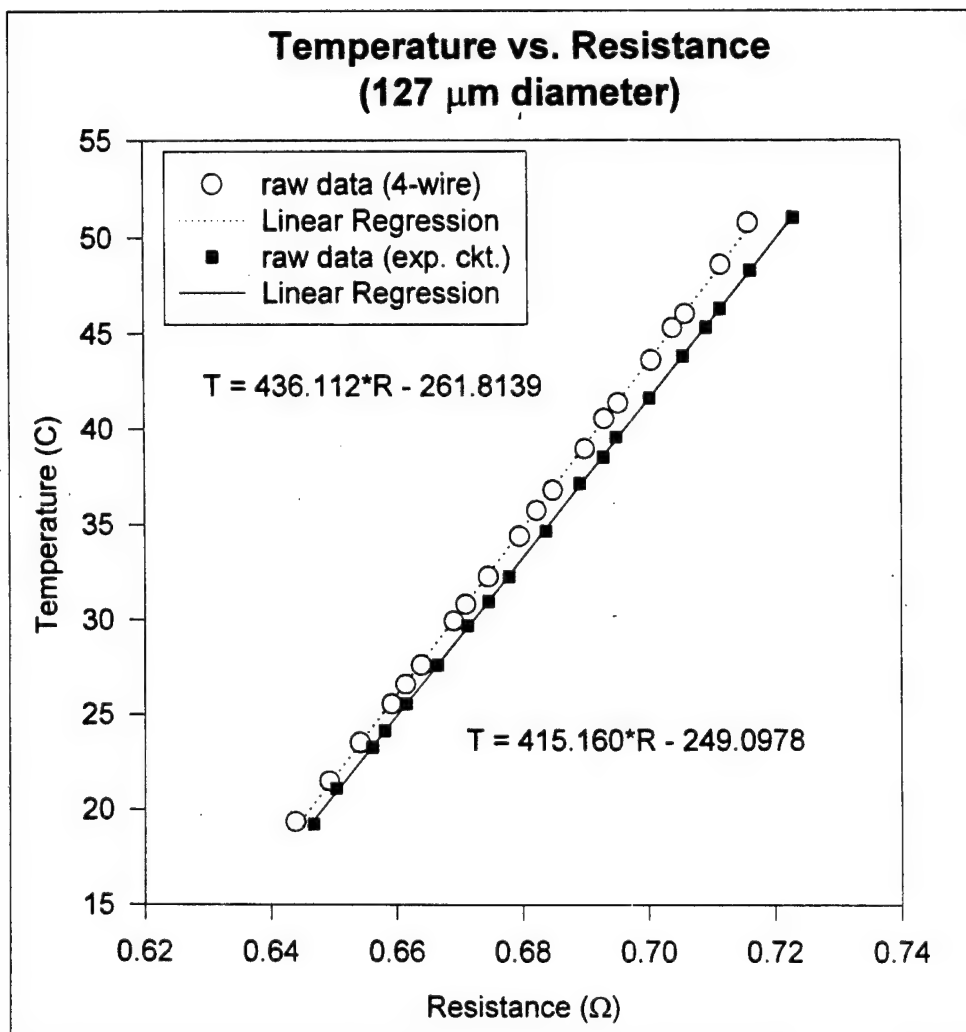


Figure 16. Platinum Wire Calibration Curve ($d = 127 \mu\text{m}$)

APPENDIX B: SAMPLE CALCULATION

The following sample calculations use data collected during an experimental run at $f \sim 1213$ Hz ($L = 64$ cm), pressure ratio $\sim 1.0\%$ and $\Delta T \sim 24^\circ\text{C}$ for the 50.8 μm diameter platinum wire. The measure values and the properties for air (at 300K) are

$$\begin{array}{ll} T_\infty = 25.3^\circ\text{C} & \gamma = \frac{c_p}{c_v} = 1.4 \\ f = 1218\text{Hz} & R = 287\frac{\text{m}^2}{\text{s}^2\text{K}} \\ V_w = 653.18\text{mV} & k = 0.026\frac{\text{W}}{\text{mK}} \\ V_{PR} = 14.0310\text{mV} & \nu = 159 \times 10^{-5}\frac{\text{m}^2}{\text{s}} \\ V_m = 0.533\text{V} & P_m = 101.35\text{kPa} \end{array}$$

where V_m is defined as the measured pressure transducer output voltage (RMS) and P_m is the mean ambient air pressure.

A. NUSSELT NUMBER

The Nusselt number equation is

$$Nu = \frac{hd}{k} \quad (\text{B.1})$$

where

$$h = \frac{\text{Power}}{A_s(T_s - T_\infty)} \quad (\text{B.2})$$

Substituting,

$$Nu = \frac{\text{Power}}{A_s(T_s - T_\infty)} \left(\frac{d}{k} \right) \quad (\text{B.3})$$

The wire surface temperature, T_s , is calculated using the equation found from the wire calibration as described in Appendix A.

$$T_s = 59.8156R_w - 224.2799 \quad (B.4)$$

and

$$R_w = \frac{V_w}{I} = V_w \left(\frac{R_{PR}}{V_{PR}} \right) = \frac{(653.18mV)(98.3m\Omega)}{(14.0310mV)} \quad (B.5)$$

$$R_w = 4576.12m\Omega$$

Therefore,

$$T_s = 49.4^\circ C$$

Power is found from

$$Power = \frac{V_w^2}{R_w} = \frac{(653.18mV)^2 \left(\frac{1V}{100mV} \right)^2}{(4576.12m\Omega) \left(\frac{1\Omega}{1000m\Omega} \right)} \quad (B.6)$$

$$Power = 0.093W$$

Substituting into the Nusselt number equation,

$$Nu = \frac{(0.093W)2(2.54 \times 10^{-5}m)}{(1.20 \times 10^{-5}m^2)(49.4 - 25.3)(K)(0.026 \frac{W}{mK})}$$

where

$$A_s = \pi dl = 2\pi(2.54 \times 10^{-5}m)(7.53 \times 10^{-2}m) \quad (B.7)$$

$$A_s = 1.20 \times 10^{-5}m^2$$

Finally,

$$Nu = 0.628$$

B. REYNOLDS NUMBER

The Reynolds number equation is

$$Re_d = \frac{U_0(2a)}{\nu} = 2\varepsilon\Lambda^2 \quad (B.8)$$

where

$$U_0 = \frac{c}{\gamma} \left(\frac{P_0}{P_m} \right) \quad (B.9)$$

$$c = \sqrt{\gamma R(T_\infty + 273.15)} \quad (B.10)$$

and

$$P_0 = \frac{V_m}{0.522} \quad (B.11)$$

Making the above substitutions into the Reynolds number equation, we get

$$Re_d = \frac{2aV_m}{0.522\nu P_m} \sqrt{\frac{R}{\gamma}} \sqrt{(T_\infty + 273.15)} \quad (B.12)$$

$$Re_d = \frac{2(2.54 \times 10^{-5} m)(0.533 V)}{(0.522 V/kPa)(1.59 \times 10^{-5} m^2/s)(101.35 kPa)} \sqrt{\frac{287 m^2/s^2 K}{1.4}} \sqrt{(25.3 + 273.15)(K)}$$

Finally,

$$Re_d = 7.96$$

APPENDIX C: UNCERTAINTY ANALYSIS

A. PLATINUM WIRE RESISTANCE

The equation for platinum wire resistance is

$$R_w = \frac{V_w}{I} \quad (C.1)$$

where

$$I = \frac{V_{PR}}{R_{PR}} \quad (C.2)$$

therefore,

$$R_w = V_w \left(\frac{R_{PR}}{V_{PR}} \right) \quad (C.3)$$

The uncertainty becomes

$$u_{R,wire} = \sqrt{\left(\frac{\partial R_w}{\partial V_w} u_{V,wire} \right)^2 + \left(\frac{\partial R_w}{\partial R_{PR}} u_{R,PR} \right)^2 + \left(\frac{\partial R_w}{\partial V_{PR}} u_{V,PR} \right)^2} \quad (C.4)$$

$$u_{R,wire} = \sqrt{\left(\frac{R_{PR}}{V_{PR}} u_{V,wire} \right)^2 + \left(\frac{V_w}{V_{PR}} u_{R,PR} \right)^2 + \left(\frac{-V_w R_{PR}}{V_{PR}^2} u_{V,PR} \right)^2} \quad (C.5)$$

$$\frac{u_{R,wire}}{R_w} = \sqrt{\left(\frac{u_{V,wire}}{V_w} \right)^2 + \left(\frac{u_{R,PR}}{R_{PR}} \right)^2 + \left(\frac{-u_{V,PR}}{V_{PR}} \right)^2} \quad (C.6)$$

$$R_{PR} = 0.0983 \Omega$$

Resistance, Precision Resistor

$$u_{R,PR} = 0.026\%$$

Uncertainty in Resistance, Precision Resistor

$$V_w = \text{measured quantity}$$

Voltage, Platinum Wire

$$u_{V,wire} = (\% \text{ reading} + \# \text{ counts})$$

Uncertainty in Voltage, Platinum Wire

V_{PR} = measure quantity

Voltage, Precision Resistor

$u_{V,PR}$ = (% reading + # counts)

Uncertainty in Voltage, Precision Resistor

The measured quantity uncertainty equations vary depending upon the Hewlett Packard HP 3478A digital multimeter range and resolution for each specific data sample. The following is an example of a data run for $f \sim 1213$ Hz ($L = 64$ cm), pressure ratio ~ 1.0 % and $\Delta T \sim 24^\circ\text{C}$ using the $50.8 \mu\text{m}$ diameter wire.

$$R_{PR} = 0.0983\Omega$$

$$V_w = 653.18mV$$

$$u_{R,PR} = 0.026\%$$

$$V_{PR} = 14.0310mV$$

$$u_{V,wire} = \left(\frac{0.006\%}{100} \right) 653.18mV + 1count \left(\frac{100 \times 10^{-6} V}{count} \right) \left(\frac{1000mV}{V} \right)$$

$$u_{V,wire} = 0.13919mV$$

$$u_{V,PR} = \left(\frac{0.035\%}{100} \right) 14.030mV + 40counts \left(\frac{100 \times 10^{-9} V}{count} \right) \left(\frac{1000mV}{V} \right)$$

$$u_{V,PR} = 0.00891mV$$

The platinum wire resistance uncertainty is

$$\frac{u_{R,wire}}{R_w} = \sqrt{\left(\frac{0.13919}{653.18} \right)^2 + \left(\frac{0.026}{100} \right)^2 + \left(\frac{-0.00891}{14.030} \right)^2}$$

$$\frac{u_{R,wire}}{R_w} = 7.186 \times 10^{-4} \quad \text{or} \quad 0.07186 \%$$

The calculated platinum wire resistance is

$$R_w = 4576.12 m\Omega$$

therefore,

$$u_{R,wire} = 3.29 m\Omega$$

B. NUSSELT NUMBER

The Nusselt number equation is

$$Nu = \frac{hd}{k} \quad (C.7)$$

where

$$h = \frac{Power}{A_s(T_s - T_\infty)} = \frac{\left(\frac{V_w^2}{R_w} \right)}{A_s(T_s - T_\infty)} \quad (C.8)$$

therefore,

$$Nu = \frac{\left(\frac{V_w^2}{R_w} \right)}{d l \pi (T_s - T_\infty)} \left(\frac{d}{k} \right) = \frac{V_w^2}{R_w l k \pi (T_s - T_\infty)} \quad (C.9)$$

From the calibration data the surface temperature of the wire can be written as

$$T_s = AR_w + B \quad (C.10)$$

where A and B represent the slope and y-intercept, respectively, from the linear regression model used for the wire calibration. Substituting, the Nusselt number becomes,

$$Nu = \frac{V_w^2}{l k \pi R_w (AR_w + B - T_\infty)} \quad (C.11)$$

and the uncertainty becomes,

$$u_{Nu} = \sqrt{\left(\frac{\partial Nu}{\partial V_w} u_{V,wire}\right)^2 + \left(\frac{\partial Nu}{\partial R_w} u_{R,wire}\right)^2 + \left(\frac{\partial Nu}{\partial T_\infty} u_{T_\infty}\right)^2 + \left(\frac{\partial Nu}{\partial l} u_l\right)^2} \quad (C.12)$$

$$\frac{u_{Nu}}{Nu} = \sqrt{\left(\frac{2}{V_w} u_{V,wire}\right)^2 + \left(\frac{(T_\infty - B - 2AR_w)}{R_w (AR_w + B - T_\infty)} u_{R,wire}\right)^2 + \left(\frac{u_{T_\infty}}{(AR_w + B - T_\infty)}\right)^2 + \left(\frac{-u_l}{l}\right)^2}$$

The following continues from the previous example where $f \sim 1213$ Hz, pressure ratio ~ 1.0 % and $\Delta T \sim 24^\circ\text{C}$.

$$A = 59.8156^\circ\text{C} / \Omega$$

$$V_w = 653.18\text{mV}$$

$$B = -224.2799^\circ\text{C}$$

$$u_{V,wire} = 0.13919\text{mV}$$

$$T_\infty = 25.3^\circ\text{C}$$

$$l = 0.0753\text{m}$$

$$u_{T_\infty} = 0.5^\circ\text{C}$$

$$u_l = 3\%$$

$$R_w = 4576.12\text{m}\Omega$$

$$u_{R,wire} = 3.29\text{m}\Omega$$

The Nusselt number uncertainty is

$$\frac{u_{Nu}}{Nu} = \sqrt{(4.26 \times 10^{-4})^2 + (-8.90 \times 10^{-3})^2 + (2.08 \times 10^{-2})^2 + (3.00 \times 10^{-2})^2}$$

$$\frac{u_{Nu}}{Nu} = 3.75 \times 10^{-2} \quad \text{or} \quad 3.75 \%$$

The calculated Nusselt number is

$$Nu = 0.628$$

therefore,

$$u_{Nu} = 0.0236$$

C. REYNOLDS NUMBER

The Reynolds number equation is

$$Re_d = \frac{(2a)U_0}{\nu} = 2 \frac{a}{\nu} \left(\frac{c}{\gamma} \frac{P_0}{P_m} \right) \quad (C.13)$$

where

$$c = \sqrt{\gamma R (T_\infty + 273.15)} \quad (C.14)$$

$$P_0 = \frac{\left(\frac{V_0}{\sqrt{2}} \right)}{0.522} \quad (C.15)$$

and

$$\frac{V_0}{\sqrt{2}} = \text{microphone output (RMS)}$$

Substituting,

$$Re_d = \sqrt{\frac{R}{\gamma}} \left(\frac{1}{\nu} \right) \left(\frac{1}{0.522 P_m} \right) (2a) \left(\frac{V_0}{\sqrt{2}} \right) \sqrt{(T_\infty + 273.15)} \quad (C.16)$$

Let

$$V_0' = \frac{V_0}{\sqrt{2}} \text{Volts}, \quad \text{and} \quad T_\infty' = (T_\infty + 273.15)K \quad (\text{C.17})$$

The uncertainty becomes

$$u_{\text{Re}} = \sqrt{\left(\frac{\partial \text{Re}_d}{\partial a} u_a\right)^2 + \left(\frac{\partial \text{Re}_d}{\partial V_0'} u_{V_0'}\right)^2 + \left(\frac{\partial \text{Re}_d}{\partial T_\infty'} u_{T_\infty'}\right)^2} \quad (\text{C.18})$$

$$\frac{u_{\text{Re}}}{\text{Re}_d} = \sqrt{\left(\frac{u_a}{a}\right)^2 + \left(\frac{u_{V_0'}}{V_0'}\right)^2 + \left(\frac{u_{T_\infty'}}{2T_\infty'}\right)^2} \quad (\text{C.19})$$

The following continues from the previous example where $f \sim 1213$ Hz, pressure ratio $\sim 1.0\%$ and $\Delta T \sim 24^\circ\text{C}$.

$$a = 2.54 \times 10^{-5} m$$

$$T_\infty' = (25.3 + 273.15)K$$

$$u_a = 5\%$$

$$u_{T_\infty'} = 0.5K$$

$$V_0' = 0.533V$$

$$u_{V_0'} = 2.3 \times 10^{-3}V + \left(\frac{0.06\%}{100}\right)0.533V + \left(\frac{0.03\%}{100}\right)1V$$

$$u_{V_0'} = 2.920 \times 10^{-3}V$$

The Reynolds number uncertainty is

$$\frac{u_{Re}}{Re_d} = \sqrt{\left(\frac{5}{100}\right)^2 + \left(\frac{2.920 \times 10^{-3}}{0.533}\right)^2 + \left(\frac{0.5}{2(298.55)}\right)^2}$$

$$\frac{u_{Re}}{Re_d} = 0.0503 \quad \text{or} \quad 5.03\%$$

The calculated Reynolds number is

$$Re_d = 7.96$$

therefore,

$$u_{Re} = 0.400$$

APPENDIX D: EXPERIMENTAL DATA

This appendix includes a representative sample of experimentally measured quantities, calculated parameters and uncertainties for the two platinum wire diameters used. Due to space constraints, some constants used in the spreadsheets for calculations have been omitted. The 50.8 μm diameter wire data is reported first followed by the 127 μm diameter wire.

Experiment Information	PR	Ta (C)	Vout (mV)	Wire	Wire	Rres (mΩ)	Is (C)	Ta (C)	Qr (mA)	Vout (V)	Freq (Hz)	mic V (μV)	Rn (Ω)	Tm (W/m²)	Corr	Fp (ReD)	N (μmD)	X	KC	NVA	Aa (2A/μA)	ReRe	GID	Ra	PR %	SPL (dB)	Power (W)
f = 1213 Hz L = 64 cm PR - 0.9 %	25.6	7.9023	348.92	4315.48	33.85	8.25	90	380	1218	0.478	41	281.2	41	7.1	0.55	0.001	11.50	36.1	0.31	0.20	8.32E-8	73.7	0.90	150	0.028		
	25.7	7.9025	348.92	4315.37	33.85	8.15	284.7	41	1218	0.478	41	284.7	41	7.1	0.56	0.001	11.50	36.1	0.31	0.20	8.21E-8	73.8	0.90	150	0.028		
	25.7	7.9028	348.94	4315.46	33.85	8.15	283.6	41	1218	0.478	41	283.6	41	7.1	0.55	0.001	11.50	36.1	0.31	0.20	8.25E-8	73.7	0.90	150	0.028		
	25.9	11.2789	511.58	4456.62	42.42	16.52	120	540	1218	0.474	40	295.8	40	7.1	0.58	0.001	11.41	35.9	0.31	0.20	1.72E-7	72.6	0.90	150	0.059		
PR - 1.1 %	26.0	11.2782	511.57	4458.41	42.40	16.40	140	660	1218	0.474	40	297.8	40	7.1	0.58	0.001	11.41	35.9	0.31	0.20	1.70E-7	72.6	0.90	150	0.059		
	26.1	11.2789	511.57	4458.53	42.41	16.31	120	540	1218	0.474	40	299.5	40	7.1	0.59	0.001	11.42	35.9	0.31	0.20	1.69E-7	72.6	0.90	150	0.059		
	26.2	13.4694	628.04	4583.45	49.88	23.68	140	660	1218	0.474	40	302.4	40	7.1	0.59	0.001	11.42	35.9	0.31	0.20	2.46E-7	72.6	0.90	150	0.086		
	26.3	13.4695	628.03	4583.34	49.88	23.58	140	660	1218	0.474	40	303.7	40	7.1	0.59	0.001	11.42	35.9	0.31	0.20	2.44E-7	72.7	0.90	150	0.086		
PR - 1.3 %	26.4	13.4690	628.04	4583.59	49.89	23.49	140	660	1218	0.474	41	304.8	41	7.1	0.60	0.001	11.42	35.9	0.31	0.20	2.43E-7	72.7	0.90	150	0.086		
	25.4	8.4543	370.76	4310.91	33.58	8.18	100	400	1218	0.586	62	324.4	62	8.8	0.63	0.001	14.10	44.3	0.31	0.20	2.44E-7	110.7	1.11	152	0.032		
	25.2	8.4541	370.77	4311.13	33.59	8.39	120	480	1218	0.586	62	316.2	62	8.8	0.62	0.001	14.09	44.3	0.31	0.20	3.76E-8	110.7	1.11	152	0.032		
	25.1	8.4542	370.76	4310.96	33.58	8.48	100	400	1218	0.586	62	312.8	62	8.8	0.61	0.001	14.09	44.3	0.31	0.20	3.81E-8	110.6	1.11	152	0.032		
PR - 1.5 %	25.4	12.0659	545.72	4445.94	41.66	16.26	130	580	1218	0.586	62	342.9	62	8.8	0.67	0.001	14.10	44.3	0.31	0.20	7.22E-8	110.8	1.11	152	0.067		
	25.5	12.0682	545.73	4445.91	41.65	16.15	130	580	1218	0.586	62	345.0	62	8.8	0.67	0.001	14.10	44.3	0.31	0.20	7.22E-8	110.8	1.11	152	0.067		
	25.6	12.0682	545.73	4445.91	41.65	16.05	130	580	1218	0.586	62	347.2	62	8.8	0.68	0.001	14.10	44.3	0.31	0.20	7.17E-8	110.4	1.11	152	0.099		
	25.4	14.4893	674.16	4573.71	49.30	23.90	160	710	1218	0.585	61	346.0	61	8.7	0.68	0.001	14.07	44.2	0.31	0.20	1.08E-7	110.4	1.11	152	0.099		
PR - 1.3 %	25.5	14.4892	674.16	4573.75	49.30	23.80	160	710	1218	0.585	62	347.4	62	8.7	0.68	0.001	14.08	44.2	0.31	0.20	1.07E-7	110.4	1.11	152	0.099		
	25.6	14.4893	674.16	4573.71	49.30	23.70	160	710	1218	0.585	62	348.9	62	8.7	0.68	0.001	14.08	44.2	0.31	0.20	1.07E-7	110.4	1.11	152	0.099		
	25.8	9.4928	417.35	4321.75	34.23	8.43	100	450	1218	0.688	85	397.9	85	10.3	0.78	0.001	16.59	52.1	0.31	0.20	1.97E-8	153.3	1.30	153	0.040		
	25.9	9.4928	417.35	4321.63	34.22	8.32	120	540	1218	0.688	85	403.0	85	10.3	0.79	0.001	16.59	52.1	0.31	0.20	1.94E-8	153.3	1.30	153	0.040		
PR - 1.5 %	25.9	9.4926	417.35	4321.84	34.23	8.33	120	540	1218	0.688	85	402.4	85	10.3	0.79	0.001	16.59	52.1	0.31	0.20	1.94E-8	153.3	1.30	153	0.040		
	25.8	13.1644	595.71	4448.23	41.79	15.99	140	630	1218	0.688	85	415.1	85	10.3	0.81	0.001	16.56	52.0	0.31	0.20	1.95E-8	153.3	1.30	153	0.080		
	25.9	13.1645	595.70	4448.12	41.79	15.89	140	630	1218	0.688	85	417.9	85	10.3	0.82	0.001	16.56	52.0	0.31	0.20	3.72E-8	152.9	1.30	153	0.080		
	26.0	13.1640	595.70	4448.29	41.80	15.80	140	630	1218	0.688	85	420.2	85	10.3	0.82	0.001	16.57	52.0	0.31	0.20	3.70E-8	152.9	1.30	153	0.080		
PR - 1.3 %	26.1	15.9349	743.51	4586.60	50.07	23.87	170	780	1218	0.687	85	417.0	85	10.3	0.82	0.001	16.56	52.0	0.31	0.20	3.72E-8	152.9	1.30	153	0.080		
	26.0	15.9349	743.51	4586.60	50.07	23.87	170	780	1218	0.687	85	417.0	85	10.3	0.81	0.001	16.54	52.0	0.31	0.20	5.66E-8	152.5	1.30	153	0.121		
	26.1	15.9345	743.35	4585.73	50.02	23.92	170	780	1218	0.687	85	419.2	85	10.3	0.82	0.001	16.55	52.0	0.31	0.20	5.63E-8	152.5	1.30	153	0.121		
	26.2	15.9349	743.51	4586.60	50.07	23.87	170	780	1218	0.687	85	420.2	85	10.3	0.82	0.001	16.55	52.0	0.31	0.20	5.61E-8	152.6	1.30	153	0.121		
PR - 1.5 %	26.4	10.5031	462.89	4329.78	34.71	8.31	110	490	1220	0.798	115	495.6	115	11.9	0.97	0.001	19.20	60.3	0.31	0.20	1.07E-8	205.5	1.51	155	0.049		
	26.5	10.5085	462.88	4329.93	34.72	8.22	120	580	1220	0.798	115	501.7	115	11.9	0.98	0.001	19.20	60.3	0.31	0.20	1.06E-8	205.6	1.51	155	0.049		
	26.5	10.5089	462.88	4329.77	34.71	8.21	120	580	1220	0.798	115	501.7	115	11.9	0.98	0.001	19.20	60.3	0.31	0.20	1.06E-8	205.6	1.51	155	0.049		
	26.5	10.5089	462.88	4329.77	34.71	8.21	120	580	1220	0.798	115	499.5	115	11.9	0.98	0.001	19.20	60.3	0.31	0.20	1.06E-8	205.6	1.51	155	0.049		
PR - 1.3 %	26.5	14.646	663.61	4453.97	42.14	15.64	180	700	1220	0.798	115	526.2	115	11.9	1.03	0.001	19.20	60.3	0.31	0.20	2.02E-8	205.6	1.51	155	0.099		
	26.6	14.642	663.62	4455.26	42.11	15.61	180	700	1220	0.798	115	526.8	115	11.9	1.03	0.001	19.20	60.3	0.31	0.20	2.01E-8	205.7	1.51	155	0.099		
	26.6	14.645	663.62	4454.34	42.16	15.56	180	700	1220	0.798	115	527.2	115	11.9	1.03	0.001	19.20	60.3	0.31	0.20	2.01E-8	205.7	1.51	155	0.099		
	26.6	14.645	663.62	4454.34	42.16	15.56	180	700	1220	0.798	115	527.2	115	11.9	1.03	0.001	19.20	60.3	0.31	0.20	2.01E-8	205.7	1.51	155	0.099		
PR - 1.3 %	26.6	18.34	859.28	4605.63	51.21	24.61	180	900	1220	0.797	114	542.1	114	11.9	1.06	0.001	19.18	60.3	0.31	0.20	3.19E-8	205.2	1.51	155	0.160		
	26.7	18.33	859.29	4608.19	51.36	24.66	180	900	1220	0.797	114	540.6	114	11.9	1.06	0.001	19.18	60.3	0.31	0.20	3.19E-8	205.2	1.51	155	0.160		
	26.8	18.33	859.30	4608.25	51.37	24.57	180	900	1220	0.797	114	542.8	114	11.9	1.06	0.001	19.19	60.3	0.31	0.20	3.18E-8	205.3	1.51	155	0.160		
	26.8	18.33	859.30	4608.25	51.37	24.57	180	900	1220	0.797	114	541.8	114	11.9	1.06	0.001	19.18	60.3	0.31	0.20	3.19E-8	205.2	1.51	155	0.160		

Element Information	Unit	Vol	Res	Cap	Ind	R	L	C	S	T	F	P	Q	V	I	W	S	D	T	F	P	Q	V	I	W	S	D	T	F	P	Q	V	I	W	S	D	T	F	P	Q	V	I	W	S	D	T	F	P	Q	V	I	W	S	D	T	F	P	Q	V	I	W	S	D	T	F	P	Q	V	I	W	S	D	T	F	P	Q	V	I	W	S	D	T	F	P	Q	V	I	W	S	D	T	F	P	Q	V	I	W	S	D	T	F	P	Q	V	I	W	S	D	T	F	P	Q	V	I	W	S	D	T	F	P	Q	V	I	W	S	D	T	F	P	Q	V	I	W	S	D	T	F	P	Q	V	I	W	S	D	T	F	P	Q	V	I	W	S	D	T	F	P	Q	V	I	W	S	D	T	F	P	Q	V	I	W	S	D	T	F	P	Q	V	I	W	S	D	T	F	P	Q	V	I	W	S	D	T	F	P	Q	V	I	W	S	D	T	F	P	Q	V	I	W	S	D	T	F	P	Q	V	I	W	S	D	T	F	P	Q	V	I	W	S	D	T	F	P	Q	V	I	W	S	D	T	F	P	Q	V	I	W	S	D	T	F	P	Q	V	I	W	S	D	T	F	P	Q	V	I	W	S	D	T	F	P	Q	V	I	W	S	D	T	F	P	Q	V	I	W	S	D	T	F	P	Q	V	I	W	S	D	T	F	P	Q	V	I	W	S	D	T	F	P	Q	V	I	W	S	D	T	F	P	Q	V	I	W	S	D	T	F	P	Q	V	I	W	S	D	T	F	P	Q	V	I	W	S	D	T	F	P	Q	V	I	W	S	D	T	F	P	Q	V	I	W	S	D	T	F	P	Q	V	I	W	S	D	T	F	P	Q	V	I	W	S	D	T	F	P	Q	V	I	W	S	D	T	F	P	Q	V	I	W	S	D	T	F	P	Q	V	I	W	S	D	T	F	P	Q	V	I	W	S	D	T	F	P	Q	V	I	W	S	D	T	F	P	Q	V	I	W	S	D	T	F	P	Q	V	I	W	S	D	T	F	P	Q	V	I	W	S	D	T	F	P	Q	V	I	W	S	D	T	F	P	Q	V	I	W	S	D	T	F	P	Q	V	I	W	S	D	T	F	P	Q	V	I	W	S	D	T	F	P	Q	V	I	W	S	D	T	F	P	Q	V	I	W	S	D	T	F	P	Q	V	I	W	S	D	T	F	P	Q	V	I	W	S	D	T	F	P	Q	V	I	W	S	D	T	F	P	Q	V	I	W	S	D	T	F	P	Q	V	I	W	S	D	T	F	P	Q	V	I	W	S	D	T	F	P	Q	V	I	W	S	D	T	F	P	Q	V	I	W	S	D	T	F	P	Q	V	I	W	S	D	T	F	P	Q	V	I	W	S	D	T	F	P	Q	V	I	W	S	D	T	F	P	Q	V	I	W	S	D	T	F	P	Q	V	I	W	S	D	T	F	P	Q	V	I	W	S	D	T	F	P	Q	V	I	W	S	D	T	F	P	Q	V	I	W	S	D	T	F	P	Q	V	I	W	S	D	T	F	P	Q	V	I	W	S	D	T	F	P	Q	V	I	W	S	D	T	F	P	Q	V	I	W	S	D	T	F	P	Q	V	I	W	S	D	T	F	P	Q	V	I	W	S	D	T	F	P	Q	V	I	W	S	D	T	F	P	Q	V	I	W	S	D	T	F	P	Q	V	I	W	S	D	T	F	P	Q	V	I	W	S	D	T	F	P	Q	V	I	W	S	D	T	F	P	Q	V	I	W	S	D	T	F	P	Q	V	I	W	S	D	T	F	P	Q	V	I	W	S	D	T	F	P	Q	V	I	W	S	D	T	F	P	Q	V	I	W	S	D	T	F	P	Q	V	I	W	S	D	T	F	P	Q	V	I	W	S	D	T	F	P	Q	V	I	W	S	D	T	F	P	Q	V	I	W	S	D	T	F	P	Q	V	I	W	S	D	T	F	P	Q	V	I	W	S	D	T	F	P	Q	V	I	W	S	D	T	F	P	Q	V	I	W	S	D	T	F	P	Q	V	I	W	S	D	T	F	P	Q	V	I	W	S	D	T	F	P	Q	V	I	W	S	D	T	F	P	Q	V	I	W	S	D	T	F	P	Q	V	I	W	S	D	T	F	P	Q	V	I	W	S	D	T	F	P	Q	V	I	W	S	D	T	F	P	Q	V	I	W	S	D	T	F	P	Q	V	I	W	S	D	T	F	P	Q	V	I	W	S	D	T	F	P	Q	V	I	W	S	D	T	F	P	Q	V	I	W	S	D	T	F	P	Q	V	I	W	S	D	T	F	P	Q	V	I	W	S	D	T	F	P	Q	V	I	W	S	D	T	F	P	Q	V	I	W	S	D	T	F	P	Q	V	I	W	S	D	T	F	P	Q	V	I	W	S	D	T	F	P	Q	V	I	W	S	D	T	F	P	Q	V	I	W	S	D	T	F	P	Q	V	I	W	S	D	T	F	P	Q	V	I	W	S	D	T	F	P	Q	V	I	W	S	D	T	F	P	Q	V	I	W	S	D	T	F	P	Q	V	I	W	S	D	T	F	P	Q	V	I	W	S	D	T	F	P	Q	V	I	W	S	D	T	F	P	Q	V	I	W	S	D	T	F	P	Q	V	I	W	S	D	T	F	P	Q	V	I	W	S	D	T	F	P	Q	V	I	W	S	D	T	F	P	Q	V	I	W	S	D	T	F	P	Q	V	I	W	S	D	T	F	P	Q	V	I	W	S	D	T	F	P	Q	V	I	W	S	D	T	F	P	Q	V	I	W	S	D	T	F	P	Q	V	I	W	S	D	T	F	P	Q	V	I	W	S	D	T	F	P	Q	V	I	W	S	D	T	F	P	Q	V	I	W	S	D	T	F	P	Q	V	I	W	S	D	T	F	P	Q	V	I	W	S	D	T	F	P	Q	V	I	W	S	D	T	F	P	Q	V	I	W	S	D	T	F	P	Q	V	I	W	S	D	T	F	P	Q	V	I	W	S	D	T	F	P	Q	V	I	W	S	D	T	F	P	Q	V	I	W	S	D	T
---------------------	------	-----	-----	-----	-----	---	---	---	---	---	---	---	---	---	---	---	---	---	---	---	---	---	---	---	---	---	---	---	---	---	---	---	---	---	---	---	---	---	---	---	---	---	---	---	---	---	---	---	---	---	---	---	---	---	---	---	---	---	---	---	---	---	---	---	---	---	---	---	---	---	---	---	---	---	---	---	---	---	---	---	---	---	---	---	---	---	---	---	---	---	---	---	---	---	---	---	---	---	---	---	---	---	---	---	---	---	---	---	---	---	---	---	---	---	---	---	---	---	---	---	---	---	---	---	---	---	---	---	---	---	---	---	---	---	---	---	---	---	---	---	---	---	---	---	---	---	---	---	---	---	---	---	---	---	---	---	---	---	---	---	---	---	---	---	---	---	---	---	---	---	---	---	---	---	---	---	---	---	---	---	---	---	---	---	---	---	---	---	---	---	---	---	---	---	---	---	---	---	---	---	---	---	---	---	---	---	---	---	---	---	---	---	---	---	---	---	---	---	---	---	---	---	---	---	---	---	---	---	---	---	---	---	---	---	---	---	---	---	---	---	---	---	---	---	---	---	---	---	---	---	---	---	---	---	---	---	---	---	---	---	---	---	---	---	---	---	---	---	---	---	---	---	---	---	---	---	---	---	---	---	---	---	---	---	---	---	---	---	---	---	---	---	---	---	---	---	---	---	---	---	---	---	---	---	---	---	---	---	---	---	---	---	---	---	---	---	---	---	---	---	---	---	---	---	---	---	---	---	---	---	---	---	---	---	---	---	---	---	---	---	---	---	---	---	---	---	---	---	---	---	---	---	---	---	---	---	---	---	---	---	---	---	---	---	---	---	---	---	---	---	---	---	---	---	---	---	---	---	---	---	---	---	---	---	---	---	---	---	---	---	---	---	---	---	---	---	---	---	---	---	---	---	---	---	---	---	---	---	---	---	---	---	---	---	---	---	---	---	---	---	---	---	---	---	---	---	---	---	---	---	---	---	---	---	---	---	---	---	---	---	---	---	---	---	---	---	---	---	---	---	---	---	---	---	---	---	---	---	---	---	---	---	---	---	---	---	---	---	---	---	---	---	---	---	---	---	---	---	---	---	---	---	---	---	---	---	---	---	---	---	---	---	---	---	---	---	---	---	---	---	---	---	---	---	---	---	---	---	---	---	---	---	---	---	---	---	---	---	---	---	---	---	---	---	---	---	---	---	---	---	---	---	---	---	---	---	---	---	---	---	---	---	---	---	---	---	---	---	---	---	---	---	---	---	---	---	---	---	---	---	---	---	---	---	---	---	---	---	---	---	---	---	---	---	---	---	---	---	---	---	---	---	---	---	---	---	---	---	---	---	---	---	---	---	---	---	---	---	---	---	---	---	---	---	---	---	---	---	---	---	---	---	---	---	---	---	---	---	---	---	---	---	---	---	---	---	---	---	---	---	---	---	---	---	---	---	---	---	---	---	---	---	---	---	---	---	---	---	---	---	---	---	---	---	---	---	---	---	---	---	---	---	---	---	---	---	---	---	---	---	---	---	---	---	---	---	---	---	---	---	---	---	---	---	---	---	---	---	---	---	---	---	---	---	---	---	---	---	---	---	---	---	---	---	---	---	---	---	---	---	---	---	---	---	---	---	---	---	---	---	---	---	---	---	---	---	---	---	---	---	---	---	---	---	---	---	---	---	---	---	---	---	---	---	---	---	---	---	---	---	---	---	---	---	---	---	---	---	---	---	---	---	---	---	---	---	---	---	---	---	---	---	---	---	---	---	---	---	---	---	---	---	---	---	---	---	---	---	---	---	---	---	---	---	---	---	---	---	---	---	---	---	---	---	---	---	---	---	---	---	---	---	---	---	---	---	---	---	---	---	---	---	---	---	---	---	---	---	---	---	---	---	---	---	---	---	---	---	---	---	---	---	---	---	---	---	---	---	---	---	---	---	---	---	---	---	---	---	---	---	---	---	---	---	---	---	---	---	---	---	---	---	---	---	---	---	---	---	---	---	---	---	---	---	---	---	---	---	---	---	---	---	---	---	---	---	---	---	---	---	---	---	---	---	---	---	---	---	---	---	---	---	---	---	---	---	---	---	---	---	---	---	---	---	---	---	---	---	---	---	---	---	---	---	---	---	---	---	---	---	---	---	---	---	---	---	---	---	---	---	---	---	---	---	---	---	---	---	---	---	---	---	---	---	---	---	---	---	---	---	---	---	---	---	---	---	---	---	---	---	---	---	---	---	---	---	---	---	---	---	---	---	---	---	---	---	---	---	---	---	---	---	---	---	---	---	---	---	---	---	---	---	---	---	---	---	---	---	---	---	---	---	---	---	---	---	---	---	---	---	---	---	---	---	---	---	---	---	---	---	---	---	---	---	---	---	---	---	---	---	---	---	---	---	---	---	---	---	---	---	---	---	---	---	---	---	---	---	---	---	---	---	---	---	---	---	---	---	---	---	---	---	---	---	---	---	---	---	---	---	---	---	---	---	---	---	---	---	---	---	---	---	---	---	---	---	---	---	---	---	---	---	---	---	---	---	---	---	---	---	---	---	---	---	---	---	---	---	---	---	---	---	---	---	---	---	---	---	---	---	---	---	---	---	---	---	---	---	---	---	---	---	---	---	---	---	---	---	---	---	---	---	---	---	---	---	---	---	---	---	---	---	---	---	---	---	---	---	---	---	---	---	---	---	---	---	---	---	---	---	---	---	---	---	---	---	---	---	---	---	---	---	---	---	---	---	---	---	---	---	---	---	---	---	---	---	---	---	---	---	---	---	---	---	---	---	---	---	---	---	---	---	---	---	---	---	---	---	---	---	---	---	---	---	---	---	---	---	---	---	---	---	---	---	---	---	---	---	---	---	---	---	---	---	---	---	---	---	---	---	---	---	---	---	---	---	---	---	---	---	---	---	---	---	---	---	---	---

Experiment Information	T _a (°C)	PR (V)	Wire Vol _t (mV)	Wire Res (mΩ)	T _s (°C)	I _s (A)	V _{be} (V)	Q _{sc} (mA)	V _{ce} (V)	f _{osc} (Hz)	R _s (Ω)	h _{FE}	Cor		β _{DC}	β _{AC}	K _{RC} (K)	ΔV _A (V)	β _{RC}	G _{RD} (K)	R _{FR} (K)	R _{FR} (K)	R _{FR} (K)	PR %	SPL (dB)	P _{out} (W)
													P _{DC} (W)	P _{RF} (W)												
PR - 1.9 %	22.4	10.9215	472.59	4253.59	30.15	7.75	120	500	1212	0.905	146	5637	146	13.5	1.10	0.001	21.77	68.4	0.31	0.20	6.22E-9	263.4	1.71	156	0.053	
	22.4	10.9213	472.59	4253.67	30.16	7.76	1212	0.905	146	1212	0.905	146	563.5	146	13.5	1.10	0.001	21.77	68.4	0.31	0.20	6.23E-9	263.4	1.71	156	0.053
	22.4	10.9214	472.59	4253.63	30.15	7.75	1212	0.905	146	1212	0.905	146	563.5	146	13.5	1.10	0.001	21.77	68.4	0.31	0.20	6.22E-9	263.4	1.71	156	0.053
	22.5	18.29	728.35	4395.14	38.62	16.12	170	770	1212	0.903	146	623.1	146	13.4	1.22	0.001	21.72	68.2	0.31	0.20	1.30E-8	262.3	1.71	156	0.121	
	22.3	16.31	728.33	4389.63	38.29	15.99	1212	0.903	146	1212	0.903	146	624.8	146	13.4	1.22	0.001	21.72	68.2	0.31	0.20	1.30E-8	262.3	1.71	156	0.121
PR - 1.7 %	22.2	16.31	728.35	4389.75	38.30	16.10	1212	0.903	146	1212	0.903	146	625.6	146	13.4	1.22	0.001	21.72	68.2	0.31	0.20	1.30E-8	262.2	1.71	156	0.121
	22.6	20.23	933.83	4537.59	47.14	24.54	210	980	1212	0.903	146	651.7	146	13.4	1.27	0.001	21.73	68.3	0.31	0.20	1.98E-8	262.4	1.71	156	0.192	
	22.5	20.25	933.83	4533.11	46.87	24.37	1212	0.903	146	1212	0.903	146	656.8	146	13.4	1.28	0.001	21.72	68.2	0.31	0.20	1.97E-8	262.3	1.71	156	0.192
	22.4	20.25	933.89	4533.40	46.89	24.49	1212	0.903	146	1212	0.903	146	653.7	146	13.4	1.28	0.001	21.72	68.2	0.31	0.20	1.98E-8	262.3	1.71	156	0.192
	22.8	17.53	785.26	4403.37	39.11	16.31	1213	1.010	182	1213	1.010	182	714.5	182	15.0	1.40	0.001	24.29	76.3	0.31	0.20	8.42E-9	328.1	1.91	157	0.140
PR - 1.9 %	22.7	12.091	524.77	4266.39	30.92	8.22	130	560	1213	1.013	183	646.2	183	15.1	1.28	0.001	24.36	76.5	0.31	0.20	4.20E-9	329.9	1.91	157	0.065	
	22.6	12.091	524.76	4266.31	30.91	8.31	1213	1.013	183	1213	1.013	183	646.2	183	15.1	1.26	0.001	24.35	76.5	0.31	0.20	4.25E-9	329.8	1.91	157	0.065
	22.5	12.091	524.76	4266.31	30.91	8.41	1213	1.013	183	1213	1.013	183	638.5	183	15.1	1.25	0.001	24.35	76.5	0.31	0.20	4.31E-9	329.7	1.91	157	0.065
	22.8	17.54	785.25	4400.80	38.96	16.16	190	830	1213	1.010	182	721.6	182	15.0	1.41	0.001	24.29	76.3	0.31	0.20	8.34E-9	328.1	1.91	157	0.140	
	22.8	17.54	785.23	4400.69	38.95	16.15	1213	1.010	182	1213	1.010	182	714.5</													

Experiment Information	PR		Wire		T-T ₀	D ₀	V ₀	F ₀	m _{KY}	R ₀	h	Cont		N ₀ (D)	L _X	K _C	ΔV _A	β	Grid		R _S	PR %	SPL (dB)	Power (W)	
	V ₀ (mV)	T _a (°C)	V ₀ (mV)	R ₀ (Ω)								R _t	R _b						R _S	R _b					R _S
f = 1213 Hz L = 64 cm PR ~ 2.5 %	23.7	13.61	592.79	4281.50	31.82	8.12	630	1215	1330	317	841.0	317	19.8	1.64	0.001	31.98	100.5	0.31	0.20	1.38E-9	569.2	2.51	159	0.082	
	23.6	13.61	592.79	4281.50	31.82	8.22		1215	1330	317	830.8	317	19.8	1.62	0.001	31.98	100.5	0.31	0.20	1.41E-9	569.0	2.51	159	0.082	
	23.5	13.61	592.79	4281.50	31.82	8.32		1215	1330	317	830.9	317	19.8	1.62	0.001	31.98	100.5	0.31	0.20	1.41E-9	569.0	2.51	159	0.082	
PR ~ 2.7 %	23.7	18.57	877.68	4408.58	39.42	15.72	210	1215	1331	317	924.8	317	19.8	1.81	0.001	32.01	100.6	0.31	0.20	2.68E-9	570.1	2.52	159	0.175	
	23.6	19.56	877.68	4410.84	39.56	15.96		1215	1331	317	910.7	317	19.8	1.78	0.001	32.00	100.5	0.31	0.20	2.72E-9	569.9	2.52	159	0.175	
	23.6	19.57	877.69	4408.63	39.43	15.93		1215	1331	317	918.8	317	19.8	1.80	0.001	32.00	100.5	0.31	0.20	2.70E-9	569.9	2.52	159	0.175	
PR ~ 2.7 %	23.7	24.32	1125.50	4549.61	47.86	24.16	250	1170	1215	1331	959.2	317	19.8	1.87	0.001	32.01	100.6	0.31	0.20	4.11E-9	570.1	2.52	159	0.278	
	23.8	24.32	1125.61	4549.65	47.86	24.06		1215	1331	317	963.1	317	19.8	1.88	0.001	32.01	100.6	0.31	0.20	4.09E-9	570.3	2.52	159	0.278	
	23.8	24.32	1125.60	4549.61	47.86	24.06		1215	1331	317	963.2	317	19.8	1.88	0.001	32.01	100.6	0.31	0.20	4.09E-9	570.3	2.52	159	0.278	
											961.9	317	19.8	1.88	0.001	32.01	100.6	0.31	0.20	4.10E-9	570.2				
PR ~ 2.7 %	23.3	14.17	616.59	4277.40	31.58	8.28	150	1215	1431	366	893.7	366	21.3	1.75	0.001	34.39	108.0	0.31	0.20	1.06E-9	657.9	2.70	160	0.089	
	23.4	14.17	616.59	4277.40	31.58	8.18		1215	1431	366	904.7	366	21.3	1.77	0.001	34.39	108.1	0.31	0.20	1.05E-9	658.2	2.70	160	0.089	
	23.4	14.17	616.59	4277.40	31.58	8.18		1215	1431	366	904.7	366	21.3	1.77	0.001	34.39	108.1	0.31	0.20	1.05E-9	658.2	2.70	160	0.089	
											901.0	366	21.3	1.76	0.001	34.39	108.0	0.31	0.20	1.05E-9	658.1				
PR ~ 2.9 %	23.4	20.21	905.93	4406.38	39.29	15.89	210	1215	1433	367	975.4	367	21.3	1.91	0.001	34.44	108.2	0.31	0.20	2.02E-9	660.0	2.71	160	0.186	
	23.3	20.20	905.95	4408.66	39.43	16.13		1215	1433	367	960.6	367	21.3	1.88	0.001	34.44	108.2	0.31	0.20	2.05E-9	659.8	2.71	160	0.186	
	23.2	20.21	905.93	4406.38	39.29	16.09		1215	1433	367	963.2	367	21.3	1.88	0.001	34.43	108.2	0.31	0.20	2.05E-9	659.5	2.71	160	0.186	
											966.4	367	21.3	1.89	0.001	34.44	108.2	0.31	0.20	2.04E-9	659.7				
PR ~ 2.9 %	23.4	24.99	1154.30	4540.52	47.31	23.91	280	1200	1215	1435	368	1021.1	368	21.4	2.00	0.001	34.49	108.4	0.31	0.20	3.02E-9	661.9	2.71	160	0.293
	23.3	24.98	1154.32	4542.42	47.43	24.13		1215	1435	368	1011.7	368	21.4	1.98	0.001	34.48	108.3	0.31	0.20	3.05E-9	661.6	2.71	160	0.293	
	23.2	24.99	1154.31	4540.56	47.32	24.12		1215	1435	368	1012.5	368	21.4	1.98	0.001	34.48	108.3	0.31	0.20	3.06E-9	661.3	2.71	160	0.293	
											1015.1	368	21.4	1.98	0.001	34.48	108.3	0.31	0.20	3.04E-9	661.6				
PR ~ 2.9 %	23.8	14.34	624.89	4283.59	31.95	8.15	150	1216	1526	417	931.2	417	22.7	1.82	0.001	36.67	115.2	0.31	0.20	8.03E-10	748.5	2.88	160	0.091	
	23.9	14.34	624.88	4283.52	31.94	8.04		1216	1526	417	943.3	417	22.7	1.84	0.001	36.68	115.2	0.31	0.20	7.92E-10	748.8	2.88	160	0.091	
	23.9	14.34	624.88	4283.52	31.94	8.04		1216	1526	417	943.3	417	22.7	1.84	0.001	36.68	115.2	0.31	0.20	7.92E-10	748.8	2.88	160	0.091	
											939.3	417	22.7	1.84	0.001	36.68	115.2	0.31	0.20	7.96E-10	748.7				
PR ~ 2.9 %	23.8	20.43	917.42	4414.21	39.76	15.96	220	1216	1527	417	994.2	417	22.8	1.94	0.001	36.70	115.3	0.31	0.20	1.57E-9	749.5	2.89	160	0.191	
	23.9	20.43	917.43	4414.26	39.76	15.86		1216	1527	418	1000.3	417	22.8	1.95	0.001	36.70	115.3	0.31	0.20	1.56E-9	749.8	2.89	160	0.191	
	23.9	20.44	917.42	4412.05	39.63	15.73		1216	1527	418	1009.2	417	22.8	1.97	0.001	36.70	115.3	0.31	0.20	1.55E-9	749.8	2.89	160	0.191	
											1001.2	417	22.8	1.96	0.001	36.70	115.3	0.31	0.20	1.56E-9	749.7				
PR ~ 2.9 %	23.9	25.26	1169.03	4549.31	47.84	23.94	280	1220	1216	1528	418	1044.2	418	22.8	2.04	0.001	36.73	115.4	0.31	0.20	2.35E-9	750.8	2.89	160	0.300
	23.9	25.27	1169.03	4547.51	47.73	23.83		1216	1528	418	1049.3	418	22.8	2.05	0.001	36.73	115.4	0.31	0.20	2.34E-9	750.8	2.89	160	0.301	
	23.9	25.27	1169.03	4547.51	47.73	23.83		1216	1528	418	1044.2	418	22.8	2.04	0.001	36.73	115.4	0.31	0.20	2.35E-9	750.8	2.89	160	0.300	
	23.9	25.26	1169.03	4549.31	47.84	23.94		1216	1528	418	1045.9	418	22.8	2.04	0.001	36.73	115.4	0.31	0.20	2.34E-9	750.8	2.89	160	0.300	

Experiment Information	T _a (°C)	PR (mV)	Wire (mV)	Wire (mV)	T _s (°C)	T _s -T _a (°C)	I _s (mA)	V _{out} (V)	Freq (Hz)	mV _{in} (mV)	R _s (Ω)	n	R _o (Ω)	Re(D)	Nu(D)	X	e	K _C (1/s)	ΔV _A (mV)	β	Re(R _o)	R _s (Ω)	PR %	SPU (dB)	Power (W)
f ~ 1053 Hz L = 58 cm PR ~ 0.9 %	24.5	7.8060	341.10	4295.43	32.65	8.15	80	370	1052	0.483	48	276.4	48	7.2	0.54	4.9E-4	13.43	42.2	0.27	0.17	6.03E-8	92.7	0.91	150	0.027
	24.4	7.8060	341.10	4295.43	32.65	8.25	80	370	1052	0.483	48	273.1	48	7.2	0.53	4.9E-4	13.43	42.2	0.27	0.17	6.13E-8	92.6	0.91	150	0.027
	24.4	7.8062	341.09	4295.19	32.64	8.24	80	370	1052	0.483	48	273.5	48	7.2	0.53	4.9E-4	13.43	42.2	0.27	0.17	6.12E-8	92.6	0.91	150	0.027
	24.5	11.0536	487.60	4425.17	40.41	15.91	120	530	1052	0.482	48	292.6	48	7.2	0.57	4.9E-4	13.40	42.1	0.27	0.17	6.10E-8	92.6	0.91	150	0.056
24.5 11.0535 24.4 11.0536	24.5	11.0535	497.59	4425.12	40.41	16.01	120	530	1052	0.482	48	290.8	48	7.2	0.57	4.9E-4	13.40	42.1	0.27	0.17	1.20E-7	92.2	0.91	150	0.056
	24.4	11.0536	497.60	4425.17	40.41	16.01	120	530	1052	0.482	48	290.7	48	7.2	0.57	4.9E-4	13.40	42.1	0.27	0.17	1.20E-7	92.2	0.91	150	0.056
	24.5	13.5320	627.57	4558.83	48.41	23.91	150	660	1052	0.482	48	300.7	48	7.2	0.59	4.9E-4	13.40	42.1	0.27	0.17	1.79E-7	92.3	0.91	150	0.086
	24.5	13.5321	627.57	4558.80	48.41	23.91	150	660	1052	0.482	48	300.7	48	7.2	0.59	4.9E-4	13.40	42.1	0.27	0.17	1.79E-7	92.3	0.91	150	0.086
24.5 13.5323 24.5 13.5323	24.5	13.5323	627.58	4558.80	48.41	23.91	150	660	1052	0.482	48	300.7	48	7.2	0.59	4.9E-4	13.40	42.1	0.27	0.17	1.79E-7	92.3	0.91	150	0.086
	24.5	13.5323	627.58	4558.80	48.41	23.91	150	660	1052	0.482	48	300.7	48	7.2	0.59	4.9E-4	13.40	42.1	0.27	0.17	1.79E-7	92.3	0.91	150	0.086
	24.5	8.3406	364.31	4293.66	32.55	8.05	90	390	1052	0.584	71	319.6	70	8.7	0.62	4.9E-4	16.24	51.0	0.27	0.17	2.79E-8	135.5	1.10	152	0.031
	24.5	8.3406	364.32	4293.62	32.55	8.05	90	390	1052	0.584	71	319.7	70	8.7	0.62	4.9E-4	16.24	51.0	0.27	0.17	2.79E-8	135.5	1.10	152	0.031
PR ~ 1.1 % 24.5 8.3406 24.5 8.3406	24.5	8.3406	364.32	4293.77	32.55	8.05	90	390	1052	0.584	71	319.3	70	8.7	0.62	4.9E-4	16.24	51.0	0.27	0.17	2.80E-8	135.5	1.10	152	0.031
	24.5	8.3406	364.32	4293.77	32.55	8.05	90	390	1052	0.584	71	319.3	70	8.7	0.62	4.9E-4	16.24	51.0	0.27	0.17	2.80E-8	135.5	1.10	152	0.031
	24.5	12.1129	545.39	4426.01	40.46	15.96	130	580	1052	0.584	71	350.3	70	8.7	0.68	4.9E-4	16.24	51.0	0.27	0.17	2.79E-8	135.5	1.10	152	0.067
	24.5	12.1129	545.39	4426.01	40.46	15.96	130	580	1052	0.584	71	350.3	70	8.7	0.68	4.9E-4	16.24	51.0	0.27	0.17	2.79E-8	135.5	1.10	152	0.067
24.5 15.4256 24.5 15.4259 24.5 15.4254	24.5	15.4256	716.18	4563.87	48.71	24.21	160	750	1052	0.584	71	386.3	70	8.7	0.75	4.9E-4	16.24	51.0	0.27	0.17	5.54E-8	135.5	1.10	152	0.067
	24.5	15.4259	716.18	4563.79	48.71	24.21	160	750	1052	0.584	71	386.4	70	8.7	0.75	4.9E-4	16.24	51.0	0.27	0.17	5.54E-8	135.5	1.10	152	0.067
	24.5	15.4254	716.18	4563.93	48.71	24.21	160	750	1052	0.584	71	386.2	70	8.7	0.75	4.9E-4	16.24	51.0	0.27	0.17	5.54E-8	135.5	1.10	152	0.067
	24.5	15.4254	716.18	4563.93	48.71	24.21	160	750	1052	0.584	71	386.2	70	8.7	0.75	4.9E-4	16.24	51.0	0.27	0.17	5.54E-8	135.5	1.10	152	0.067
PR ~ 1.3 % 24.3 9.2479 24.3 9.2481	24.3	9.2479	403.89	4293.03	32.51	8.21	100	430	1052	0.691	99	386.5	98	10.3	0.76	4.9E-4	19.21	60.4	0.27	0.17	1.44E-8	189.6	1.31	153	0.038
	24.3	9.2481	403.89	4293.03	32.51	8.21	100	430	1052	0.691	99	386.5	98	10.3	0.76	4.9E-4	19.21	60.4	0.27	0.17	1.44E-8	189.6	1.31	153	0.038
	24.3	9.2481	403.89	4293.03	32.51	8.21	100	430	1052	0.691	99	386.5	98	10.3	0.76	4.9E-4	19.21	60.4	0.27	0.17	1.44E-8	189.6	1.31	153	0.038
	24.3	9.2481	403.89	4293.03	32.51	8.21	100	430	1052	0.691	99	386.5	98	10.3	0.76	4.9E-4	19.21	60.4	0.27	0.17	1.44E-8	189.6	1.31	153	0.038
24.4 13.6010 24.5 13.6016 24.5 13.6013	24.4	13.6010	613.00	4430.40	40.73	16.33	150	650	1052	0.690	99	432.3	98	10.3	0.85	4.9E-4	19.19	60.3	0.27	0.17	2.91E-8	189.0	1.30	153	0.085
	24.5	13.6016	613.01	4430.28	40.72	16.22	150	650	1052	0.690	99	432.3	98	10.3	0.85	4.9E-4	19.19	60.3	0.27	0.17	2.91E-8	189.0	1.30	153	0.085
	24.5	13.6013	613.01	4430.38	40.73	16.23	150	650	1052	0.690	99	432.3	98	10.3	0.85	4.9E-4	19.19	60.3	0.27	0.17	2.91E-8	189.0	1.30	153	0.085
	24.5	13.6013	613.01	4430.38	40.73	16.23	150	650	1052	0.690	99	432.3	98	10.3	0.85	4.9E-4	19.19	60.3	0.27	0.17	2.91E-8	189.0	1.30	153	0.085
24.4 16.628 24.4 16.632 24.4 16.633	24.4	16.628	771.13	4558.70	48.40	24.00	180	810	1052	0.691	99	452.2	98	10.3	0.88	4.9E-4	19.21	60.4	0.27	0.17	4.26E-8	189.6	1.31	153	0.130
	24.4	16.632	771.12	4557.55	48.33	23.93	180	810	1052	0.691	99	452.2	98	10.3	0.88	4.9E-4	19.21	60.4	0.27	0.17	4.26E-8	189.6	1.31	153	0.130
	24.4	16.633	771.12	4557.27	48.32	23.92	180	810	1052	0.691	99	452.2	98	10.3	0.88	4.9E-4	19.21	60.4	0.27	0.17	4.26E-8	189.6	1.31	153	0.130
	24.4	16.633	771.12	4557.27	48.32	23.92	180	810	1052	0.691	99	452.2	98	10.3	0.88	4.9E-4	19.21	60.4	0.27	0.17	4.26E-8	189.6	1.31	153	0.130
PR ~ 1.5 % 24.2 10.135 24.2 10.134 24.2 10.134	24.2	10.135	441.75	4284.56	32.00	7.80	110	470	1051	0.796	131	485.7	130	11.9	0.95	4.9E-4	22.15	69.6	0.27	0.17	7.84E-9	252.1	1.50	155	0.046
	24.2	10.134	441.75	4284.98	32.03	7.83	110	470	1051	0.796	131	485.7	130	11.9	0.95	4.9E-4	22.15	69.6	0.27	0.17	7.84E-9	252.1	1.50	155	0.046
	24.2	10.134	441.76	4285.08	32.03	7.83	110	470	1051	0.796	131	485.7	130	11.9	0.95	4.9E-4	22.15	69.6	0.27	0.17	7.84E-9	252.1	1.50	155	0.046
	24.2	10.134	441.76	4285.08	32.03	7.83	110	470	1051	0.796	131	485.7	130	11.9	0.95	4.9E-4	22.15	69.6	0.27	0.17	7.84E-9	252.1	1.50	155	0.046
24.2 14.665 24.3 14.671 24.3 14.668	24.2	14.665	659.46	4420.38	40.13	15.93	160	700	1051	0.796	131	514.0	130	11.9	1.00	4.9E-4	22.15	69.6	0.27	0.17	1.60E-8	252.1	1.50	155	0.098
	24.3	14.671	659.44	4418.44	40.01	15.71	160	700	1051	0.796	131	514.0	130	11.9	1.00	4.9E-4	22.15	69.6	0.27	0.17	1.60E-8	252.1	1.50	155	0.098
	24.3	14.668	659.43	4419.28	40.06	15.76	160	700	1051	0.796	131	514.0	130	11.9	1.00	4.9E-4	22.15	69.6	0.27	0.17	1.60E-8	252.1	1.50	155	0.098
	24.3	14.668	659.43	4419.28	40.06	15.76	160	700	1051	0.796	131	514.0	130	11.9	1.00	4.9E-4	22.15	69.6	0.27	0.17	1.60E-8	252.1	1.50	155	0.098
24.3 17.96 24.4 17.85 24.4 17.96	24.3	17.96	831.42	4550.59	47.92	23.62	190	870	1051	0.794	131	535.2	130	11.8	1.05	4.9E-4	22.09	69.4	0.27	0.17	2.39E-8	251.0	1.50	155	0.152
	24.4	17.85	831.40	4553.02	48.06	23.66	190	870	1051	0.794	131	533.9	130	11.8	1.04	4.9E-4	22.10	69.4	0.27	0.17	2.39E-8	251.1	1.50	155	0.152
	24.4	17.96	831.39	4550.43	47.91	23.51	190	870	1051	0.794	131	537.7	130	11.8	1.05	4.9E-4	22.10	69.4	0.27	0.17	2.38E-8	251.1	1.50	155	0.152
	24.4	17.96	831.39	4550.43	47.91	23.51	190	870	1051	0.794	131	537.7	130	11.8	1.05	4.9E-4	22.10	69.4	0.27	0.17	2.38E-8	251.1	1.50	155	0.152

[illegible]

Experiment Information	T _A (°C)	PR Volt	Wire			I _g (A)	T _s -T _a (°C)	Cur (mA)	Volt (V)	Freq (Hz)	mV _{CE} (V)	R _s (Ω)	V _{WIR2K} (V)	Cort		Nu(D)	X	s	K _C (m)	Δ ⁺ A	β (ΔI _{CE} /I _{CE})	G _{ND} Re-Te	R _s Δ ⁺ A	PR %	SPL (dB)	Power (W)
			R _a	Re(D)	R _a									Re(D)												
f = 564 Hz L = 47 cm PR - 0.9 %	22.7	8.147	353.06	4259.95	30.53	7.83	90	380	565	0.478	88	310.9	86	7.1	0.61	2.6E-4	24.68	77.5	0.14	0.09	1.81E-8	227.4	0.90	150	0.029	
	22.8	8.147	353.06	4259.95	30.53	7.73			565	0.478	88	314.9	86	7.1	0.62	2.6E-4	24.68	77.5	0.14	0.09	1.78E-8	227.5	0.90	150	0.029	
	22.8	8.147	353.06	4259.95	30.53	7.73			565	0.478	88	314.9	86	7.1	0.62	2.6E-4	24.68	77.5	0.14	0.09	1.78E-8	227.5	0.90	150	0.029	
												313.8	86	7.1	0.61	2.6E-4	24.68	77.5	0.14	0.09	1.79E-8	227.5	0.90	150	0.029	
PR - 1.1 %	22.7	12.128	541.96	4392.70	38.47	15.77	130	580	565	0.478	88	352.8	86	7.1	0.69	2.6E-4	24.68	77.5	0.14	0.09	3.64E-8	227.4	0.90	150	0.067	
	22.8	12.128	541.97	4392.78	38.48	15.68			565	0.478	88	354.9	86	7.1	0.69	2.6E-4	24.68	77.5	0.14	0.09	3.61E-8	227.5	0.90	150	0.067	
	22.8	12.128	541.97	4392.78	38.48	15.68			565	0.478	88	354.2	86	7.1	0.69	2.6E-4	24.68	77.5	0.14	0.09	3.62E-8	227.5	0.90	150	0.067	
												376.1	86	7.1	0.73	2.6E-4	24.63	77.4	0.14	0.09	5.51E-8	226.6	0.90	150	0.107	
PR - 1.3 %	22.8	15.118	696.20	4526.82	46.49	23.69	160	730	565	0.477	87	376.0	86	7.1	0.73	2.6E-4	24.63	77.4	0.14	0.09	5.51E-8	226.6	0.90	150	0.107	
	22.8	15.117	696.20	4527.12	46.51	23.71			565	0.477	87	375.7	86	7.1	0.73	2.6E-4	24.63	77.4	0.14	0.09	5.51E-8	226.6	0.90	150	0.107	
	22.8	15.118	696.19	4526.75	46.49	23.69			565	0.477	87	376.1	86	7.1	0.73	2.6E-4	24.63	77.4	0.14	0.09	5.51E-8	226.6	0.90	150	0.107	
												375.9	86	7.1	0.73	2.6E-4	24.63	77.4	0.14	0.09	5.51E-8	226.6	0.90	150	0.107	
PR - 1.5 %	22.8	9.240	400.86	4264.56	30.81	8.01	100	430	565	0.582	130	391.6	128	8.7	0.77	2.6E-4	30.05	94.4	0.14	0.09	8.40E-9	337.3	1.10	152	0.038	
	22.9	9.240	400.86	4264.56	30.81	7.91			565	0.582	130	396.5	128	8.7	0.77	2.6E-4	30.06	94.4	0.14	0.09	8.28E-9	337.5	1.10	152	0.038	
	23.0	9.240	400.86	4264.56	30.81	7.81			565	0.582	130	401.6	128	8.7	0.78	2.6E-4	30.06	94.4	0.14	0.09	8.17E-9	337.7	1.10	152	0.038	
												443.9	128	8.7	0.87	2.6E-4	30.07	94.5	0.14	0.09	1.62E-8	338.0	1.10	152	0.083	
PR - 1.3 %	22.9	13.485	603.15	4396.71	38.71	15.81	140	540	565	0.582	130	435.4	128	8.7	0.85	2.6E-4	30.06	94.4	0.14	0.09	1.66E-8	337.5	1.10	152	0.083	
	23.1	13.485	603.15	4396.71	38.71	15.61			565	0.582	130	441.0	128	8.7	0.86	2.6E-4	30.07	94.5	0.14	0.09	1.63E-8	337.9	1.10	152	0.083	
	23.2	13.485	603.15	4396.71	38.71	15.51			565	0.582	130	440.1	128	8.7	0.87	2.6E-4	30.07	94.5	0.14	0.09	1.62E-8	338.0	1.10	152	0.083	
												443.9	128	8.7	0.86	2.6E-4	30.06	94.4	0.14	0.09	1.63E-8	337.8	1.10	152	0.083	
PR - 1.3 %	23.1	16.857	778.57	4540.16	47.29	24.19	180	820	565	0.581	130	459.2	128	8.6	0.90	2.6E-4	30.01	94.3	0.14	0.09	2.54E-8	336.7	1.10	152	0.134	
	23.3	16.857	778.59	4540.27	47.30	24.00			565	0.581	130	462.9	128	8.6	0.91	2.6E-4	30.02	94.3	0.14	0.09	2.52E-8	337.1	1.10	152	0.134	
	23.4	16.857	778.58	4540.22	47.30	23.90			565	0.581	130	464.9	128	8.7	0.91	2.6E-4	30.03	94.4	0.14	0.09	2.50E-8	337.2	1.10	152	0.134	
												513.1	180	10.3	1.02	2.6E-4	35.66	112.0	0.14	0.09	4.14E-9	475.0	1.31	153	0.049	
PR - 1.3 %	23.4	10.48	455.64	4273.80	31.36	7.96	110	490	566	0.691	183	507.8	180	10.3	0.99	2.6E-4	35.65	112.0	0.14	0.09	4.20E-9	474.7	1.31	153	0.049	
	23.5	10.48	455.64	4273.80	31.36	7.86			566	0.691	183	514.3	180	10.3	1.00	2.6E-4	35.66	112.0	0.14	0.09	4.14E-9	475.0	1.31	153	0.049	
	23.6	10.48	455.63	4273.71	31.35	7.75			566	0.691	184	521.3	181	10.3	1.02	2.6E-4	35.66	112.0	0.14	0.09	4.08E-9	475.3	1.31	153	0.049	
												514.5	180	10.3	1.01	2.6E-4	35.66	112.0	0.14	0.09	4.14E-9	475.0	1.31	153	0.049	
PR - 1.5 %	23.4	14.76	660.74	4400.46	38.94	15.54	160	700	566	0.691	183	531.4	180	10.3	1.04	2.6E-4	35.65	112.0	0.14	0.09	8.19E-9	474.7	1.31	153	0.099	
	23.3	14.76	660.73	4400.39	38.93	15.63			566	0.691	183	528.1	180	10.3	1.03	2.6E-4	35.65	112.0	0.14	0.09	8.26E-9	474.5	1.31	153	0.099	
	23.2	14.76	660.71	4400.26	38.92	15.72			566	0.691	183	525.0	180	10.3	1.03	2.6E-4	35.64	112.0	0.14	0.09	8.32E-9	474.2	1.31	153	0.099	
												528.2	180	10.3	1.03	2.6E-4	35.65	112.0	0.14	0.09	8.26E-9	474.5	1.31	153	0.099	
PR - 1.5 %	23.4	18.39	849.74	4542.11	47.41	24.01	190	890	566	0.690	183	551.0	180	10.3	1.08	2.6E-4	35.60	111.8	0.14	0.09	1.27E-8	473.4	1.30	153	0.159	
	23.5	18.41	849.76	4537.28	47.12	23.62			566	0.690	183	560.7	180	10.3	1.10	2.6E-4	35.61	111.9	0.14	0.09	1.25E-8	473.6	1.30	153	0.159	
	23.5	18.38	849.77	4544.74	47.57	24.07			566	0.690	183	549.4	180	10.3	1.07	2.6E-4	35.61	111.9	0.14	0.09	1.27E-8	473.6	1.30	153	0.159	
												553.7	180	10.3	1.08	2.6E-4	35.60	111.9	0.14	0.09	1.27E-8	473.5	1.30	153	0.159	
PR - 1.5 %	23.4	11.59	504.82	4281.61	31.83	8.43	130	540	566	0.797	244	587.7	240	11.9	1.15	2.6E-4	41.12	129.2	0.14	0.09	2.51E-9	631.6	1.51	155	0.060	
	23.5	11.59	504.81	4281.52	31.82	8.32			566	0.797	244	595.2	240	11.9	1.16	2.6E-4	41.13	129.2	0.14	0.09	2.48E-9	631.9	1.51	155	0.060	
	23.6	11.59	504.80	4281.44	31.82	8.22			566	0.797	244	602.8	240	11.9	1.18	2.6E-4	41.13	129.2	0.14	0.09	2.44E-9	632.3	1.51	155	0.060	
												595.2	240	11.9	1.16	2.6E-4	41.13	129.2	0.14	0.09	2.48E-9	631.9	1.51	155	0.060	
PR - 1.5 %	23.4	16.48	739.93	4413.54	39.72	16.32	180	780	566	0.796	243	632.6	239	11.9	1.24	2.6E-4	41.07	129.0	0.14	0.09	4.99E-9	630.0	1.50	155	0.124	
	23.5	16.47	739.90	4416.04	39.87	16.37			566	0.796	243	630.3	239	11.9	1.23	2.6E-4	41.08	129.0	0.14	0.09	4.90E-9	630.3	1.50	155	0.124	
	23.5	16.48	739.93	4413.54	39.72	16.22			566	0.796	243	636.5	239	11.9	1.24	2.6E-4	41.08	129.0	0.14	0.09	4.85E-9	630.3	1.50	155	0.124	
												633.1	239	11.9	1.24	2.6E-4	41.07	129.0	0.14	0.09	4.78E-9	630.2	1.50	155	0.124	
PR - 1.5 %	23.5	20.10	927.60	4536.47	47.07	23.57	210	970	566	0.796	243	669.6	239	11.9	1.31	2.6E-4	41.08	129.0	0.14	0.09	7.05E-9	630.3	1.50	155	0.190	
	23.5	20.10	927.70	4536.96	47.10	23.60			566	0.796	243	668.8	239	11.9	1.31	2.6E-4	41.08	129.0	0.14	0.09	7.06E-9	630.3	1.50	155	0.190	
	23.5	20.10	927.70	4536.96	47.10	23.60			566	0.796	243	668.1	239	11.9	1.31	2.6E-4	41.08	129.0	0.14	0.09	7.06E-9	630.3	1.50	155	0.190	
												669.1	239	11.9	1.31	2.6E-4	41.08	129.0	0.14	0.09	7.06E-9	630.3	1.50	155	0.190	

Exposure Information										Exposure Information									
Frequency	Power	Power Spectral Density	Power Spectral Density	Power Spectral Density	Power Spectral Density	Power Spectral Density	Power Spectral Density	Power Spectral Density	Power Spectral Density	Frequency	Power	Power Spectral Density	Power Spectral Density	Power Spectral Density	Power Spectral Density	Power Spectral Density	Power Spectral Density	Power Spectral Density	Power Spectral Density
Hz	W	W/Hz	W/Hz	W/Hz	W/Hz	W/Hz	W/Hz	W/Hz	W/Hz	Hz	W	W/Hz	W/Hz	W/Hz	W/Hz	W/Hz	W/Hz	W/Hz	W/Hz
1 ~ 564 Hz	3.43E-4	2.60E-4	-8.4E-4	0.094	6.86E-4	-0.032	-0.030	0.064	7.73	0.050	-8.5E-4	6.04E-3	5.04						
L = 47 cm PR - 0.9 %	3.43E-4	2.60E-4	-8.4E-4	0.094	6.86E-4	-0.032	-0.030	0.065	7.82	0.050	-8.4E-4	6.04E-3	5.04						
	3.43E-4	2.60E-4	-8.4E-4	0.094	6.86E-4	-0.032	-0.030	0.065	7.82	0.050	-8.4E-4	6.04E-3	5.04						
				0.094					7.79				5.04						
	2.45E-4	2.60E-4	-6.8E-4	0.077	4.89E-4	-0.014	-0.030	0.032	4.57	0.050	-8.5E-4	6.04E-3	5.04						
	2.45E-4	2.60E-4	-6.8E-4	0.077	4.89E-4	-0.014	-0.030	0.032	4.59	0.050	-8.4E-4	6.04E-3	5.04						
	2.45E-4	2.60E-4	-6.8E-4	0.077	4.89E-4	-0.014	-0.030	0.032	4.59	0.050	-8.4E-4	6.04E-3	5.04						
				0.077					4.58				5.04						
	2.04E-4	2.60E-4	-6.1E-4	0.070	4.07E-4	-0.009	-0.030	0.021	3.77	0.050	-8.4E-4	6.05E-3	5.04						
	2.04E-4	2.60E-4	-6.1E-4	0.070	4.07E-4	-0.009	-0.030	0.021	3.77	0.050	-8.4E-4	6.05E-3	5.04						
	2.04E-4	2.60E-4	-6.1E-4	0.070	4.07E-4	-0.009	-0.030	0.021	3.77	0.050	-8.4E-4	6.05E-3	5.04						
				0.070					3.77				5.04						
PR - 1.1 %	3.09E-4	2.60E-4	-7.8E-4	0.088	6.19E-4	-0.029	-0.030	0.062	7.51	0.050	-8.4E-4	5.07E-3	5.03						
	3.09E-4	2.60E-4	-7.8E-4	0.088	6.19E-4	-0.029	-0.030	0.063	7.59	0.050	-8.4E-4	5.07E-3	5.03						
	3.09E-4	2.60E-4	-7.8E-4	0.088	6.19E-4	-0.030	-0.030	0.064	7.67	0.050	-8.4E-4	5.07E-3	5.03						
				0.088					7.59				5.03						
	2.26E-4	2.60E-4	-6.5E-4	0.073	4.52E-4	-0.013	-0.030	0.032	4.55	0.050	-8.4E-4	5.07E-3	5.03						
	2.26E-4	2.60E-4	-6.5E-4	0.073	4.52E-4	-0.013	-0.030	0.032	4.58	0.050	-8.4E-4	5.07E-3	5.03						
	2.26E-4	2.60E-4	-6.5E-4	0.073	4.52E-4	-0.013	-0.030	0.032	4.60	0.050	-8.4E-4	5.07E-3	5.03						
				0.073					4.57				5.03						
	1.88E-4	2.60E-4	-5.9E-4	0.067	3.77E-4	-0.008	-0.030	0.021	3.73	0.050	-8.4E-4	5.08E-3	5.03						
	1.88E-4	2.60E-4	-5.9E-4	0.067	3.77E-4	-0.008	-0.030	0.021	3.74	0.050	-8.4E-4	5.08E-3	5.03						
	1.88E-4	2.60E-4	-5.9E-4	0.067	3.77E-4	-0.008	-0.030	0.021	3.75	0.050	-8.4E-4	5.08E-3	5.03						
				0.067					3.74				5.03						
PR - 1.3 %	2.79E-4	2.60E-4	-4.2E-3	0.418	5.59E-4	-0.139	-0.030	0.063	15.51	0.050	-8.4E-4	4.36E-3	5.02						
	2.79E-4	2.60E-4	-4.2E-3	0.418	5.59E-4	-0.140	-0.030	0.064	15.69	0.050	-8.4E-4	4.36E-3	5.02						
	2.79E-4	2.60E-4	-4.2E-3	0.418	5.59E-4	-0.142	-0.030	0.064	15.89	0.050	-8.4E-4	4.36E-3	5.02						
				0.418					15.70				5.02						
	2.11E-4	2.60E-4	-3.1E-3	0.308	4.23E-4	-0.055	-0.030	0.032	7.06	0.050	-8.4E-4	4.36E-3	5.02						
	2.11E-4	2.60E-4	-3.1E-3	0.308	4.23E-4	-0.055	-0.030	0.032	7.03	0.050	-8.4E-4	4.36E-3	5.02						
	2.11E-4	2.60E-4	-3.1E-3	0.308	4.23E-4	-0.055	-0.030	0.032	7.00	0.050	-8.4E-4	4.36E-3	5.02						
				0.308					7.03				5.02						
	1.78E-4	2.60E-4	-2.5E-3	0.254	3.55E-4	-0.031	-0.030	0.021	4.81	0.050	-8.4E-4	4.37E-3	5.02						
	1.78E-4	2.60E-4	-2.5E-3	0.254	3.55E-4	-0.032	-0.030	0.021	4.85	0.050	-8.4E-4	4.37E-3	5.02						
	1.78E-4	2.60E-4	-2.5E-3	0.255	3.55E-4	-0.031	-0.030	0.021	4.81	0.050	-8.4E-4	4.37E-3	5.02						
				0.254					4.82				5.02						
PR - 1.5 %	2.58E-4	2.60E-4	-3.8E-3	0.382	5.16E-4	-0.120	-0.030	0.059	13.71	0.050	-8.4E-4	3.86E-3	5.02						
	2.58E-4	2.60E-4	-3.8E-3	0.382	5.16E-4	-0.121	-0.030	0.060	13.87	0.050	-8.4E-4	3.86E-3	5.02						
	2.58E-4	2.60E-4	-3.8E-3	0.382	5.16E-4	-0.123	-0.030	0.061	14.03	0.050	-8.4E-4	3.86E-3	5.02						
				0.382					13.87				5.02						
	1.95E-4	2.60E-4	-2.8E-3	0.280	3.90E-4	-0.048	-0.030	0.031	6.44	0.050	-8.4E-4	3.87E-3	5.02						
	1.95E-4	2.60E-4	-2.8E-3	0.280	3.90E-4	-0.048	-0.030	0.031	6.43	0.050	-8.4E-4	3.87E-3	5.02						
	1.95E-4	2.60E-4	-2.8E-3	0.280	3.90E-4	-0.048	-0.030	0.031	6.43	0.050	-8.4E-4	3.87E-3	5.02						
				0.280					6.45				5.02						
	1.68E-4	2.60E-4	-2.3E-3	0.236	3.36E-4	-0.030	-0.030	0.021	4.71	0.050	-8.4E-4	3.87E-3	5.02						
	1.68E-4	2.60E-4	-2.3E-3	0.236	3.36E-4	-0.030	-0.030	0.021	4.71	0.050	-8.4E-4	3.87E-3	5.02						
	1.68E-4	2.60E-4	-2.3E-3	0.236	3.36E-4	-0.030	-0.030	0.021	4.71	0.050	-8.4E-4	3.87E-3	5.02						
				0.236					4.71				5.02						

Experiment Information	T _a (°C)	PR (mV)	Wire Volt (mV)	Wire Res (mΩ)	T _s (°C)	I _s -I _e (G)	Cur (mA)	V _o (V)	Freq (Hz)	mic-V (V)	R _s (Ω)	h _{FE}	Corr		X (Ω)	β (m)	KC (m)	Av _i (2ΔV _i)	PR % SPL (dB)	R _s (Ω)	ReRe (Ω)	Gr(D)			
													R _s (Ω)	Re(D) (mΩ)											
f = 564 Hz L = 47 cm PR ~ 1.7 %	23.6	12.10	526.39	4276.37	31.51	7.91	130	560	566	0.902	313	681.3	308	13.4	1.33	2.6E-4	46.55	146.3	0.14	0.09	1.43E-9	809.8	170	156	0.065
	23.5	12.10	526.40	4276.46	31.52	8.02	130	560	566	0.902	313	672.4	307	13.4	1.31	2.6E-4	46.55	146.2	0.14	0.09	1.45E-9	809.4	170	156	0.065
	23.4	12.10	526.40	4276.46	31.52	8.12	130	560	566	0.902	313	664.1	307	13.4	1.30	2.6E-4	46.54	146.2	0.14	0.09	1.47E-9	808.9	170	156	0.065
	23.6	17.63	792.22	4417.20	39.94	16.34	190	830	566	0.902	313	723.7	308	13.4	1.31	2.6E-4	46.55	146.2	0.14	0.09	1.45E-9	808.4	170	156	0.142
PR ~ 1.9 %	23.5	17.64	792.23	4414.75	39.79	16.29	16.39	830	566	0.902	313	726.2	307	13.4	1.42	2.6E-4	46.55	146.2	0.14	0.09	2.96E-9	809.4	170	156	0.142
	23.4	17.64	792.22	4414.70	39.79	16.39	16.39	830	566	0.902	313	721.9	307	13.4	1.41	2.6E-4	46.54	146.2	0.14	0.09	2.98E-9	808.9	170	156	0.142
	24.1	21.37	989.72	4552.62	48.04	23.94	220	130	566	0.903	314	747.9	309	13.5	1.46	2.6E-4	46.64	146.5	0.14	0.09	4.33E-9	813.4	171	156	0.215
	24.0	21.36	989.72	4552.62	48.17	24.17	24.17	130	566	0.903	314	740.6	309	13.5	1.45	2.6E-4	46.64	146.5	0.14	0.09	4.31E-9	813.4	171	156	0.215
PR ~ 2.1 %	23.6	18.31	822.66	4416.57	39.90	16.30	190	860	566	1.008	391	782.3	384	15.0	1.53	2.6E-4	52.03	163.5	0.14	0.09	1.86E-9	1011.9	191	157	0.153
	23.5	18.31	822.61	4416.31	39.98	16.38	16.38	860	566	1.008	390	778.2	384	15.0	1.52	2.6E-4	52.02	163.4	0.14	0.09	1.89E-9	1011.3	191	157	0.153
	22.7	22.20	1023.50	4531.98	46.80	24.10	230	1070	566	1.011	392	798.0	385	15.0	1.56	2.6E-4	52.02	163.4	0.14	0.09	1.89E-9	1011.3	191	157	0.231
	22.7	22.22	1023.60	4528.35	46.59	23.89	23.89	1070	566	1.011	392	806.1	385	15.0	1.57	2.6E-4	52.02	163.4	0.14	0.09	2.78E-9	1012.3	191	157	0.231
PR ~ 2.3 %	24.8	18.32	822.62	4413.95	39.74	16.04	190	860	567	1.117	481	819.8	473	16.7	1.60	2.6E-4	57.68	181.2	0.14	0.09	6.00E-10	1245.4	211	158	0.078
	24.8	18.31	822.61	4416.31	39.98	16.38	16.38	860	567	1.117	481	799.5	473	16.7	1.56	2.6E-4	57.66	181.2	0.14	0.09	6.17E-10	1244.0	211	158	0.078
	24.7	18.31	822.61	4416.31	39.98	16.38	16.38	860	567	1.117	481	790.1	473	16.7	1.54	2.6E-4	57.66	181.2	0.14	0.09	6.25E-10	1243.3	211	158	0.078
	24.7	18.31	822.61	4416.31	39.98	16.38	16.38	860	567	1.117	481	803.1	473	16.7	1.57	2.6E-4	57.67	181.2	0.14	0.09	6.14E-10	1244.2	211	158	0.078
PR ~ 2.3 %	24.9	18.65	840.02	4427.56	40.56	15.66	200	880	567	1.117	481	847.0	473	16.7	1.65	2.6E-4	57.67	181.2	0.14	0.09	1.19E-9	1244.7	211	158	0.159
	24.8	18.64	840.01	4429.86	40.70	15.90	15.90	880	567	1.117	481	833.8	473	16.7	1.63	2.6E-4	57.66	181.2	0.14	0.09	1.21E-9	1244.0	211	158	0.159
	24.8	18.65	840.01	4427.51	40.55	15.75	200	880	567	1.117	481	841.8	473	16.7	1.64	2.6E-4	57.68	181.2	0.14	0.09	1.20E-9	1244.0	211	158	0.159
	24.8	18.65	840.01	4427.51	40.55	15.75	200	880	567	1.117	481	840.9	473	16.7	1.64	2.6E-4	57.67	181.2	0.14	0.09	1.20E-9	1244.2	211	158	0.159
PR ~ 2.3 %	25.0	22.94	1064.84	4562.94	48.65	23.65	240	1110	567	1.117	481	874.2	473	16.7	1.71	2.6E-4	57.68	181.2	0.14	0.09	1.80E-9	1245.4	211	158	0.248
	24.9	22.95	1064.80	4561.21	48.53	23.63	240	1110	567	1.117	481	874.2	473	16.7	1.71	2.6E-4	57.67	181.2	0.14	0.09	1.80E-9	1244.7	211	158	0.249
	24.9	22.95	1064.80	4560.78	48.53	23.63	240	1110	567	1.117	481	874.2	473	16.7	1.71	2.6E-4	57.68	181.2	0.14	0.09	1.80E-9	1244.7	211	158	0.249
	24.9	22.95	1064.80	4560.78	48.53	23.63	240	1110	567	1.117	481	874.2	473	16.7	1.71	2.6E-4	57.68	181.2	0.14	0.09	1.80E-9	1244.7	211	158	0.249
PR ~ 2.3 %	24.8	13.76	602.04	4300.91	32.98	8.18	150	640	567	1.220	573	857.1	564	18.2	1.67	2.6E-4	62.98	197.9	0.14	0.09	4.39E-10	1484.0	231	158	0.084
	24.7	13.76	602.05	4300.96	32.99	8.29	150	640	567	1.220	573	846.3	564	18.2	1.65	2.6E-4	62.97	197.8	0.14	0.09	4.45E-10	1483.2	231	158	0.084
	24.7	13.76	602.04	4300.91	32.98	8.28	150	640	567	1.220	573	846.8	564	18.2	1.65	2.6E-4	62.97	197.8	0.14	0.09	4.45E-10	1483.2	231	158	0.084
	24.7	13.76	602.04	4300.91	32.98	8.28	150	640	567	1.220	573	850.1	564	18.2	1.66	2.6E-4	62.98	197.8	0.14	0.09	4.43E-10	1483.5	231	158	0.084
PR ~ 2.3 %	24.7	18.18	863.73	4426.73	40.51	15.81	200	910	567	1.222	575	887.2	566	18.2	1.73	2.6E-4	63.07	198.2	0.14	0.09	8.43E-10	1488.1	231	158	0.169
	24.6	18.18	863.75	4426.83	40.51	15.91	15.91	910	567	1.222	575	881.3	565	18.2	1.72	2.6E-4	63.06	198.1	0.14	0.09	8.50E-10	1487.3	231	158	0.169
	24.5	19.17	893.73	4429.04	40.65	16.15	250	1150	567	1.222	575	913.9	565	18.2	1.70	2.6E-4	63.05	198.1	0.14	0.09	8.64E-10	1486.4	231	158	0.168
	24.5	19.17	893.73	4429.04	40.65	16.15	250	1150	567	1.222	575	912.4	565	18.2	1.72	2.6E-4	63.06	198.1	0.14	0.09	8.53E-10	1487.3	231	158	0.168
PR ~ 2.3 %	24.6	23.73	1102.20	4565.79	48.83	24.23	250	1150	567	1.221	574	913.9	565	18.2	1.79	2.6E-4	63.01	198.0	0.14	0.09	1.30E-9	1484.8	231	158	0.266
	24.6	23.72	1102.19	4567.68	48.94	24.34	24.34	1150	567	1.221	574	909.3	565	18.2	1.78	2.6E-4	63.01	198.0	0.14	0.09	1.30E-9	1484.8	231	158	0.266
	24.6	23.73	1102.20	4565.79	48.83	24.23	24.23	1150	567	1.221	574	913.9	565	18.2	1.79	2.6E-4	63.01	198.0	0.14	0.09	1.30E-9	1484.8	231	158	0.266
	24.6	23.73	1102.20	4565.79	48.83	24.23	24.23	1150	567	1.221	574	912.4	565	18.2	1.78	2.6E-4	63.01	198.0	0.14	0.09	1.30E-9	1484.8	231	158	0.266

Experiment Information	T _a (°C)	PR Volt (mV)	Wire Volt (mV)	Wire Res (mΩ)	T _s (°C)	T _s -T _a (°C)	Cur (mA)	Vol _t (V)	Freq (Hz)	mic V (V)	Re	h W/m ² K	Corr		Re(D)	Nu(D)	X	ε	KC (m)	A ^{1/2}	β (2A/A ^{1/2})	Gr(D)		PR %	SPL (dB)	Power (W)
													Rs	Rs								Rs/Rs	Rs			
f ~ 1213 Hz L = 64 cm PR ~ 1.5 %	23.5	39.51	270.65	673.37	31.85	8.35	410	340	1213	0.795	113	433.6	113	29.6	2.12	0.001	7.66	24.1	1.93	1.23	174E-7	81.5	1.50	155	0.109	
	23.5	39.46	270.28	673.30	31.82	8.32	410	340	1213	0.795	113	434.0	113	29.6	2.12	0.001	7.66	24.1	1.93	1.23	174E-7	81.5	1.50	155	0.108	
	23.5	39.43	270.10	673.37	31.85	8.35	410	340	1213	0.795	113	433.2	113	29.6	2.12	0.001	7.66	24.1	1.93	1.23	174E-7	81.5	1.50	155	0.108	
	23.7	52.59	369.76	691.15	39.60	15.90	540	460	1213	0.796	114	414.0	114	29.6	2.02	0.001	7.67	24.1	1.93	1.23	330E-7	81.8	1.50	155	0.198	
PR ~ 1.7 %	23.8	63.66	459.70	709.84	47.76	23.96	650	560	1213	0.792	113	413.6	113	29.5	2.02	0.001	7.63	24.0	1.93	1.23	506E-7	81.0	1.50	155	0.298	
	23.8	63.65	459.73	710.00	47.63	24.03	650	560	1213	0.792	113	412.4	113	29.5	2.01	0.001	7.63	24.0	1.93	1.23	508E-7	81.0	1.50	155	0.298	
	23.8	63.59	459.64	710.53	48.06	24.26	650	560	1213	0.792	113	408.0	113	29.5	1.99	0.001	7.63	24.0	1.93	1.23	513E-7	81.0	1.50	155	0.297	
	24.3	41.09	282.02	674.68	32.42	8.12	430	350	1215	0.901	146	483.1	146	33.6	2.36	0.001	8.68	27.3	1.94	1.23	102E-7	104.7	1.70	156	0.118	
PR ~ 1.9 %	24.3	41.09	282.01	674.66	32.41	8.11	430	350	1215	0.901	146	483.7	146	33.6	2.36	0.001	8.68	27.3	1.94	1.23	102E-7	104.7	1.70	156	0.118	
	24.3	41.09	282.01	674.66	32.41	8.11	430	350	1215	0.901	146	483.5	146	33.6	2.35	0.001	8.68	27.3	1.94	1.23	102E-7	104.7	1.70	156	0.118	
	24.4	56.69	398.57	692.85	40.35	15.95	580	490	1215	0.900	145	481.0	145	33.6	2.35	0.001	8.67	27.2	1.94	1.23	201E-7	104.5	1.70	156	0.230	
	24.4	56.67	398.57	693.10	40.45	16.05	580	490	1215	0.900	145	477.6	145	33.6	2.33	0.001	8.67	27.2	1.94	1.23	203E-7	104.5	1.70	156	0.230	
PR ~ 1.9 %	24.4	56.68	398.57	692.97	40.40	16.00	580	490	1215	0.900	145	479.3	145	33.6	2.34	0.001	8.67	27.2	1.94	1.23	202E-7	104.5	1.70	156	0.230	
	24.4	68.14	492.77	710.88	48.21	23.81	700	600	1215	0.899	145	477.5	145	33.5	2.33	0.001	8.66	27.2	1.94	1.23	302E-7	104.3	1.70	156	0.342	
	24.4	68.13	492.72	710.91	48.22	23.82	700	600	1215	0.899	145	477.1	145	33.5	2.33	0.001	8.66	27.2	1.94	1.23	302E-7	104.3	1.70	156	0.341	
	24.4	68.09	492.67	711.26	48.37	23.97	700	600	1215	0.899	145	476.2	145	33.5	2.31	0.001	8.66	27.2	1.94	1.23	304E-7	104.3	1.70	156	0.341	
PR ~ 1.9 %	23.1	43.544	297.7	672.05	31.28	8.18	450	370	1213	1.009	182	536.8	182	37.5	2.62	0.001	9.71	30.5	1.93	1.23	600E-8	131.1	1.91	157	0.132	
	23.1	43.544	297.5	671.60	31.08	7.98	450	370	1213	1.009	182	549.7	182	37.5	2.69	0.001	9.71	30.5	1.93	1.23	644E-8	131.1	1.91	157	0.132	
	23.1	43.544	297.7	672.05	31.28	8.18	450	370	1213	1.009	182	536.8	182	37.5	2.62	0.001	9.71	30.5	1.93	1.23	660E-8	131.1	1.91	157	0.132	
	22.9	58.982	414.2	690.31	39.24	16.34	610	510	1213	1.008	182	506.3	182	37.5	2.47	0.001	9.70	30.5	1.93	1.23	655E-8	131.1	1.91	157	0.249	
PR ~ 1.9 %	22.9	58.982	413.7	689.48	38.88	15.98	610	510	1213	1.008	182	517.2	182	37.5	2.53	0.001	9.70	30.5	1.93	1.23	133E-7	130.8	1.91	157	0.248	
	22.9	58.982	413.9	689.81	39.02	16.12	610	510	1213	1.008	182	512.8	182	37.5	2.50	0.001	9.70	30.5	1.93	1.23	131E-7	130.8	1.91	157	0.248	
	22.9	70.558	507.5	707.04	46.53	23.63	720	620	1213	1.009	182	513.0	182	37.5	2.51	0.001	9.71	30.5	1.93	1.23	131E-7	130.8	1.91	157	0.364	
	22.9	70.558	508.6	708.57	47.20	24.30	720	620	1213	1.009	182	500.0	182	37.5	2.44	0.001	9.71	30.5	1.93	1.23	197E-7	131.0	1.91	157	0.365	
22.9	70.558	508.0	707.74	46.84	23.94	720	620	1213	1.009	182	507.0	182	37.5	2.48	0.001	9.71	30.5	1.93	1.23	194E-7	131.0	1.91	157	0.365		
												506.7	182	37.5	2.47	0.001	9.71	30.5	1.93	1.23	194E-7	131.0	1.91	157	0.365	

Experiment Information	Wire Res Volt uncent	PR Res Volt uncent	Wire R Volt uncent (%)	Wire Res Volt uncent	Wire Length uncent	Ta uncent	Nu(D) uncent	Wire Res Volt uncent	Ta uncent	Re Volt uncent (%)
I ~ 1213 Hz L = 64 cm PR ~ 1.5 %	1.07E-4	2.60E-4	0.262	2.14E-4	-0.095	0.060	11.59	0.020	-8.4E-4	3.87E-3
	1.07E-4	2.60E-4	0.262	2.14E-4	-0.095	0.060	11.64	0.020	-8.4E-4	3.87E-3
	1.07E-4	2.60E-4	0.262	2.14E-4	-0.095	0.060	11.61	0.020	-8.4E-4	3.87E-3
	3.30E-4	2.60E-4	0.202	6.61E-4	-0.040	0.031	5.92	0.020	-8.4E-4	3.87E-3
	3.30E-4	2.60E-4	0.202	6.61E-4	-0.040	0.031	5.94	0.020	-8.4E-4	3.87E-3
	3.30E-4	2.60E-4	0.202	6.61E-4	-0.040	0.031	5.93	0.020	-8.4E-4	3.87E-3
	2.78E-4	2.60E-4	0.168	5.55E-4	-0.023	0.021	4.34	0.020	-8.4E-4	3.88E-3
	2.78E-4	2.60E-4	0.168	5.55E-4	-0.023	0.021	4.34	0.020	-8.4E-4	3.88E-3
	2.78E-4	2.60E-4	0.168	5.55E-4	-0.023	0.021	4.32	0.020	-8.4E-4	3.88E-3
PR ~ 1.7 %	1.05E-4	2.60E-4	0.252	2.11E-4	-0.094	0.062	11.61	0.020	-8.4E-4	3.49E-3
	1.05E-4	2.60E-4	0.252	2.11E-4	-0.094	0.062	11.63	0.020	-8.4E-4	3.49E-3
	1.05E-4	2.60E-4	0.252	2.11E-4	-0.094	0.062	11.63	0.020	-8.4E-4	3.49E-3
	3.10E-4	2.60E-4	0.188	6.21E-4	-0.037	0.031	5.73	0.020	-8.4E-4	3.49E-3
	3.10E-4	2.60E-4	0.188	6.21E-4	-0.037	0.031	5.71	0.020	-8.4E-4	3.49E-3
	3.10E-4	2.60E-4	0.188	6.21E-4	-0.037	0.031	5.72	0.020	-8.4E-4	3.49E-3
	2.63E-4	2.60E-4	0.158	5.26E-4	-0.022	0.021	4.28	0.020	-8.4E-4	3.49E-3
	2.63E-4	2.60E-4	0.158	5.26E-4	-0.022	0.021	4.28	0.020	-8.4E-4	3.49E-3
	2.63E-4	2.60E-4	0.158	5.26E-4	-0.022	0.021	4.27	0.020	-8.4E-4	3.49E-3
PR ~ 1.9 %	1.68E-3	2.60E-4	0.173	3.36E-3	-0.064	0.061	9.32	0.020	-8.4E-4	3.18E-3
	1.04E-4	2.60E-4	0.238	2.07E-4	-0.090	0.063	11.36	0.020	-8.4E-4	3.18E-3
	1.04E-4	2.60E-4	0.238	2.07E-4	-0.088	0.061	11.11	0.020	-8.4E-4	3.18E-3
	3.01E-4	2.60E-4	0.181	6.03E-4	-0.035	0.031	5.54	0.020	-8.4E-4	3.18E-3
	3.02E-4	2.60E-4	0.181	6.03E-4	-0.036	0.031	5.63	0.020	-8.4E-4	3.18E-3
	3.02E-4	2.60E-4	0.181	6.03E-4	-0.036	0.031	5.59	0.020	-8.4E-4	3.18E-3
	2.57E-4	2.60E-4	0.153	5.14E-4	-0.022	0.021	4.26	0.020	-8.4E-4	3.18E-3
	2.57E-4	2.60E-4	0.153	5.14E-4	-0.021	0.021	4.20	0.020	-8.4E-4	3.18E-3
	2.57E-4	2.60E-4	0.153	5.14E-4	-0.021	0.021	4.23	0.020	-8.4E-4	3.18E-3

Experiment Information	T _a	PR Volt (mV)	Wire Volt (mV)	Wire Res (mΩ)	T _s	T _a -T _s (C)	Our Volt (mA)	Freq (Hz)	mic V (V)	Re	h	Ra	Corr	Re(D)	Nu(D)	x	ε	KC	ΔV _A	β (2ΔV/h)	Gr(D)				
																					Ra ² /Ts	Ra ² /Ts	Ra ² /Ts		
f = 1213 Hz L = 64 cm PR - 2.1 %	22.6	36.665	250.4	671.33	30.96	8.36	380	320	1212	1.115	222	371.8	222	41.5	1.82	0.001	10.73	33.7	1.93	1.23	4.54E-8	160.0	2.11	158	0.093
	22.6	36.665	250.6	671.87	31.20	8.60	380	320	1212	1.115	222	362.0	222	41.5	1.77	0.001	10.73	33.7	1.93	1.23	4.67E-8	160.0	2.11	158	0.093
	22.6	36.665	250.5	671.60	31.08	8.48	380	320	1212	1.115	222	366.8	222	41.5	1.79	0.001	10.73	33.7	1.93	1.23	4.61E-8	160.0	2.11	158	0.093
	22.4	49.580	347.4	688.77	38.57	16.17	510	430	1212	1.116	223	360.7	223	41.5	1.76	0.001	10.74	33.7	1.93	1.23	8.77E-8	160.2	2.11	158	0.175
	22.4	49.580	347.6	689.17	38.74	16.34	510	430	1212	1.116	223	357.1	223	41.5	1.74	0.001	10.74	33.7	1.93	1.23	8.87E-8	160.2	2.11	158	0.175
	22.4	49.580	347.5	688.97	38.66	16.26	510	430	1212	1.116	223	358.9	223	41.5	1.75	0.001	10.74	33.7	1.93	1.23	8.82E-8	160.2	2.11	158	0.175
	22.2	59.646	429.3	707.51	46.74	24.54	610	530	1212	1.114	222	353.3	222	41.4	1.73	0.001	10.71	33.7	1.93	1.23	1.34E-7	159.5	2.11	158	0.260
	22.2	59.646	430.2	708.99	47.39	25.19	610	530	1212	1.114	222	345.0	222	41.4	1.69	0.001	10.71	33.7	1.93	1.23	1.38E-7	159.5	2.11	158	0.261
	22.2	59.646	428.9	706.85	46.45	24.25	610	530	1212	1.114	222	357.2	222	41.4	1.74	0.001	10.71	33.7	1.93	1.23	1.33E-7	159.5	2.11	158	0.260
PR - 2.3 %	21.6	36.320	247.2	669.05	29.97	8.37	380	310	1210	1.222	267	363.4	267	45.4	1.78	0.001	11.76	36.9	1.93	1.23	3.17E-8	192.1	2.31	158	0.091
	21.6	36.320	248.9	668.23	29.61	8.01	380	310	1210	1.222	267	379.0	267	45.4	1.85	0.001	11.76	36.9	1.93	1.23	3.04E-8	192.1	2.31	158	0.091
	21.6	36.320	247.0	668.50	29.73	8.13	380	310	1210	1.222	267	373.7	267	45.4	1.83	0.001	11.76	36.9	1.93	1.23	3.08E-8	192.1	2.31	158	0.091
	21.3	49.247	343.5	685.65	37.20	15.90	510	430	1210	1.223	267	360.1	267	45.4	1.76	0.001	11.76	36.9	1.93	1.23	6.03E-8	192.2	2.31	158	0.172
	21.3	49.247	343.8	686.25	37.47	16.17	510	430	1210	1.223	267	354.6	267	45.4	1.73	0.001	11.76	37.0	1.93	1.23	6.13E-8	192.2	2.31	158	0.172
	21.3	49.247	343.2	685.05	36.94	15.64	510	430	1210	1.223	267	365.8	267	45.4	1.79	0.001	11.76	37.0	1.93	1.23	5.93E-8	192.2	2.31	158	0.172
PR - 2.5 %	21.1	59.127	423.6	704.24	45.32	24.22	610	520	1210	1.221	266	350.2	266	45.3	1.71	0.001	11.74	36.9	1.93	1.23	9.26E-8	191.4	2.31	158	0.255
	21.1	59.127	422.6	702.58	44.59	23.49	610	520	1210	1.221	266	360.2	266	45.3	1.76	0.001	11.74	36.9	1.93	1.23	8.99E-8	191.4	2.31	158	0.254
	21.1	59.127	423.8	704.58	45.46	24.36	610	520	1210	1.221	266	348.3	266	45.3	1.70	0.001	11.74	36.9	1.93	1.23	9.32E-8	191.4	2.31	158	0.255
PR - 2.5 %	21.2	37.657	255.6	687.22	29.17	7.97	390	320	1210	1.324	313	409.0	313	49.1	2.00	0.001	12.73	40.0	1.93	1.23	2.20E-8	225.1	2.50	159	0.098
	21.2	37.657	255.8	687.74	29.40	8.20	390	320	1210	1.324	313	398.0	313	49.1	1.94	0.001	12.73	40.0	1.93	1.23	2.26E-8	225.1	2.50	159	0.098
	21.2	37.657	255.9	688.00	29.51	8.31	390	320	1210	1.324	313	392.7	313	49.1	1.92	0.001	12.73	40.0	1.93	1.23	2.30E-8	225.1	2.50	159	0.098
	21.4	44.201	304.3	676.74	33.32	11.92	460	380	1210	1.324	313	382.0	313	49.1	1.87	0.001	12.74	40.0	1.93	1.23	3.29E-8	225.3	2.50	159	0.137
	21.4	44.201	303.9	675.85	32.93	11.53	460	380	1210	1.324	313	394.4	313	49.1	1.93	0.001	12.74	40.0	1.93	1.23	3.18E-8	225.3	2.50	159	0.137
	21.4	44.201	304.3	676.74	33.32	11.92	460	380	1210	1.324	313	382.0	313	49.1	1.87	0.001	12.74	40.0	1.93	1.23	3.29E-8	225.3	2.50	159	0.137
	21.5	50.408	351.3	685.07	36.95	15.45	520	430	1210	1.325	313	388.1	313	49.2	1.90	0.001	12.75	40.1	1.93	1.23	4.24E-8	225.7	2.50	159	0.180
	21.5	50.408	351.5	685.46	37.12	15.62	520	430	1210	1.325	313	384.1	313	49.2	1.88	0.001	12.75	40.1	1.93	1.23	4.29E-8	225.7	2.50	159	0.180
	21.5	50.408	351.2	684.87	36.87	15.37	520	430	1210	1.325	313	390.1	313	49.2	1.91	0.001	12.75	40.1	1.93	1.23	4.22E-8	225.7	2.50	159	0.180

Experiment Information	T _a (C)	PR Volt (mV)	Wire Volt (mV)	Wire Res (mΩ)	T _a (C)	T _a -T _a (C)	Cur (mA)	Volt (V)	Freq (Hz)	μV (V)	R _s	h Wmm ² K	Corr		Re(D)	Nu(D)	X	ε	KC (28)	A _ν A	β (2A/73)	Gr(D)		PR %	SPL (dB)	Power (W)
													R _s	R _s								ReTs	A			
I ~ 1053 Hz L = 59 cm PR ~ 0.9 %	20.2	25.7579	174.206	664.82	28.12	7.92	270	230	1045	0.479	47	191.8	47	17.7	0.94	0.001	5.33	16.7	167	1.06	9.81E-7	36.3	0.91	150	0.046	
	20.2	25.7563	174.204	664.86	28.14	7.94			1045	0.479	47	191.4	47	17.7	0.93	0.001	5.33	16.7	167	1.06	9.83E-7	36.3	0.91	150	0.046	
	20.2	25.7558	174.189	664.81	28.12	7.92			1045	0.479	47	191.7	47	17.7	0.94	0.001	5.33	16.7	167	1.06	9.82E-7	36.3	0.91	150	0.046	
PR ~ 1.1 %	20.2	35.124	244.101	683.15	36.12	15.92	360	310	1045	0.479	47	182.4	47	17.7	0.89	0.001	5.33	16.7	167	1.06	1.97E-6	36.3	0.91	150	0.087	
	20.2	35.122	244.084	683.17	36.13	15.93			1045	0.479	47	182.3	47	17.7	0.89	0.001	5.33	16.7	167	1.06	1.97E-6	36.3	0.91	150	0.087	
	20.2	35.121	244.088	683.18	36.13	15.93			1045	0.479	47	182.2	47	17.7	0.89	0.001	5.33	16.7	167	1.06	1.97E-6	36.3	0.91	150	0.087	
PR ~ 1.1 %	20.2	42.061	299.842	700.76	43.79	23.59	430	370	1045	0.480	47	181.0	47	17.8	0.88	0.001	5.34	16.8	167	1.06	2.90E-6	36.4	0.91	150	0.128	
	20.2	42.060	299.837	700.76	43.80	23.60			1045	0.480	47	181.0	47	17.8	0.88	0.001	5.34	16.8	167	1.06	2.90E-6	36.4	0.91	150	0.128	
	20.2	42.059	299.825	700.75	43.79	23.59			1045	0.480	47	181.0	47	17.8	0.88	0.001	5.34	16.8	167	1.06	2.90E-6	36.4	0.91	150	0.128	
PR ~ 1.1 %	20.0	31.634	213.82	684.43	27.95	7.95	330	270	1045	0.583	70	288.1	69	21.6	1.41	0.001	6.48	20.4	167	1.06	4.50E-7	53.6	1.10	152	0.069	
	20.0	31.628	213.79	684.46	27.97	7.97			1045	0.583	70	287.4	69	21.6	1.40	0.001	6.48	20.4	167	1.06	4.51E-7	53.6	1.10	152	0.069	
	20.0	31.628	213.79	684.46	27.97	7.97			1045	0.583	70	287.4	69	21.6	1.40	0.001	6.48	20.4	167	1.06	4.51E-7	53.6	1.10	152	0.069	
PR ~ 1.3 %	20.0	42.760	296.99	682.74	35.94	15.94	440	370	1045	0.584	70	289.8	69	21.6	1.32	0.001	6.49	20.4	167	1.06	8.96E-7	53.8	1.10	152	0.129	
	20.0	42.759	296.98	682.74	35.94	15.94			1045	0.584	70	289.8	69	21.6	1.32	0.001	6.49	20.4	167	1.06	8.96E-7	53.8	1.10	152	0.129	
	20.0	42.759	296.98	682.74	35.94	15.94			1045	0.584	70	289.8	69	21.6	1.32	0.001	6.49	20.4	167	1.06	8.96E-7	53.8	1.10	152	0.129	
PR ~ 1.3 %	20.0	51.208	365.20	701.05	43.92	23.92	530	450	1045	0.584	70	264.7	69	21.6	1.29	0.001	6.49	20.4	167	1.06	1.35E-6	53.8	1.10	152	0.190	
	20.0	51.198	365.14	701.07	43.93	23.93			1045	0.584	70	264.5	69	21.6	1.29	0.001	6.49	20.4	167	1.06	1.35E-6	53.8	1.10	152	0.190	
	20.0	51.192	365.08	701.05	43.92	23.92			1045	0.584	70	264.5	69	21.6	1.29	0.001	6.49	20.4	167	1.06	1.35E-6	53.8	1.10	152	0.190	
PR ~ 1.3 %	20.2	36.803	249.323	665.94	28.61	8.41	380	320	1045	0.690	98	369.5	97	25.5	1.80	0.001	7.67	24.1	167	1.06	2.42E-7	75.2	1.30	153	0.093	
	20.2	36.796	249.284	665.96	28.62	8.42			1045	0.690	98	368.9	97	25.5	1.80	0.001	7.67	24.1	167	1.06	2.42E-7	75.2	1.30	153	0.093	
	20.2	36.794	249.282	665.99	28.63	8.43			1045	0.690	98	368.3	97	25.5	1.80	0.001	7.67	24.1	167	1.06	2.42E-7	75.2	1.30	153	0.093	
PR ~ 1.5 %	20.4	49.32	343.27	684.17	36.56	16.16	510	430	1045	0.690	98	354.7	97	25.6	1.73	0.001	7.67	24.1	167	1.06	4.63E-7	75.3	1.30	153	0.172	
	20.4	49.31	343.33	684.43	36.68	16.28			1045	0.690	98	352.2	97	25.6	1.72	0.001	7.67	24.1	167	1.06	4.66E-7	75.3	1.30	153	0.172	
	20.4	49.31	343.30	684.37	36.65	16.25			1045	0.690	98	352.8	97	25.6	1.72	0.001	7.67	24.1	167	1.06	4.66E-7	75.3	1.30	153	0.172	
PR ~ 1.5 %	20.4	59.67	426.22	702.15	44.40	24.00	610	520	1045	0.690	98	358.8	97	25.6	1.73	0.001	7.67	24.1	167	1.06	6.88E-7	75.3	1.30	153	0.259	
	20.4	59.67	426.20	702.12	44.39	23.99			1045	0.690	98	359.0	97	25.6	1.75	0.001	7.67	24.1	167	1.06	6.87E-7	75.3	1.30	153	0.259	
	20.4	59.72	426.25	701.61	44.17	23.77			1045	0.690	98	362.6	97	25.6	1.77	0.001	7.67	24.1	167	1.06	6.81E-7	75.3	1.30	153	0.259	
PR ~ 1.5 %	23.3	38.99	266.39	671.61	31.08	7.78	400	340	1051	0.799	132	451.8	131	29.7	2.21	0.001	8.88	27.9	167	1.07	1.22E-7	101.0	1.51	155	0.106	
	23.3	38.97	266.30	671.73	31.14	7.84			1051	0.799	132	448.5	131	29.7	2.19	0.001	8.88	27.9	167	1.07	1.23E-7	101.0	1.51	155	0.106	
	23.3	38.95	266.23	671.90	31.21	7.91			1051	0.799	132	444.0	131	29.7	2.17	0.001	8.88	27.9	167	1.07	1.24E-7	101.0	1.51	155	0.106	
PR ~ 1.5 %	23.0	53.84	377.56	689.34	38.82	15.82	560	470	1051	0.801	133	435.2	131	29.8	2.13	0.001	8.90	27.9	167	1.07	1.23E-7	101.2	1.51	155	0.207	
	23.0	53.83	377.51	689.38	38.83	15.83			1051	0.801	133	434.6	131	29.8	2.12	0.001	8.90	27.9	167	1.07	1.24E-7	101.2	1.51	155	0.207	
	23.0	53.85	377.66	689.40	38.84	15.84			1051	0.801	133	434.9	131	29.8	2.12	0.001	8.90	27.9	167	1.07	1.24E-7	101.2	1.51	155	0.207	
PR ~ 1.5 %	22.6	64.88	467.04	707.61	46.79	24.19	670	570	1050	0.801	132	424.2	131	29.8	2.07	0.001	8.90	28.0	167	1.07	3.78E-7	101.3	1.51	155	0.308	
	22.6	64.84	467.03	708.04	46.97	24.37			1050	0.801	132	420.8	131	29.8	2.06	0.001	8.90	28.0	167	1.07	3.81E-7	101.3	1.51	155	0.308	
	22.6	64.83	467.05	708.18	47.03	24.43			1050	0.801	132	419.7	131	29.8	2.05	0.001	8.90	28.0	167	1.07	3.82E-7	101.3	1.51	155	0.308	

Experiment Information	T _a (°C)	PR (mV)	V _{out} (mV)	W _{in} (mW)	T _s (°C)	T _e -T _a (°C)	I _{out} (mA)	V _{out} (V)	Freq (Hz)	Inc V (V)	R _s (Ω)	h (W/m ² K)	Corr		Re(D)	N _u (D)	X	s	KC (m)	β (2ΔA/Δx)	Gr(D)		PR %	SPL (dB)	Power (W)
													R _s	R _s							R _s H _s	Λ			
T = 1053 Hz L = 58 cm PR = 1.7 %	22.6	42.26	288.48	671.03	30.83	8.23	440	360	1049	0.901	168	501.7	166	33.5	2.45	0.001	10.02	31.5	167	1.06	7.99E-8	128.6	170	156	0.124
	22.6	42.25	288.46	671.14	30.88	8.28			1049	0.901	168	498.5	166	33.5	2.44	0.001	10.02	31.5	167	1.06	8.04E-8	128.6	170	156	0.124
	22.6	42.24	288.49	671.37	30.98	8.38			1049	0.901	168	492.5	166	33.5	2.41	0.001	10.02	31.5	167	1.06	8.14E-8	128.6	170	156	0.124
22.6	56.25	394.04	688.61		38.50	15.90	580	430	1049	0.898	167	472.1	165	33.4	2.31	0.001	9.99	31.4	167	1.06	1.57E-7	127.8	170	156	0.225
	56.25	394.01	688.55		38.47	15.87			1049	0.898	167	472.8	165	33.4	2.31	0.001	9.99	31.4	167	1.06	1.56E-7	127.8	170	156	0.225
	56.26	394.02	688.45		38.43	15.83			1049	0.898	167	474.3	165	33.4	2.32	0.001	9.99	31.4	167	1.06	1.56E-7	127.8	170	156	0.226
22.9	68.43	493.55	708.99		47.38	24.48	700	600	1049	0.893	165	487.1	164	33.2	2.28	0.001	9.94	31.2	167	1.06	2.45E-7	126.6	169	156	0.344
	68.40	493.42	709.11		47.44	24.54			1049	0.893	165	465.7	164	33.2	2.27	0.001	9.94	31.2	167	1.06	2.46E-7	126.6	169	156	0.343
	68.45	493.63	708.89		47.34	24.44			1049	0.893	165	468.1	164	33.2	2.29	0.001	9.94	31.2	167	1.06	2.45E-7	126.6	169	156	0.344
PR = 1.9 %	20.8	36.255	245.8	665.45	28.83	8.03	380	310	1046	1.008	209	375.6	207	37.4	1.83	0.001	11.21	35.2	167	1.06	5.03E-8	160.7	191	157	0.091
	36.255	245.9	666.72		28.95	8.15			1046	1.008	209	370.3	207	37.4	1.81	0.001	11.21	35.2	167	1.06	5.12E-8	160.7	191	157	0.091
	36.255	246.0	666.99		29.07	8.27			1046	1.008	209	365.2	207	37.4	1.78	0.001	11.21	35.2	167	1.06	5.20E-8	160.7	191	157	0.091
20.9	49.349	343.9	685.03		36.93	16.03	510	430	1046	1.005	208	358.4	206	37.3	1.75	0.001	11.18	35.1	167	1.06	1.02E-7	159.8	190	157	0.173
	49.349	344.1	685.42		37.11	16.21			1046	1.005	208	354.8	206	37.3	1.73	0.001	11.18	35.1	167	1.06	1.03E-7	159.8	190	157	0.173
	49.349	344.2	685.62		37.19	16.29			1046	1.005	208	353.0	206	37.3	1.72	0.001	11.18	35.1	167	1.06	1.03E-7	159.8	190	157	0.173
21.1	60.106	429.3	702.10		44.38	23.28	620	530	1046	1.006	209	375.3	207	37.3	1.83	0.001	11.19	35.2	167	1.06	1.47E-7	160.4	190	157	0.262
	60.106	430.5	704.06		45.23	24.13			1046	1.006	209	363.0	207	37.3	1.77	0.001	11.19	35.2	167	1.06	1.52E-7	160.4	190	157	0.263
	60.106	429.9	703.08		44.81	23.71			1046	1.006	209	369.1	207	37.3	1.80	0.001	11.19	35.2	167	1.06	1.49E-7	160.4	190	157	0.263
PR = 2.1 %	21.6	34.953	237.6	668.21	29.60	8.00	360	300	1048	1.117	257	351.4	255	41.5	1.72	0.001	12.41	39.0	167	1.06	3.33E-8	197.0	211	158	0.084
	34.953	237.9	669.06		29.97	8.37			1048	1.117	257	336.4	255	41.5	1.64	0.001	12.41	39.0	167	1.06	3.48E-8	197.0	211	158	0.085
	34.953	238.0	669.34		30.09	8.49			1048	1.117	257	331.7	255	41.5	1.62	0.001	12.41	39.0	167	1.06	3.53E-8	197.0	211	158	0.085
21.7	47.199	329.5	686.24		37.46	15.76	490	410	1048	1.118	258	334.1	255	41.5	1.63	0.001	12.43	39.0	167	1.06	6.52E-8	197.5	211	158	0.158
	47.199	330.2	687.70		38.10	16.40			1048	1.118	258	321.8	255	41.5	1.57	0.001	12.43	39.0	167	1.06	6.79E-8	197.5	211	158	0.159
	47.199	329.3	685.82		37.28	15.58			1048	1.118	258	337.8	255	41.5	1.65	0.001	12.43	39.0	167	1.06	6.45E-8	197.5	211	158	0.158
21.7	57.940	414.9	703.91		45.17	23.47	600	510	1048	1.116	257	346.8	254	41.4	1.69	0.001	12.40	39.0	167	1.06	9.78E-8	196.8	211	158	0.245
	57.940	416.2	706.12		46.13	24.43			1048	1.116	257	334.2	254	41.4	1.63	0.001	12.40	39.0	167	1.06	1.02E-7	196.8	211	158	0.245
	57.940	415.3	704.59		45.47	23.77			1048	1.116	257	342.8	254	41.4	1.67	0.001	12.40	39.0	167	1.06	9.91E-8	196.8	211	158	0.245
PR = 2.3 %	22.1	36.275	247.0	669.33	30.09	7.99	370	320	1049	1.221	308	379.7	304	45.4	1.85	0.001	13.57	42.6	167	1.06	2.32E-8	235.4	231	158	0.091
	36.275	247.5	670.69		30.68	8.58			1049	1.221	308	354.2	304	45.4	1.73	0.001	13.57	42.6	167	1.06	2.49E-8	235.4	231	158	0.091
	36.275	247.8	671.50		31.04	8.94			1049	1.221	308	340.6	304	45.4	1.66	0.001	13.57	42.6	167	1.06	2.60E-8	235.4	231	158	0.091
22.2	41.509	286.3	678.00		33.87	11.67	430	360	1049	1.220	307	344.8	304	45.4	1.75	0.001	13.56	42.6	167	1.06	2.47E-8	235.4	231	158	0.121
	41.509	285.8	676.82		33.36	11.16			1049	1.220	307	360.1	304	45.3	1.76	0.001	13.56	42.6	167	1.06	3.25E-8	235.2	231	158	0.121
	41.509	286.0	677.29		33.56	11.36			1049	1.220	307	353.8	304	45.3	1.73	0.001	13.56	42.6	167	1.06	3.31E-8	235.2	231	158	0.121
22.1	47.216	330.4	687.87		38.17	16.07	490	410	1049	1.221	308	328.6	304	45.4	1.61	0.001	13.57	42.6	167	1.06	4.67E-8	235.4	231	158	0.159
	47.216	330.3	687.66		38.08	15.98			1049	1.221	308	330.4	304	45.4	1.61	0.001	13.57	42.6	167	1.06	4.64E-8	235.4	231	158	0.159
	47.216	329.6	686.20		37.45	15.35			1049	1.221	308	343.4	304	45.4	1.68	0.001	13.57	42.6	167	1.06	4.46E-8	235.4	231	158	0.158

Experiment Information	T _a (°C)	P _R (mV)	Wire Volt (mV)	Wire Res (mΩ)	T _s (°C)	T _s -T _a (°C)	Cur (mA)	Volt (V)	Freq (Hz)	mic V (V)	R _s (Ω)	h _w (W/m ² K)	Corr R _s (Ω)	Re(D) (mm)	X (mm)	ε	KQ (mV)	ΔA (mV)	ρ (2ΔA/V)	Gr(D) Re(Ts)	R _g (Ω)	PR %	SPL (dB)	Power (W)
f = 564 Hz L = 47 cm PR ~ 0.9 %	20.8	31.261	211.923	666.39	28.81	8.01	330	270	563	0.481	89	280.2	87	17.8	1.37	0.001	9.94	31.2	0.90	2.85E-7	92.0	0.91	150	0.067
	20.8	31.259	211.909	666.39	28.81	8.01	330	270	563	0.481	89	280.1	87	17.8	1.37	0.001	9.94	31.2	0.90	2.85E-7	92.0	0.91	150	0.067
	20.8	31.259	211.906	666.38	28.80	8.00	330	270	563	0.481	89	280.3	87	17.8	1.37	0.001	9.94	31.2	0.90	2.85E-7	92.0	0.91	150	0.067
	20.8	31.259	211.906	666.38	28.80	8.00	330	270	563	0.481	89	280.2	87	17.8	1.37	0.001	9.94	31.2	0.90	2.85E-7	92.0	0.91	150	0.067
PR ~ 1.1 %	20.8	42.231	294.129	684.64	36.76	15.96	440	370	563	0.479	88	263.5	86	17.8	1.29	0.001	9.89	31.1	0.90	5.78E-7	91.3	0.91	150	0.126
	20.8	42.229	294.120	684.65	36.77	15.97	440	370	563	0.479	88	263.4	86	17.8	1.29	0.001	9.89	31.1	0.90	5.78E-7	91.3	0.91	150	0.126
	20.8	42.231	294.132	684.64	36.77	15.97	440	370	563	0.479	88	263.4	86	17.8	1.29	0.001	9.89	31.1	0.90	5.78E-7	91.3	0.91	150	0.126
	20.8	42.231	294.132	684.64	36.77	15.97	440	370	563	0.479	88	263.4	86	17.8	1.29	0.001	9.89	31.1	0.90	5.78E-7	91.3	0.91	150	0.126
PR ~ 1.3 %	20.8	50.703	362.98	703.72	45.09	24.49	520	450	563	0.479	88	254.5	86	17.7	1.24	0.001	9.89	31.1	0.90	8.89E-7	91.2	0.91	150	0.187
	20.8	50.698	362.98	703.72	45.12	24.52	520	450	563	0.479	88	254.1	86	17.7	1.24	0.001	9.89	31.1	0.90	8.89E-7	91.2	0.91	150	0.187
	20.8	50.698	362.98	703.72	45.12	24.52	520	450	563	0.479	88	254.1	86	17.7	1.24	0.001	9.89	31.1	0.90	8.89E-7	91.2	0.91	150	0.187
	20.8	50.698	362.98	703.72	45.12	24.52	520	450	563	0.479	88	254.1	86	17.7	1.24	0.001	9.89	31.1	0.90	8.89E-7	91.2	0.91	150	0.187
PR ~ 1.5 %	20.8	36.902	250.389	666.99	29.07	8.27	380	320	563	0.584	131	378.4	129	21.6	1.85	0.001	12.06	37.9	0.90	1.35E-7	135.7	1.10	152	0.094
	20.8	36.904	250.396	666.97	29.06	8.26	380	320	563	0.584	131	378.4	129	21.6	1.85	0.001	12.06	37.9	0.90	1.35E-7	135.7	1.10	152	0.094
	20.8	36.894	250.371	667.09	29.11	8.31	380	320	563	0.584	131	378.4	129	21.6	1.85	0.001	12.06	37.9	0.90	1.35E-7	135.7	1.10	152	0.094
	20.8	36.894	250.371	667.09	29.11	8.31	380	320	563	0.584	131	378.4	129	21.6	1.85	0.001	12.06	37.9	0.90	1.35E-7	135.7	1.10	152	0.094
PR ~ 1.5 %	20.7	48.92	340.72	684.64	36.77	16.07	510	420	563	0.585	131	351.3	129	21.7	1.72	0.001	12.06	38.0	0.90	2.62E-7	136.1	1.11	152	0.170
	20.7	48.91	340.76	684.86	36.86	16.16	510	420	563	0.585	131	349.1	129	21.7	1.71	0.001	12.06	38.0	0.90	2.63E-7	136.1	1.11	152	0.170
	20.7	48.92	340.69	684.58	36.74	16.04	510	420	563	0.585	131	351.8	129	21.7	1.72	0.001	12.06	38.0	0.90	2.61E-7	136.1	1.11	152	0.170
	20.7	48.92	340.69	684.58	36.74	16.04	510	420	563	0.585	131	351.8	129	21.7	1.72	0.001	12.06	38.0	0.90	2.62E-7	136.1	1.11	152	0.170
PR ~ 1.5 %	20.8	59.16	423.64	703.92	45.17	24.37	610	520	563	0.584	131	348.2	129	21.6	1.70	0.001	12.06	37.9	0.90	3.99E-7	135.7	1.10	152	0.255
	20.8	59.16	423.64	703.92	45.17	24.37	610	520	563	0.584	131	348.2	129	21.6	1.70	0.001	12.06	37.9	0.90	3.99E-7	135.7	1.10	152	0.255
	20.8	59.16	423.64	703.92	45.17	24.37	610	520	563	0.584	131	348.2	129	21.6	1.70	0.001	12.06	37.9	0.90	3.99E-7	135.7	1.10	152	0.255
	20.8	59.16	423.64	703.92	45.17	24.37	610	520	563	0.584	131	348.2	129	21.6	1.70	0.001	12.06	37.9	0.90	3.99E-7	135.7	1.10	152	0.255
PR ~ 1.5 %	20.9	53.54	374.33	687.27	37.91	16.21	550	460	565	0.689	182	433.5	178	25.6	2.04	0.001	14.20	44.6	0.90	1.37E-7	187.9	1.30	153	0.204
	20.9	53.56	374.36	687.07	37.83	16.13	550	460	565	0.689	182	433.2	178	25.6	2.06	0.001	14.20	44.6	0.90	1.37E-7	187.9	1.30	153	0.204
	20.9	53.56	374.36	687.05	37.82	16.12	550	460	565	0.689	182	433.6	178	25.6	2.06	0.001	14.20	44.6	0.90	1.37E-7	187.9	1.30	153	0.204
	20.9	53.56	374.36	687.05	37.82	16.12	550	460	565	0.689	182	433.6	178	25.6	2.06	0.001	14.20	44.6	0.90	1.37E-7	187.9	1.30	153	0.204
PR ~ 1.5 %	20.9	63.58	454.47	702.65	44.62	23.72	650	560	565	0.688	181	412.5	177	25.5	2.01	0.001	14.16	44.5	0.90	2.05E-7	186.5	1.30	153	0.294
	20.9	63.58	454.47	702.65	44.62	23.72	650	560	565	0.688	181	412.5	177	25.5	2.01	0.001	14.16	44.5	0.90	2.05E-7	186.5	1.30	153	0.294
	20.9	63.58	454.47	702.65	44.62	23.72	650	560	565	0.688	181	412.5	177	25.5	2.01	0.001	14.16	44.5	0.90	2.05E-7	186.5	1.30	153	0.294
	20.9	63.58	454.47	702.65	44.62	23.72	650	560	565	0.688	181	412.5	177	25.5	2.01	0.001	14.16	44.5	0.90	2.05E-7	186.5	1.30	153	0.294
PR ~ 1.5 %	20.1	42.31	286.21	664.96	28.18	8.08	440	360	562	0.796	242	507.3	239	29.5	2.48	0.001	16.45	51.7	0.90	3.84E-8	252.3	1.50	155	0.123
	20.1	42.31	286.18	664.89	28.15	8.05	440	360	562	0.796	242	509.1	239	29.5	2.49	0.001	16.45	51.7	0.90	3.83E-8	252.3	1.50	155	0.123
	20.1	42.30	286.21	665.12	28.25	8.15	440	360	562	0.796	242	502.9	239	29.5	2.46	0.001	16.45	51.7	0.90	3.88E-8	252.3	1.50	155	0.123
	20.1	42.30	286.21	665.12	28.25	8.15	440	360	562	0.796	242	502.9	239	29.5	2.46	0.001	16.45	51.7	0.90	3.88E-8	252.3	1.50	155	0.123
PR ~ 1.5 %	20.2	56.68	393.42	682.31	35.75	15.55	580	490	562	0.795	242	485.6	238	29.4	2.37	0.001	16.43	51.6	0.90	7.42E-8	251.8	1.50	155	0.227
	20.2	56.65	393.48	682.77	35.95	15.75	580	490	562	0.795	242	479.2	238	29.4	2.34	0.001	16.43	51.6	0.90	7.52E-8	251.8	1.50	155	0.227
	20.2	56.64	393.43	682.81	35.97	15.77	580	490	562	0.795	242	478.6	238	29.4	2.34	0.001	16.43	51.6	0.90	7.52E-8	251.8	1.50	155	0.227
	20.2	56.64	393.43	682.81	35.97	15.77	580	490	562	0.795	242	478.6	238	29.4	2.34	0.001	16.43	51.6	0.90	7.52E-8	251.8	1.50	155	0.227
PR ~ 1.5 %	20.2	69.17	494.55	702.82	44.70	24.50	710	600	562	0.795	242	472.9	238	29.4	2.31	0.001	16.43	51.6	0.90	1.17E-7	251.8	1.50	155	0.348
	20.2	69.17	494.45	702.68	44.63	24.43	710	600	562	0.795	242	474.0	238	29.4	2.32	0.001	16.43	51.6	0.90	1.17E-7	251.8	1.50	155	0.348
	20.2	69.17	494.42	702.64	44.62	24.42	710	600	562	0.795	242	474.3	238	29.4	2.32	0.001	16.43	51.6	0.90	1.16E-7	251.8	1.50	155	0.348
	20.2	69.17	494.42	702.64	44.62	24.42	710	600	562	0.795	242	473.7	238	29.4	2.31	0.001	16.43	51.6	0.90	1.17E-7	251.8	1.50	155	0.348

Experiment Information	T _a (°C)	PR Volt (mV)	Wire Volt (mV)	Wire Res (mΩ)	T _s (°C)	T _e -T _a (°C)	Cur (mA)	Volt (V)	Freq (Hz)	micV (V)	R _s (Ω)	h (mm ² K)	Corr R _s (Ω)	Re(Ω)	Nu(°D)	X	ε	KC (mm)	Δ ¹ Δ (2ΔΔ ₀)	Gr(Ω)	R _s /R ₀	R _s Δ	PR %	SPL (dB)	Power (W)
f = 564 Hz L = 47 cm PR = 1.7 %	20.4	44.14	289.03	665.94	28.61	8.21	460	380	563	0.902	311	544.3	306	33.4	2.65	0.001	18.62	58.5	0.90	0.57	2.38E-8	323.0	1.70	156	0.134
	20.4	44.13	299.01	666.05	28.66	8.26			563	0.902	311	541.1	306	33.4	2.64	0.001	18.62	58.5	0.90	0.57	2.39E-8	323.0	1.70	156	0.134
	20.4	44.13	299.01	666.05	28.66	8.26			563	0.902	311	546.8	306	33.4	2.67	0.001	18.62	58.5	0.90	0.57	2.36E-8	323.0	1.70	156	0.134
	20.4	44.14	298.99	665.95	28.57	8.17			563	0.902	311	544.1	306	33.4	2.68	0.001	18.62	58.5	0.90	0.57	2.38E-8	323.0	1.70	156	0.134
PR = 1.9 %	20.3	58.78	408.94	683.89	36.44	16.14	610	490	563	0.902	311	504.4	306	33.4	2.46	0.001	18.62	58.5	0.90	0.57	4.68E-8	322.8	1.70	156	0.245
	20.3	58.78	408.87	683.77	36.39	16.09			563	0.902	311	505.9	306	33.4	2.47	0.001	18.62	58.5	0.90	0.57	4.66E-8	322.8	1.70	156	0.244
	20.3	58.78	408.85	683.74	36.37	16.07			563	0.902	311	506.3	306	33.4	2.47	0.001	18.62	58.5	0.90	0.57	4.66E-8	322.8	1.70	156	0.244
	20.4	70.42	503.49	702.83	44.70	24.30	720	620	563	0.902	311	494.1	306	33.4	2.41	0.001	18.62	58.5	0.90	0.57	7.03E-8	323.0	1.70	156	0.361
PR = 2.1 %	20.4	70.43	503.67	702.98	44.76	24.36			563	0.902	311	493.0	306	33.4	2.41	0.001	18.62	58.5	0.90	0.57	7.05E-8	323.0	1.70	156	0.361
	20.4	70.42	503.40	702.70	44.64	24.24			563	0.902	311	495.1	306	33.4	2.42	0.001	18.62	58.5	0.90	0.57	7.02E-8	323.0	1.70	156	0.361
	20.4	45.00	304.64	665.47	28.41	8.01	460	380	562	1.009	390	579.9	384	37.4	2.83	0.001	20.87	65.6	0.90	0.57	1.47E-8	406.1	1.91	157	0.139
	20.4	45.00	304.63	665.45	28.40	8.00			562	1.009	390	580.5	384	37.4	2.84	0.001	20.87	65.6	0.90	0.57	1.47E-8	406.1	1.91	157	0.139
PR = 2.3 %	20.4	45.00	304.62	665.43	28.39	7.99			562	1.009	390	581.2	384	37.4	2.84	0.001	20.87	65.6	0.90	0.57	1.46E-8	406.1	1.91	157	0.139
	20.4	60.29	419.12	683.36	36.21	15.81	620	520	562	1.009	390	541.3	384	37.4	2.64	0.001	20.87	65.6	0.90	0.57	2.90E-8	406.1	1.91	157	0.257
	20.4	60.31	419.06	683.03	36.06	15.66			562	1.009	390	546.3	384	37.4	2.67	0.001	20.87	65.6	0.90	0.57	2.87E-8	406.1	1.91	157	0.257
	20.4	60.28	419.08	683.40	36.23	15.83			562	1.009	390	540.5	384	37.4	2.64	0.001	20.87	65.6	0.90	0.57	2.90E-8	406.1	1.91	157	0.257
PR = 2.1 %	20.4	72.23	515.37	701.38	44.07	23.67	740	630	562	1.009	390	532.6	384	37.4	2.60	0.001	20.87	65.6	0.90	0.57	2.89E-8	406.1	1.91	157	0.379
	20.4	72.22	515.38	701.49	44.12	23.72			562	1.009	390	531.4	384	37.4	2.60	0.001	20.87	65.6	0.90	0.57	4.35E-8	406.1	1.91	157	0.379
	20.4	72.24	515.38	701.30	44.03	23.63			562	1.009	390	533.5	384	37.4	2.61	0.001	20.87	65.6	0.90	0.57	4.33E-8	406.1	1.91	157	0.379
	20.4	46.046	314.0	670.33	30.53	8.03	480	390	564	1.112	475	609.9	468	41.3	2.98	0.001	23.00	72.3	0.90	0.57	9.84E-9	494.1	2.10	158	0.147
PR = 2.3 %	22.5	46.046	314.0	670.33	30.53	8.03			564	1.112	475	609.9	468	41.3	2.98	0.001	23.00	72.3	0.90	0.57	9.84E-9	494.1	2.10	158	0.147
	22.5	46.046	314.0	670.33	30.53	8.03			564	1.112	475	609.9	468	41.3	2.98	0.001	23.00	72.3	0.90	0.57	9.84E-9	494.1	2.10	158	0.147
	22.6	61.997	434.0	688.13	38.29	15.69	640	530	564	1.112	475	580.7	468	41.3	2.84	0.001	23.00	72.3	0.90	0.57	1.92E-8	494.4	2.10	158	0.274
	22.6	61.997	434.2	688.45	38.43	15.83			564	1.112	475	575.9	469	41.3	2.81	0.001	23.00	72.3	0.90	0.57	1.94E-8	494.4	2.10	158	0.274
PR = 2.3 %	22.6	61.997	434.3	688.61	38.50	15.90			564	1.112	475	573.5	469	41.3	2.80	0.001	23.00	72.3	0.90	0.57	1.95E-8	494.4	2.10	158	0.274
	22.6	61.997	434.3	688.61	38.50	15.90			564	1.112	475	576.7	469	41.3	2.82	0.001	23.00	72.3	0.90	0.57	1.93E-8	494.4	2.10	158	0.274
	22.6	74.595	536.9	707.52	46.74	24.14	760	650	564	1.112	475	561.7	469	41.3	2.74	0.001	23.00	72.3	0.90	0.57	2.95E-8	494.4	2.10	158	0.407
	22.6	74.595	536.8	707.39	46.69	24.09			564	1.112	475	562.9	469	41.3	2.75	0.001	23.00	72.3	0.90	0.57	2.95E-8	494.4	2.10	158	0.407
PR = 2.3 %	22.9	41.876	286.1	671.59	31.08	8.18	430	360	565	1.219	571	496.2	562	45.3	2.42	0.001	25.18	79.1	0.90	0.57	6.95E-9	592.2	2.30	158	0.122
	22.9	41.876	285.4	669.95	30.36	7.46			565	1.219	571	542.5	562	45.3	2.65	0.001	25.18	79.1	0.90	0.57	6.34E-9	592.2	2.30	158	0.122
	22.9	41.876	285.7	670.65	30.67	7.77			565	1.218	571	521.6	562	45.3	2.55	0.001	25.18	79.1	0.90	0.57	6.60E-9	592.2	2.30	158	0.122
	22.9	41.876	285.7	670.65	30.67	7.77			565	1.218	571	520.1	562	45.3	2.54	0.001	25.18	79.1	0.90	0.57	6.63E-9	592.2	2.30	158	0.122
PR = 2.3 %	22.9	50.373	348.0	679.10	34.35	11.45	520	430	565	1.220	572	518.4	563	45.4	2.53	0.001	25.20	79.2	0.90	0.57	9.70E-9	593.2	2.31	158	0.178
	22.9	50.373	348.8	680.66	35.03	12.13			565	1.220	572	490.2	563	45.4	2.40	0.001	25.20	79.2	0.90	0.57	1.03E-8	593.2	2.31	158	0.178
	22.9	50.373	347.8	678.71	34.18	11.28			565	1.220	572	525.9	563	45.4	2.57	0.001	25.20	79.2	0.90	0.57	9.58E-9	593.2	2.31	158	0.178
	22.9	50.373	347.8	678.71	34.18	11.28			565	1.220	572	511.6	563	45.4	2.50	0.001	25.20	79.2	0.90	0.57	9.85E-9	593.2	2.31	158	0.178
PR = 2.3 %	23.0	62.000	435.6	690.64	39.38	16.38	640	540	565	1.219	571	568.3	562	45.3	2.73	0.001	25.18	79.1	0.90	0.57	1.39E-8	592.5	2.30	158	0.275
	23.0	62.000	434.9	689.53	38.90	15.90			565	1.219	571	574.3	562	45.3	2.81	0.001	25.18	79.1	0.90	0.57	1.35E-8	592.5	2.30	158	0.274
	23.0	62.000	436.7	692.38	40.14	17.14			565	1.219	571	534.8	562	45.3	2.61	0.001	25.18	79.1	0.90	0.57	1.46E-8	592.5	2.30	158	0.275
	23.0	62.000	436.7	692.38	40.14	17.14			565	1.219	571	558.8	562	45.3	2.71	0.001	25.18	79.1	0.90	0.57	1.40E-8	592.5	2.30	158	0.275

LIST OF REFERENCES

1. Garrett, S. L., Adeff, J. A., Hofler, T. J., Thermoacoustic Refrigerator for Space Applications, *Journal Thermophysics and Heat Transfer*, Vol. 7, No. 4, 1993, pp. 595-599.
2. Lee, B. H., Richardson, P. D., Effect of Sound on Heat Transfer from a Horizontal Circular Cylinder at Large Wavelengths, *Journal of Mechanical Engineering Science*, Vol. 7, No. 2 1965, pp. 127-130.
3. Swift, G. W., Thermoacoustic Engines and Refrigerators, *Physics Today*, July 1995, pp. 22-28.
4. A. D. Little, Inc., Energy Efficient Alternatives to Chlorofluorocarbons, Revised Final Report - Ref. 66384 (US Dept. of Energy, ER-33, GTW), April 1992.
5. Garrett, S. L., Hofler, T. J., Perkins, D. K., Thermoacoustic Refrigeration, Greenpeace Ozone-Safe Cooling Conference, 1993.
6. Gebhart, B., Jaluria, Y., Mahajan, R. L., Sammakia, B., Buoyancy Induced Flows and Transport, Hemisphere: New York, 1988.
7. Fand, R. M., Cheng, P., The Influence of Sound on Heat Transfer from a Cylinder in Crossflow, *International Journal of Heat and Mass Transfer*, Vol. 6, 1963, pp. 571-596.
8. Fand, R. M., Kaye, J., Acoustic Streaming near a Heated Cylinder, *The Journal of the Acoustical Society of America*, Vol. 32, No. 5, May 1960, pp. 579-584.
9. Fand, R. M., Kaye, J., The Influence of Sound on Free Convection from a Horizontal Cylinder, *Journal of Heat Transfer*, May 1961, pp. 133-148.
10. Fand, R. M., Mechanism of Interaction between Vibrations and Heat Transfer, *Journal of the Acoustical Society of America*, Vol. 34, No. 12, December 1962, pp. 1887-1894.
11. Morse, P. M., Ingard, K. U., *Theoretical Acoustics*, McGraw-Hill: New York, 1968.
12. Stuart, J. T., Double Boundary Layers in Oscillatory Viscous Flow, *Journal of Fluid Mechanics*, Vol. 24, 1966, pp. 673-685.

13. Honji, H., Streaked Flow Around an Oscillating Circular Cylinder, *Journal of Fluid Mechanics*, Vol. 107, 1981, pp. 509-520.
14. Williamson, C. H. K., Sinusoidal Flow Relative to Circular Cylinders, *Journal of Fluid Mechanics*, Vol. 155, 1985, pp. 141-174.
15. Faltinsen, O. M., *Sea Loads on Ships and Offshore Structures*, Cambridge University Press, 1990.
16. Sarpkaya, T., Force on a Circular Cylinder in Viscous Oscillatory Flow at Low Keulegan-Carpenter Numbers, *Journal of Fluid Mechanics*, Vol. 165, 1986, pp. 61-71.
17. Harder, D., Convective Heat Transfer From a Cylinder in a Strong Acoustic Field, Masters Thesis, Naval Postgraduate School, 1995.
18. Mozerkewich, G., Heat Transfer from a Cylinder in an Acoustic Standing Wave, *Journal of the Acoustical Society of America*, Vol. 98, No. 4, October 1995, pp. 2209-2216.
19. Richardson, P. D., Effects of Sound and Vibrations on Heat Transfer, *Applied Mechanics Reviews*, Vol. 20, No. 3, March 1967, pp. 201-217.
20. Beckwith, T. G., Marangoni, R. D., Lienhard, J. H., *Mechanical Measurements*, 5th ed., Addison-Wesley: New York, 1993.

INITIAL DISTRIBUTION LIST

1. Defense Technical Information Center.....2
 8725 John J. Kingman Rd., STE 0944
 Ft. Belvoir, VA 22060-6218

2. Dudley Knox Library.....2
 Naval Postgraduate School
 411 Dyer Rd.
 Monterey, CA 93943-5101

3. Naval/Mechanical Engineering Curriculum.....1
 Code 34
 Naval Postgraduate School
 700 Dyer Road, Room 115
 Monterey, CA 93943-5107

4. Professor A. Gopinath.....2
 Code ME/GK
 Naval Postgraduate School
 700 Dyer Road, Room 333
 Monterey, CA 93943

5. Mr. Don P. Bridenstine.....1
 831 Lightstreet Road
 Bloomsburg, PA 17815

6. Mark Bridenstine.....1
 20 Beaver Dam Road
 South Berwick, ME 03908